Multirate Schemes and Multiuser Decoding in DS/CDMA Systems

by

Tony Ottosson
Department of Information Theory
Chalmers University of Technology
S-412 96 Göteborg, Sweden

Submitted to the School of Electrical and Computer Engineering,
Chalmers University of Technology, in partial fulfillment of the requirements
for the degree of Licentiate of Engineering

Technical report no. 214L
ISBN 91-7197-217-X
Göteborg, November 1995

ABSTRACT

Direct-Sequence Code Division Multiple-Access (DS/CDMA) has for some years been considered as a candidate for future personal and mobile communications. The reasons are mainly the properties of universal frequency reuse and the multipath mitigation. Generally, the focus has been on low rate services such as speech, and very little has been done on evaluating the performance for a system that can support many types of services, such as speech, fax, image and data transmission.

In this thesis, we present several schemes for multirate support and evaluate their relative performance. It is shown that the multi-channel scheme, using several channels (codes) in parallel, is the most efficient scheme. The main advantage is a high processing-gain even in “narrowband” systems (a few MHz). The drawback, though, is the need for linear amplifiers also in the mobile.

Furthermore, we present a new multiuser receiver for the synchronous CDMA channel. The receiver is optimum in the maximum likelihood sense, and has a lower complexity than the previously known optimum receiver. Also, the thesis includes a survey of multiuser detection for the synchronous DS/CDMA channel. The optimum and several suboptimal receivers are described and their advantages and disadvantages discussed.

The third part of this thesis considers joint optimization of several components in a multiuser system. For a synchronous DS/CDMA channel, we optimize the source and channel decoders, and the multiuser detector jointly, resulting in a soft multiuser decoder for transmission of vector quantized data. The optimum and several suboptimal receivers are presented. We also show that the performance gains for these decoders, with respect to individual optimization of the source and channel decoders and the detectors, are significant.

Keywords: Direct-Sequence Code Division Multiple-Access (DS/CDMA), multirate, multi processing-gain, multi-channel, multi-modulation, multiuser detection, joint optimization, soft decoding, vector quantization.

CONTENTS

ACKNOWLEDGEMENTS

Firstly, I would like to give my most sincere gratitude to my supervisor, professor Arne Svensson. I have really appreciated the flying start he gave me by presenting some ideas that was possible to pursue. I did that, and this thesis is based on some of those ideas. Furthermore, he has never been too busy to answer a question, discuss some recent results or just chat. I have also enjoyed our weekly discussions on research topics.

I would also sincerely like to thank Mikael Skoglund, who has had a difficult task in teaching me the business of vector quantization. His insight in source coding has really broadened my view of communications and for that, I am very grateful. Our common work and the many discussions during its progress, have been very inspiring. I would also like to thank Mikael for all his suggestions to improve this manuscript.

Erik's insight in the world of geometry and optimization has given me a new, fresh look on multiuser detection and made our collaboration very fruitful. It has been a pleasure working with him and hopefully there will be a continuation in the future. I would also like to thank him for providing some very illustrative pictures for the third chapter, and for valuable comments during the work of writing this thesis.

I also appreciate the effort Lars Kollberg has put into maintaining the computers, without which this work would not have been possible.

Furthermore, I will also like to thank Thomas Eriksson for his extraordinary library of C++ routines, and his service minded soul. He is always eager to add new features, before we ask for them. I have also enjoyed our many discussions. I regret to say so, but when it comes to wrestling, I have met my superior.

Finally, I would like to thank everybody at the Department of Information Theory, for all their support (time for laughs) and for all good company, both at work and at all the numerous parties we spent together. I (at least) have never had a boring minute.

CHAPTER
1

INTRODUCTION

1-1 BACKGROUND

Spread spectrum communications basically means that the system uses more bandwidth than what is necessary to transmit the data [48]. The main reason for the use of spreading was and still is, the interference resistance [48]. For example, in military communication systems a communication link may switch frequency in a random like pattern making it very hard for the enemy to intercept and/or jam the communication. This type of technique is commonly known as *Frequency Hopping Spread Spectrum* (FH/SS). For many years, the military spread spectrum applications, aiming at avoiding jamming and interception, dominated. The reason was mainly that the technique was very expensive and immature [41]. With the development of LSI (large scale integration) commercial applications such as the GPS (Global Positioning System) was developed. GPS is a *Direct Sequence Spread Spectrum* (DS/SS) system which, in contrast to FH/SS, occupies the whole bandwidth all the time and uses randomized codes to spread and collect the signals.

With the growth of mobile communications, and the need for highly efficient communications, multiuser systems based on spread spectrum, called *Code Division Multiple Access* (CDMA), became interesting [41]. The most commonly discussed technique is the *Direct-Sequence CDMA* (DS/CDMA) technique, which has some desired properties in universal frequency reuse, multipath mitigation [67] and macro diversity. The universal frequency

reuse means that no frequency planning has to be done, since all frequencies are used in all cells. This also means that base stations may be able to receive the signals from not only their own cell, but also from the neighboring cells. Therefore, combining these signals in the mobile switching center or elsewhere (macro diversity), results in decreased bit error rate and/or increased system range.

Consider a mobile near the base station transmitting with a given power. In the case of non orthogonal codes, the power from the nearest mobile cross-couples to the receiver of the distant mobile. In some cases the distant mobile is completely hidden in the interference from the nearer user, and hence, communication is impossible. This problem is known as the *near-far effect* [13]. The solutions are good code construction, yielding low cross-correlations for all time delays (assuming an asynchronous system), accurate and fast power control, and the use of a more complex multiuser receiver. Orthogonal code construction for all time shifts is an impossible task, at least if many users coexist in the same system. Power control, on the other hand, may be possible and is, for example, used in the standardized IS-95 system in USA [66]. However, the power control is difficult to realize in fast fading channels. Furthermore, the performance of the users with good channel conditions decreases, since their powers are limited by the weakly received users. Hence, the overall capacity is limited by power control [13]. Therefore, multiuser detection may be a more efficient solution that has received much attention in the last few years [13].

Besides the rapid growth of mobile communications, the evolution of services is of great importance. For example, today more than 10 million computers are connected to the Internet, either through a direct line or by a modem connection. All use the electronic mail service and many also the popular world-wide-web (WWW) service. In the future speech, fax, image, video, data, electronic billing and many other services will struggle for their existence in the present and coming communication systems. Furthermore, more people today than ever move around, travelling from home to work, and at work hurrying from one meeting to another. Thus, the need for a mobile and highly efficient communication system supporting the requested services are of great importance [30]. Support of all these types of services, means that the system has to be able to transmit at several data rates, both high and low rates, and at different service qualities. It must be able to

switch from one rate to another, quickly and all this must be functioning reliably, and at a low cost.

1-2 OUTLINE

This thesis deals with three in some ways very different topics: modulation, multiuser detection, and optimization of a communication system including source and channel coding and multiuser detection. The common factor in all cases is that the system in question uses Direct-Sequence Code Division Multiple-Access (DS/CDMA).

One hot topic, due to the rapid evolution of new services in personal and mobile communications, is the ability to support many data rates within the same system. However, this has been neglected in the research, and most work published is on single rate systems. In Chapter 2, we present some possible modulation schemes together with a comparison analysis for the DS/CDMA system.

A survey of multiuser detection for synchronous CDMA channels, corrupted by additive white Gaussian noise, is presented in Chapter 3. Furthermore, we derive a low complexity maximum likelihood optimal receiver. Several suboptimal receivers are reviewed and the advantages and disadvantages discussed.

In Chapter 4, we present a receiver, for the synchronous CDMA case, where we jointly optimize the source and channel decoders and the multiuser detector for transmission of vector quantized data. The mean square error optimal receiver, and several suboptimal versions are presented together with an analysis of the complexity and some numerical results.

1-3 CONTRIBUTIONS

The main results presented in this thesis can be summarized as:

- Different modulation schemes to support multiple data rates in a DS/CDMA system are compared. The analysis is made both for the AWGN and multipath fading channels. Previously published work include [43], [44] and [45] by Ottosson and Svensson.

- A maximum likelihood optimum receiver for the synchronous CDMA system with lower complexity than the previously known is derived (originally published by Agrell and Ottosson in [1]).
- A jointly optimized source, channel and multiuser decoder for transmission of vector quantized data over a synchronous CDMA channel is presented. This work was originally published by Skoglund and Ottosson in [61], [62] and [46].

1-4 NOTATION

Throughout this thesis we write variables in italics. However, if the variables are random, we use capital letters for the random variables and lower-case letters for their outcomes. Vectors and matrices are given in boldface, with lower-case and capital letters, for vectors and matrices, respectively. Observe, though, that we do not distinguish between deterministic and random vectors and matrices, but this will be clear from the context. Further, we let the random vectors and matrices denote both the random vectors and matrices as well as their outcomes. A few examples of the notation are:

x, y, z	Scalar variables
X, Y, Z	Random variables and their corresponding outcomes x, y, z.
$\mathbf{x}, \mathbf{y}, \mathbf{z}$	Vectors of deterministic or random variables.
$\mathbf{X}, \mathbf{Y}, \mathbf{Z}$	Matrices of deterministic or random variables.
$\{a, b, c\}$	A set consisting of the elements a, b, and c.
$\otimes$	The Kronecker product (see Appendix 4B for the definition).
$\{\mathbf{A}\}_{i,j}$	The (i,j)-th element of the matrix $\mathbf{A}$.
$\{\mathbf{A}\}_{i}$	The ith column of the matrix $\mathbf{A}$.
$\mathbf{x}^T, \mathbf{A}^T$	The transpose of the vector $\mathbf{x}$ and matrix $\mathbf{A}$, respectively.
$E[X]$	The expected value of the random variable X.
$Var[X]$	The variance of the random variable X.

CHAPTER
2

MULTIRATE SCHEMES FOR MULTIMEDIA APPLICATIONS

2-1 INTRODUCTION

In the last few years there have been much discussion on future Personal Communications Services (PCS) [30]. The existing mobile communication systems mainly support speech services. Also in future systems speech is expected to be the main service, but with higher quality than in the systems of today, and maybe in conjunction with video. Other expected services are image transmission (facsimile) with high resolution and color and video. Further, the increasing demand for information in our society requires an easy way to access and process information. Therefore, data transmission and wireless computing will be necessary services in any future system.

There have been some proposals for systems supporting PCS. They are known as Personal Communications Networks (PCN), Future Public Land Mobile Telecommunication Systems (FPLMTS) and Universal Mobile Telecommunication Systems (UMTS) [7] [12] [36] [78]. The main focus has been on the access method, and the competitors seem to be Time Division Multiple Access (TDMA) ([35], page 774) and Code Division Multiple Access (CDMA) ([35], page 789). However, in this chapter we consider Direct Sequence CDMA (DS/CDMA) as access method and focus on how to support the services in PCS. As seen from the discussion above there are many different services to support and they have very different requirements on data rate and quality of transmission. Translating this to transmission of bits, we require rates from about 10 kbps to 1 Mbps, with bit error

rates from about 10^{-2} for speech and images, depending on the type of speech and image encoders used in the system, to 10^{-6} or lower for data transmission.

There are of course many ways to design a multirate system. In the IS-95 standard [66] repetition coding is used to support different rates, but this is only practical in supporting a few rates. A more conventional way is to alter the processing gain and spread all signals, independently of the bit rate, to the same bandwidth [43] [44] [4] [8]. Furthermore, it is possible to alter the chip rate as in [75], or the modulation format [44], use multiple channels [44] [10] [64] [9] [17] or maybe combine several of these schemes. In this work we evaluate these and other schemes regarding the multirate support capabilities in Additive White Gaussian Noise (AWGN) and multipath Rayleigh fading channels.

In Section 2-2, the system models are presented together with some basic assumptions. Multirate schemes for AWGN and multipath are discussed in Section 2-3 and Section 2-4, respectively. In Section 2-5 we construct some test systems and present their performance. The conclusions are drawn in Section 2-6.

2-2 SYSTEM MODELS

Amplitude Modulated DS/CDMA Systems

Usually BPSK is used as modulation in a DS/CDMA system. In spite of this, assume that all users, independent of the bit rate, use amplitude modulation (AM) and that the multirate CDMA system supports n different rates, or subsystems. The transmitted signal of user number k, in subsystem i, then is of the form

$$s_{ik}(t) = \sqrt{2P_i}\, b_{ik}(t)\, c_{ik}(t) \cos(\omega_c t + \theta_{ik}) \tag{2-1}$$

where P_i is the power of each user in the subsystem and $b_{ik}(t)$ is a pulse amplitude modulation (PAM) signal with a rectangular pulse shape of duration T_i. Moreover, $c_{ik}(t)$ is the spreading code waveform of period N_i, consisting of chips in a binary polar format with rectangular pulse shape of duration T_c such that $T_i = N_i T_c$. That is, short spreading codes are used.

The modulator phases θ_{ik} are modeled as independent random variables, uniformly distributed over $[0, 2\pi)$. Using the assumption of an AWGN channel, and asynchronous transmission, the received signal can be modeled as

$$r(t) = w(t) + \sum_{i=1}^{n} \sum_{k=1}^{K_i} s_{ik}(t - \tau_{ik}) \tag{2-2}$$

where $w(t)$ is zero-mean white Gaussian noise, with double-sided spectral density $N_0/2$, K_i the number of users in subsystem i and τ_{ik} are the delays, modeled as independent random variables, uniformly distributed over $[0, T_i)$.

For simplicity a correlation (matched filter) receiver is used[1], and therefore the output of the lth receiver in subsystem j can be written as

$$Z_{jl} = \int_0^{T_j} r(t)\, c_{jl}(t) \cos(\omega_c t)\, dt \tag{2-3}$$

assuming without loss of generality that θ_{jl} and τ_{jl} is zero, because we are only interested in the relative phase and time differences between the users. In calculation of Z_{jl} we see that different parts can be identified as

$$Z_{jl} = \sqrt{\frac{P_j}{2}} T_j (b_{jl}^{(0)} + I_{jl} + W_j) \tag{2-4}$$

where $b_{jl}^{(0)}$ is the transmitted symbol and W_j is the Gaussian noise term with zero-mean and variance $N_0/2E_j$. Here E_j is the average energy per symbol and user in the jth subsystem. The interference from the other users, in all subsystems is

$$I_{jl} = \sum_{\substack{i=1 \\ i \neq j,\, k \neq l}}^{n} \sum_{k=1}^{K_i} \frac{1}{T_j} \sqrt{\frac{P_i}{P_j}} \int_0^{T_j} b_{ik}(t - \tau_{ik})\, c_{ik}(t - \tau_{ik})\, c_{jl}(t) \cos\varphi_{ik} dt \tag{2-5}$$

where $\varphi_{ik} = \theta_{ik} - \omega_c \tau_{ik}$.

1. The sufficient statistics are a bank of filters matched to each of the spreading sequences [73].

Quadrature Amplitude Modulated DS/CDMA Systems

It is sometimes convenient to transmit information in quadrature format, to increase the data throughput. We can therefore reformulate our model above such that the transmitted signal of user k in the subsystem i is

$$\begin{aligned} s_{ik}(t) \;=\; & \sqrt{2P_i}\, b_{ik}^{I}(t)\, c_{ik}^{I}(t) \cos(\omega_c t + \theta_{ik}) \;+ \\ & \sqrt{2P_i}\, b_{ik}^{Q}(t)\, c_{ik}^{Q}(t) \sin(\omega_c t + \theta_{ik}) \end{aligned} \tag{2-6}$$

where $b_{ik}^{I}(t)$ and $b_{ik}^{Q}(t)$ are the In-phase and Quadrature-phase PAM signals, each with a rectangular pulse shape of duration T_i. The spreading code waveforms, $c_{ik}^{I}(t)$ and $c_{ik}^{Q}(t)$ of period N_i, consisting of chips in binary polar format and rectangular pulse shapes of duration T_c. Therefore, the decision variables now depend on both the In-phase and the Quadrature-phase components of the other users and are given by

$$\begin{cases} Z_{jl}^{I} \;=\; \displaystyle\int_0^{T_j} r(t)\, c_{jl}^{I}(t) \cos(\omega_c t)\, dt \;=\; \sqrt{\frac{P_j}{2}}\, T_j \left(b_{jl}^{I(0)} + I_{jl}^{I} + W_j^{I}\right) \\ Z_{jl}^{Q} \;=\; \displaystyle\int_0^{T_j} r(t)\, c_{jl}^{Q}(t) \sin(\omega_c t)\, dt \;=\; \sqrt{\frac{P_j}{2}}\, T_j \left(b_{jl}^{Q(0)} + I_{jl}^{Q} + W_j^{Q}\right) \end{cases} \tag{2-7}$$

Here I_{jl}^{I} and I_{jl}^{Q} are the interference from the other users onto the In-phase and Quadrature-phase components given as

$$I_{jl}^{I} = \sum_{\substack{i=1 \\ i \neq j,\, k \neq l}}^{n} \sum_{k=1}^{K_i} \frac{1}{T_j} \sqrt{\frac{P_i}{P_j}} \cdot \left\{ \int_0^{T_j} b_{ik}^{I}(t-\tau_{ik})\, c_{ik}^{I}(t-\tau_{ik})\, c_{jl}^{I}(t) \cos\varphi_{ik} dt + \right. \tag{2-8}$$

$$\left. \int_0^{T_j} b_{ik}^{Q}(t-\tau_{ik})\, c_{ik}^{Q}(t-\tau_{ik})\, c_{jl}^{I}(t) \sin\varphi_{ik} dt \right\}$$

$$I_{jl}^{Q} = \sum_{\substack{i=1 \\ i \neq j,\, k \neq l}}^{n} \sum_{k=1}^{K_i} \frac{1}{T_j} \sqrt{\frac{P_i}{P_j}} \cdot \left\{ \int_0^{T_j} b_{ik}^{Q}(t-\tau_{ik})\, c_{ik}^{Q}(t-\tau_{ik})\, c_{jl}^{Q}(t) \cos\varphi_{ik} dt + \right.$$

$$\left. \int_0^{T_j} b_{ik}^{I}(t-\tau_{ik})\, c_{ik}^{I}(t-\tau_{ik})\, c_{jl}^{Q}(t) \sin\varphi_{ik} dt \right\}$$

and the AWGN noise components are denoted W_j^I and W_j^Q, respectively.

2-3 PERFORMANCE IN AWGN CHANNELS

Multi-Modulation Systems

The performance of a BPSK single rate system ($n = 1$) with K users and processing gain N can be approximated by assuming that the interference is Gaussian with zero mean. This approximation has been proven to be very accurate for low signal-to-noise ratios and many users, or alternatively for few users but with a high processing gain [18] [19]. In addition, this approximation is more accurate for amplitude modulation using many levels (see Appendix 2C and [45]). It is observed, though, that the approximation is generally slightly optimistic. With this approximation, the bit error probability can be written as (see Appendix 2A and [50])

$$P_b = Q\left(\left[\frac{N_0}{2E_b} + \frac{K-1}{3N} \right]^{-1/2} \right) \tag{2-9}$$

where

$$Q(x) = (1/\sqrt{2\pi}) \int_x^\infty \exp(-z^2/2)\, dz. \tag{2-10}$$

For a QPSK system the expression is

$$P_b = Q\left(\left[\frac{N_0}{2E_b} + \frac{2(K-1)}{3N} \right]^{-1/2} \right). \tag{2-11}$$

This can be reformulated for squared lattice M-ary Quadrature modulation schemes to express the symbol error probability for each quadrature phase (I and Q) as

$$P_e^{I/Q} = 2\frac{(\sqrt{M}-1)}{\sqrt{M}} Q\left(\left[\frac{M-1}{3} \left(\frac{N_0}{E} + \frac{2(K-1)}{3N} \right) \right]^{-1/2} \right) \tag{2-12}$$

where E is the average signal-to-noise ratio per symbol. After the observation that the I and Q quadrature phases are independent, the bit error probability for high signal-to-noise ratios can be approximated to

$$P_b \approx \frac{2P_e^{I/Q} - (P_e^{I/Q})^2}{\log_2(M)}. \tag{2-13}$$

Now assume a *multi-modulation system* with n rates $R_1 > R_2 > \ldots > R_n$, where all users have the same symbol rate, signal-to-noise ratio per bit and processing gain $N = B/R_n$. Here B is the system bandwidth and R_n is the bit rate for the BPSK users. The performance of an M-ary QAM user in subsystem j then is (Appendix 2A)

$$P_{e,jl}^{I/Q} = 2\frac{(\sqrt{M}-1)}{\sqrt{M}} Q\left(\left[\frac{M_j-1}{3} \left(\frac{N_0}{\log(M_j) E_b} + \frac{2}{3N} \left(\sum_{i=1}^{n} \frac{R_i}{R_j} \cdot K_i - 1 \right) \right) \right]^{-1/2} \right) \tag{2-14}$$

where R_i is the bit rate of subsystem i and K_i is the number of users in the ith subsystem. The modulation level, that is, the number of symbols in the signal space, is controlled by the bit rate and is given by

$$M_j = 2^{(R_j/R_n)}. \tag{2-15}$$

However, if the subsystem j is a BPSK system the performance is

$$P_{b_{jl}} = Q\left(\left[\frac{N_0}{2E_b} + \frac{1}{3N}\left(\sum_{i=1}^{n} \frac{R_i}{R_j} \cdot K_i - 1 \right) \right]^{-1/2} \right). \tag{2-16}$$

To understand these formulas, observe that we assume that all users have the same signal-to-noise ratio per bit E_b/N_0, and that the average symbol energy ratio between subsystem i and subsystem j is given by

$$\frac{E_i}{E_j} = \frac{(R_i/R_1)\,E_b}{(R_j/R_1)\,E_b} = \frac{R_i}{R_j}. \tag{2-17}$$

Since all users have the same signal-to-noise ratio per bit the transmitted powers will be different for different rates. Thus, users with very high rates transmit with higher power than the low rate users. In situations where a high rate user is near the base-station and the low rate user far away, the low-rate user has a much lower power at the receiver than the high rate user, due to the cross-correlation between the user codes. This is called the *near-far effect.* Nevertheless, if all users should transmit at the same power, the performance for high rate users would degrade significantly compared to the low rate users, due to their low E_b/N_0 in this case.

Multi Processing-Gain Systems

The most natural way, or at least the most conventional way, to achieve multirate is to vary the processing gain, and accordingly spread all users independently of their bit rates to the same bandwidth B. The European RACE project CODIT [4] use this type of multirate scheme in combination with several chip rates.

We assume a *multi processing-gain system* where all users use BPSK modulation and a constant chip period T_c. Also, assume that the subsystems are ordered in descending bit rate order. That is, the bit rates are ordered as $R_1 > R_2 > \ldots > R_n$ with the corresponding processing gains $N_i = B/R_i$. In addition, assume that all bit rates are multiples of the lowest rate R_n and that the powers P_i are such that all users in all subsystems transmit at same signal-to-noise ratio per bit E_{b_i}, that is,

$$E_{b_1} = P_1 T_1 = \ldots = E_{b_n} = P_n T_n. \tag{2-18}$$

Note that this assumption, as in the multi-modulation system, causes near-far effects, because the powers from the different users depend on the bit rate. If, however, all users have the same power, the performance degrades for the high bit rate users, due to their low E_b/N_0. The performance of user l with rate R_l in a BPSK modulated system may be expressed as (Appendix 2A)

$$P_{b_{jl}} = Q\left(\left[\frac{N_0}{2E_b} + \frac{1}{3N_j}\left(\sum_{i=1}^{n} \frac{R_i}{R_j} \cdot K_i - 1 \right) \right]^{-1/2} \right). \tag{2-19}$$

It is easy to see this result if we recognize that $R_i/R_j = P_i/P_j$ and therefore the interference from the other subsystems is weighted according to their transmitted powers. The correlation properties between the different spreading codes of the users remain the same, independent of the period N_i, because random codes and equal chip rates are assumed. Observe that the performance is the same as for the BPSK rates in a multi-modulation scheme (see (2-16)) if $N_j = N$.

Multi-Channel Systems

As we shall see later, QPSK is the most efficient modulation scheme. A conclusion of this is that many QPSK channels in parallel can be used to achieve a high data rate. This is called the multi-channel scheme.

Assume a *multi-channel system* with constant processing gain N and chip period T_c. Moreover, assume that the modulation is QPSK for all users and that all users transmit at the same signal-to-noise ratio per bit, which in this case does not lead to near-far effects, because all channels transmit at the same power. The bit error performance for such a system is very easily derived, because all QPSK channels have the same performance if all channels and users are transmitted asynchronously. Therefore, we get from (2-11)

$$P_{b_{jl}} = Q\left(\left[\frac{N_0}{2E_b} + \frac{2}{3N}\left(\sum_{i=1}^{n} \frac{R_i}{R_0} K_i - 1 \right) \right]^{-1/2} \right) \tag{2-20}$$

where R_0 is the bit rate for a single QPSK channel and N the processing gain such that $NR_0 = B$. Notice that the performance is about the same as for the multi processing-gain scheme. The result of a practical multi-chan-

nel system is slightly better than this, because the parallel channels of each user would be transmitted synchronous and, therefore, have good cross-correlation properties. If, for example, the codes are orthogonal at zero time-shifts (synchronous) and have random properties for all other shifts, the bit error rate would decrease to

$$P_{b_{jl}} = Q\left(\left[\frac{N_0}{2E_b} + \frac{2}{3N}\left(\sum_{i=1}^{n} \frac{R_i}{R_0} K_i - \frac{R_j}{R_0} \right) \right]^{-1/2} \right). \tag{2-21}$$

Codes with these properties can indeed be constructed. Walsh-Hadamard codes and Orthogonal Gold codes [65], for example, fulfill such requirements. The Orthogonal Gold codes are constructed by adding the chip symbol +1 to the end of each Gold sequence.

A drawback of this scheme, though, is the need for linear amplifiers also in the mobile, caused by the summation of many parallel channels. Usually, the linearity is measured by the *Peak-to-Mean Envelope Power Ratio* (PMEPR), and it can be shown assuming random codes (see Appendix 2B) that PMEPR $= R_i/R_0$, that is, linear with the number of parallel channels. The same type of linearity problem arises in multi-carrier systems [5], but here the number of channels may be in the order of a 1000 or more. It would of course be possible to precode the data in a such a way that the envelope variations decrease, that is, avoid sequences of data with a high peak envelope power.

Multi Chip-Rate Systems

The use of spreading results in a processing gain that suppresses external interference. In the use of a multi processing-gain system, this suppression level is not constant. Therefore, all users do not accomplish the same bandwidth efficiency. A way to accomplish a multirate system that has a constant processing gain, is to let the bit rate change the chip-rate [75]. Hence a *multi chip-rate system* is achieved. This means that users with different rates have different bandwidths and therefore we can, by the use of Frequency Division Multiplex (FDM), squeeze many such subsystems within the system bandwidth. It has been shown [75] that this scheme outperforms the multi processing-gain scheme in a synchronous CDMA system over an AWGN channel. But, the condition of that comparison was no sidelobes in the spectrum of a subsystem, that is, ideal frequency compression of subsystems.

Also, the comparison was done in an AWGN channel and consequently any diversity gain for wideband channels is neglected. (It has been shown that a wideband system performs better than a FDM combined narrowband system [14][27] due to the utilization of RAKE diversity on frequency selective channels). Thus, drawbacks of the multi chip-rate scheme are: more complex frequency management and increased technology complexity because the transmitters and receivers need filters with several bandwidths. Furthermore, a multiuser detector may be more complex to implement. All things considered, the performance of the multi-chip scheme will significantly degrade in a more realistic comparison and the system and technology complexity may be inhibiting in realizing such a system.

Miscellaneous Multirate Schemes

There are other possible schemes that are not discussed above. *Parallel Combinatory Spread Spectrum* (PC/SS) [76][53] is a scheme where each user have a set of P sequences to choose from and use k data bits to select r sequences and then BPSK modulate r bits onto these sequences. This gives the following expression

$$k = r + \log_2\binom{P}{r} \tag{2-22}$$

for the number of input bits. If, for example, $P = N = 128$ and $r = 2N/3$, we get $k = 1.56N$ and the system can transmit more bits than the sequence length. Thus, PC/SS is useful for high rate transmission. Disadvantages are the high complexity, due to the need of P matched filters for each user and that very few users and bit rates could be supported, because each user consume many sequences. Furthermore, the detection of which of the sequences that are used at a specific time is very sensitive to channel noise and ought therefore to be protected using error correction encoding.

Another possibility is to transmit the information as *Pulse Position Modulation* (PPM) [42]. Assume, as earlier, that the sequence length is N and that there are M possible time slots to choose from. The rate of the system is then given by

$$R_{PPM} = \frac{\log_2(M)}{M + N - 1} \cdot \frac{1}{T_c} \tag{2-23}$$

and the system can transmit more than one bit per N chips. If the number of available slots vary with the bit rate we get a multirate scheme. However, a difficulty is that this system is very sensitive to multipath propagation and can not utilize the frequency selective fading of a wideband signal in a RAKE receiver.

2-4 PERFORMANCE IN MULTIPATH RAYLEIGH FADING CHANNELS

Channel Model

One of the advantages of DS/CDMA is the possibility to resolve and detect propagation paths and therefore achieve diversity gain. This is usually done in a RAKE receiver. The number of resolvable paths L_{max} can be estimated to be [31]

$$L_{max} \leq \frac{\Delta}{T_c} + 1 \tag{2-24}$$

where Δ is the delay spread of the channel, and T_c is the chip period. A typical value of the delay spread is $3\ \mu s$ for urban areas. We can therefore expect that a narrowband CDMA channel of about 1 MHz will have at least 2 paths, but a wideband channel of about 5 to 6 MHz will have 3 or more paths. As a result, the channel can be modeled as a discrete channel with random delays and Rayleigh fading amplitudes as

$$h_{jl}(t) = \sum_{m=1}^{L} \alpha_{jl,m} \delta(t - \tau_{jl,m}) e^{j\theta_{jl,m}} \tag{2-25}$$

where, for the mth path of user l in subsystem j, $\alpha_{jl,m}$ is the Rayleigh fading amplitude, $\tau_{jl,m}$ is the delay, assumed uniformly distributed on $[0, T_j)$, and $\theta_{jl,m}$ is the channel phase assumed uniformly distributed on $[0, 2\pi)$. Furthermore, L is the number of received paths, such that $L \leq L_{max}$.

Performance Without Diversity Reception

If we, as above, approximate the interference as Gaussian, it can be shown [31] that the performance is equivalent to the performance of a system with $K_i L$ users in each subsystem, and with Rayleigh fading amplitudes. Therefore, we can use the previously derived formulas for the performance on a single path given the amplitudes. In a single-rate BPSK system the performance without a RAKE receiver and antenna diversity is

$$P_b(\alpha_1) = Q\left(\left(\alpha_1^{-2}\left[\frac{N_0}{2E_b} + \frac{LK-1}{3N}\mathrm{E}[\alpha^2]\right]\right)^{-1/2}\right) \tag{2-26}$$

where α_1 is the Rayleigh fading amplitude of the first path of the desired user and $\mathrm{E}[\alpha^2]$ is the expected signal strength. The performance is then given by averaging over the fading. For convenience, we use known results for the performance of BPSK on a Rayleigh fading channel. We identify the bit error probability given the amplitude $P_b(\alpha_1)$ with the bit error rate for a single user BPSK given the fading amplitude $P_b(\gamma) = Q(\sqrt{2\gamma})$. Equality between the arguments are obtained when

$$\gamma = \frac{1}{2} \cdot \frac{\alpha_1^2}{\dfrac{N_0}{2E_b} + \dfrac{LK-1}{3N}\mathrm{E}[\alpha^2]} \tag{2-27}$$

and by observing that α_1^2 is exponentially distributed we see that γ is exponentially distributed with the expected signal strength

$$\bar{\gamma} = E[\gamma] = \frac{1}{2}\left(\frac{N_0}{2\bar{E}_b} + \frac{LK-1}{3N}\right)^{-1}. \tag{2-28}$$

Consequently, the bit error performance is given through integrating as [49]

$$P_b = \int_0^\infty P_b(\gamma)\frac{1}{\bar{\gamma}}e^{-\gamma/\bar{\gamma}}d\gamma = \frac{1}{2}\cdot\left(1 - \sqrt{\frac{\bar{\gamma}}{1+\bar{\gamma}}}\right) \tag{2-29}$$

In a similar way it is possible to obtain the performance of user l in subsystem j for the multirate schemes proposed if γ is replaced with $\gamma_{jl,m}$ and P_b with $P_{b_{jl}}$ in the formulas above. Observe, though, that for M-ary QAM in the multi-modulation scheme we first have to find the symbol error per-

formance for each quadrature phase symbol (I and Q) $P_{e_{jl}}^{I/Q}(\gamma_{jl,m})$. Accordingly, we identify the performance with

$$P_{e_{ik}}^{I/Q}(\gamma_{ik,l}) = 2\frac{(\sqrt{M}-1)}{\sqrt{M}}Q(\sqrt{2\gamma_{ik,l}}) . \tag{2-30}$$

The equivalent expected signal-to-noise interference ratio $\bar{\gamma}_{jl,m}$ per path and user number l in subsystem j in an L-path Rayleigh fading channel is found in Table 2-1 for the different multirate schemes. Also, note that the performance on a Rayleigh fading channel for M-ary QAM, in contrast to BPSK and QPSK, is

Table 2-1. Equivalent average signal-to-interference level $\bar{\gamma}_{jl,m}$.

Scheme	Average signal-to-interference $\bar{\gamma}_{ik,l}$
Multi-Modulation	$\bar{\gamma}_{jl,m} = \frac{1}{2}\left[\frac{M-1}{3}\left(\frac{N_0}{\log(M)\bar{E}_b} + \frac{2}{3N}\left(\sum_{i=1}^{n}\frac{R_i}{R_j}\cdot K_i L - 1\right)\right)\right]^{-1}$
Multi Processing-Gain	$\bar{\gamma}_{jl,m} = \frac{1}{2}\left[\frac{N_0}{2\bar{E}_b} + \frac{1}{3N_j}\left(\sum_{i=1}^{n}\frac{R_i}{R_j}\cdot K_i L - 1\right)\right]^{-1}$
Multi-Channel	$\bar{\gamma}_{jl,m} = \frac{1}{2}\left[\frac{N_0}{2\bar{E}_b} + \frac{2}{3N}\left(\sum_{i=1}^{n}\frac{R_i}{R_0}K_i L - 1\right)\right]^{-1}$
Multi-Channel (orthogonal codes)	$\bar{\gamma}_{jl,m} = \frac{1}{2}\left[\frac{N_0}{2\bar{E}_b} + \frac{2}{3N}\left(\sum_{i=1}^{n}\frac{R_i}{R_0}K_i L - \frac{R_j}{R_0}\right)\right]^{-1}$

$$P_{e_{jl}}^{I/Q} = \frac{(\sqrt{M}-1)}{\sqrt{M}}\left(1 - \sqrt{\frac{\bar{\gamma}_{jl,m}}{1+\bar{\gamma}_{jl,m}}}\right). \tag{2-31}$$

Performance of Diversity Receivers using Maximum Ratio Combining

To increase the rather bad system performance on an multipath Rayleigh fading channel, diversity can be used. Thus, several approximately independent copies of the same information must be found. In a DS/CDMA system the different paths in the multipath propagation can be used and combined in a suitable way (RAKE receiver). It is also possible to obtain diversity with multiple receiving antennas. The optimum solution for maximum sig-

nal-to-noise ratio at the output of the receiver is to combine them according to the complex (amplitude and phase) channel gain as in the *maximum ratio combining* (MRC). Hence, we have to estimate the multipath channel. With the use of the results in [31] [49] we can generalize the bit error performance for BPSK and QPSK and the symbol error performance for each quadrature phase (I and Q) for M-ary QAM as

$$P_{e_{jl}}^{I/Q} = A \cdot P_{b_{jl}}(\bar{\gamma}_{jl,m}) \sum_{n=0}^{D-1} \binom{D-1+n}{n} [1 - P_{b_{jl}}(\bar{\gamma}_{jl,m})]^n \qquad (2\text{-}32)$$

where $P_{b_{jl}}(\bar{\gamma}_{jl,m})$ is given by (2-29), $\bar{\gamma}_{jl,m}$ is the average signal-to-interference level per received path and D is the number of paths that are combined in the receiver. Furthermore, A is a constant that depends on the modulation. For BPSK and QPSK, $A = 1$, but for M-ary QAM, $A = 2(\sqrt{M} - 1)/\sqrt{M}$. The received average signal-to-interference level is given by

$$\bar{\gamma}_{jl} = \bar{\gamma}_{jl,m} \cdot D. \qquad (2\text{-}33)$$

Performance of Diversity Receivers using Selection Combining

Selection combining (SC) means that only the best path, that is the path with the highest signal-to-noise ratio of D received paths is chosen. Thus, the performance is worse than that of MRC. On the other hand the receiver only needs to estimate the path strengths, which yields a less complex receiver. The performance can be found in [31] and is given by

$$P_{b_{jl}} = D \sum_{n=0}^{D-1} \binom{D-1}{n} P_{b_{jl}}\left(\frac{\bar{\gamma}_{jl,m}}{1+n}\right) \qquad (2\text{-}34)$$

for BPSK and QPSK. For M-ary QAM the symbol error rate for the I and Q quadrature phases is

$$P_{e_{jl}}^{I/Q} = D \sum_{n=0}^{D-1} \binom{D-1}{n} P_{e_{jl}}^{I/Q}\left(\frac{\bar{\gamma}_{jl,m}}{1+n}\right) \qquad (2\text{-}35)$$

where $P_{e_{jl}}^{I/Q}(\bar{\gamma}_{jl,m}/(1+n))$ is given by (2-30). Here the received average signal-to-interference level is

$$\bar{\gamma}_{jl} = \bar{\gamma}_{jl,m} \cdot \sum_{d=1}^{D} \frac{1}{d}. \tag{2-36}$$

2-5 NUMERICAL RESULTS

In the following examples we have, if not stated otherwise, used the Gaussian approximations found above. To validate the accuracy of the Gaussian approximation we have simulated some of the systems and compared the results. In general, we can see that the approximations are fairly good, especially for low signal-to-noise ratios and many users. As we will note, however, the approximations are slightly optimistic.

In the evaluation of a multi-modulation scheme, we first calculate the performance of various modulations in a single rate system. The assumptions are random sequences, processing gain $N = 128$ and AWGN channel. The results are shown in Figure 2-1. We see that BPSK and QPSK have almost the same performance and that these modulation formats perform much better than 16-QAM. This is due to the fact that 16-QAM is worse than BPSK and QPSK in a single user AWGN channel (about 4-5 dB). In the case of a CDMA channel, with non-orthogonal user codes, the powers of the interfering users cross-couple to the user of interest. Hence, the performance is even worse for 16-QAM on a CDMA channel using a matched filter receiver. Furthermore, as seen in the figure, QPSK is slightly better than BPSK. The reason for this is that the comparison is made for constant throughput i.e., the number of QPSK users is only half of the number of BPSK users. Hence, each of the K users of BPSK type are disturbed by $K-1$ users. In the QPSK case, the interfering users quadrature phase symbols can be seen as equivalent BPSK users with the same power as in the BPSK system. Thus, each of the phases of the $K/2$ QPSK users are disturbed by $(K/2-1)\cdot 2 = K-2$ equivalent BPSK users, resulting in slightly lower interference power level for the QPSK system. These results indicate that the suggested multi-modulation scheme is inefficient in achieving multirate.

Another possibility for multirate system design is the multi processing-gain scheme. To evaluate the performance of such a system we first compare the Gaussian approximation with a simulated system in a AWGN channel. We

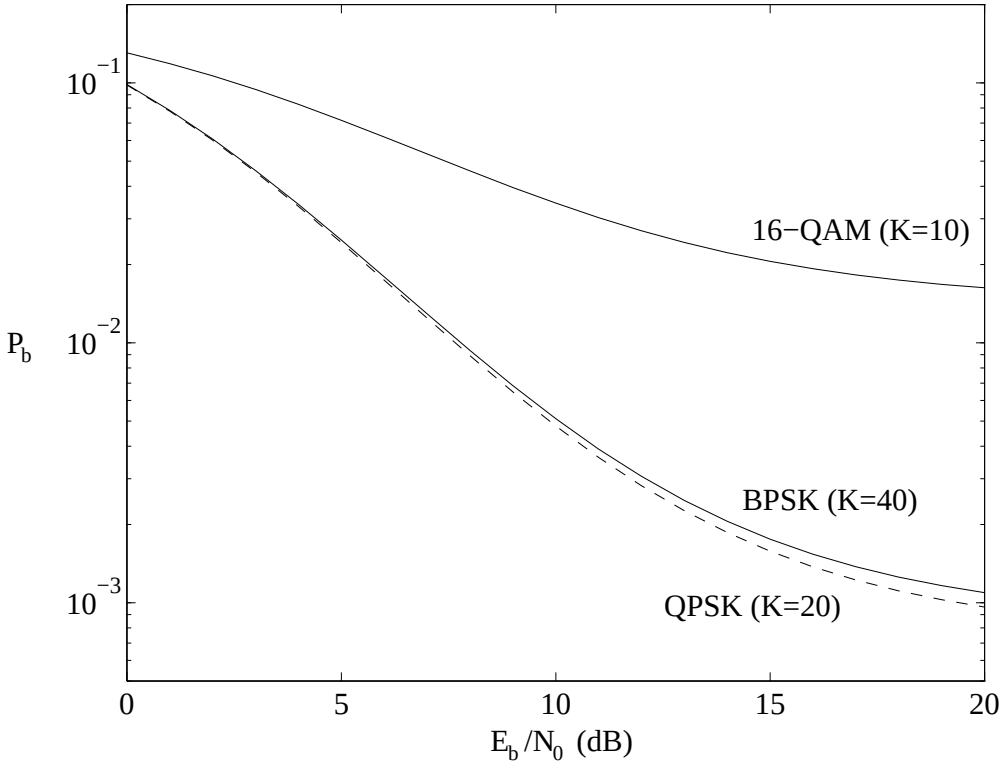

Figure 2-1. Comparison of different single-rate modulation formats in an AWGN channel. Random sequences and processing gain $N = 128$ are used. K is the number of users in the system.

use $N_1 = 64$ and $N_2 = 128$ as processing gains, that is, subsystem 1 have two times higher data rate than subsystem 2. The number of users is $K_1 = 5$ in subsystem 1 and $K_2 = 10$ in subsystem 2, and random codes are used. The results are shown in Figure 2-2. We see a discrepancy of about 1 dB at high signal-to-noise ratios between the simulated and calculated performance. The relative performance between the subsystem 1 and subsystem 2 users remain the same though.

To compare the different multirate schemes we have constructed test systems according to Table 2-2. Firstly, we present results for SYSTEM II, where we compare the multi processing-gain scheme, the multi-channel scheme and the multi-modulation scheme for an AWGN channel, using the Gaussian approximation. For the multi processing-gain scheme the processing gain is set to $N_i = B/R_i$, where the system bandwidth is $B = R_0 N_{max}$ and $N_{max} = 256$. Translating this to a multi-modulation scheme we get the processing gain $N = N_{max}$. In the multi-channel scheme, however, the processing gain is $N = 2N_{max}$, because R_0 is the bit rate for a QPSK channel

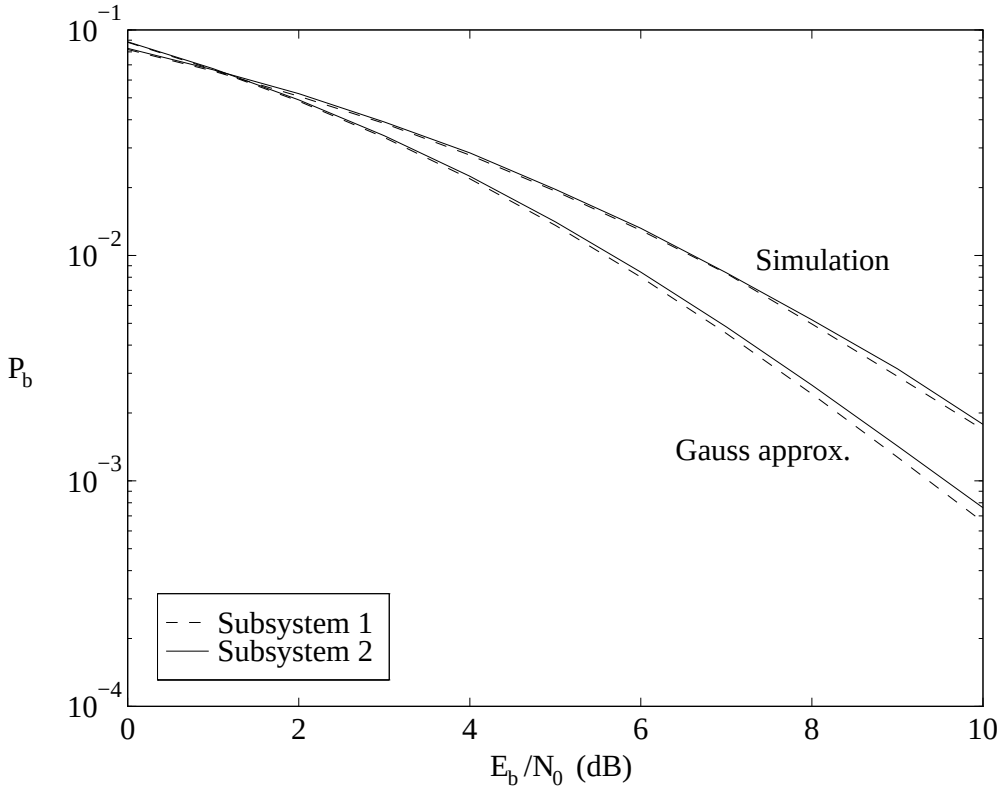

Figure 2-2. Comparison between the Gaussian approximation and a simulation of a multi processing-gain system with $N_1 = 64$ and $N_2 = 128$ in an AWGN channel. The number of users are $K_1 = 5$ and $K_2 = 10$ in subsystem 1 and 2, respectively.

Table 2-2. Test systems for multirate evaluation.

System	Bandwidth	Bit rates
SYSTEM I	B	$R_2 = R_0, R_1 = 2R_0$
SYSTEM II	B	$R_3 = R_0, R_2 = 2R_0, R_1 = 4R_0$

and therefore the symbol rate is $R_0/2$. For a summary of these constructions see Table 2-3. In Figure 2-3, we see that the multi processing-gain scheme and the multi-channel scheme have almost the same performance. The multi-channel scheme has the highest processing gain $N = 512$ and therefore suppression level. The multi-modulation scheme has much worse performance for the higher levels of modulation, here 16-QAM. Observe, though, that the users using BPSK and QPSK have the same performance as the users in the other schemes with the same rates as for the BPSK and QPSK users. This means that the high rate users have worse performance

Table 2-3. Summary of the different multirate scheme constructions.

Parameter	**Multi-Modulation Scheme**	**Multi Processing-Gain Scheme**	**Multi-Channel Scheme**
Bandwidth	$B = R_n N_{max}$	$B = R_0 N_{max}$	$B = (R_0/2)\,N$
Modulation	BPSK/M-ary QAM $M_j = 2^{(R_j/R_n)}$	BPSK	QPSK
Symbol rate	R_n	R_i	$R_0/2$
Processing gain	$N = N_{max}$	$N_i = B/R_i$	$N = 2N_{max}$

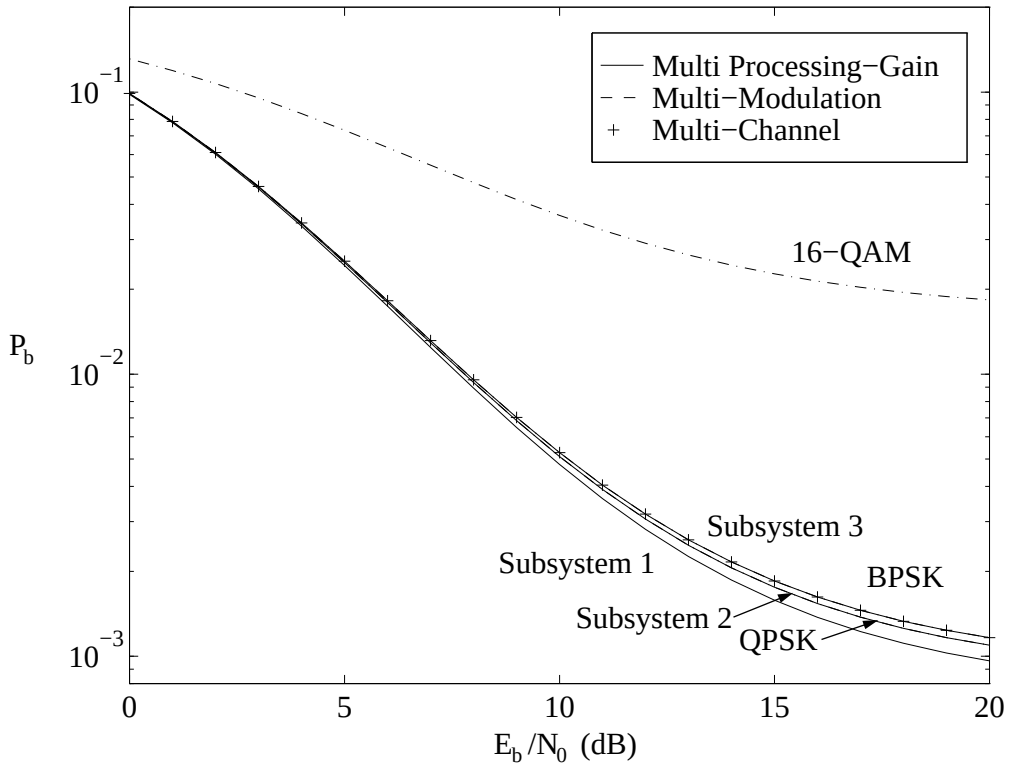

Figure 2-3. Performance of various multirate schemes for SYSTEM II in an AWGN channel. Observe that “BPSK”, “QPSK”, and “16-QAM” denotes the performance of the different rate users of the multi-modulation scheme. Further “Subsystem 1”, “Subsystem 2” and “Subsystem 3” denotes multi processing-gain performance for bit rate R_1, R_2 and R_3, respectively. There exist $K_1 = 5$, $K_2 = 10$ and $K_3 = 40$ users in subsystem 1, 2, and 3, respectively.

than the low rate users. In spite of this appealing property we conclude that the multi-modulation scheme has a low multirate support. It would of course be possible to increase the energy for the higher rates to decrease the bit error probability to a certain level. However, this will increase the bit error rate for the other users.

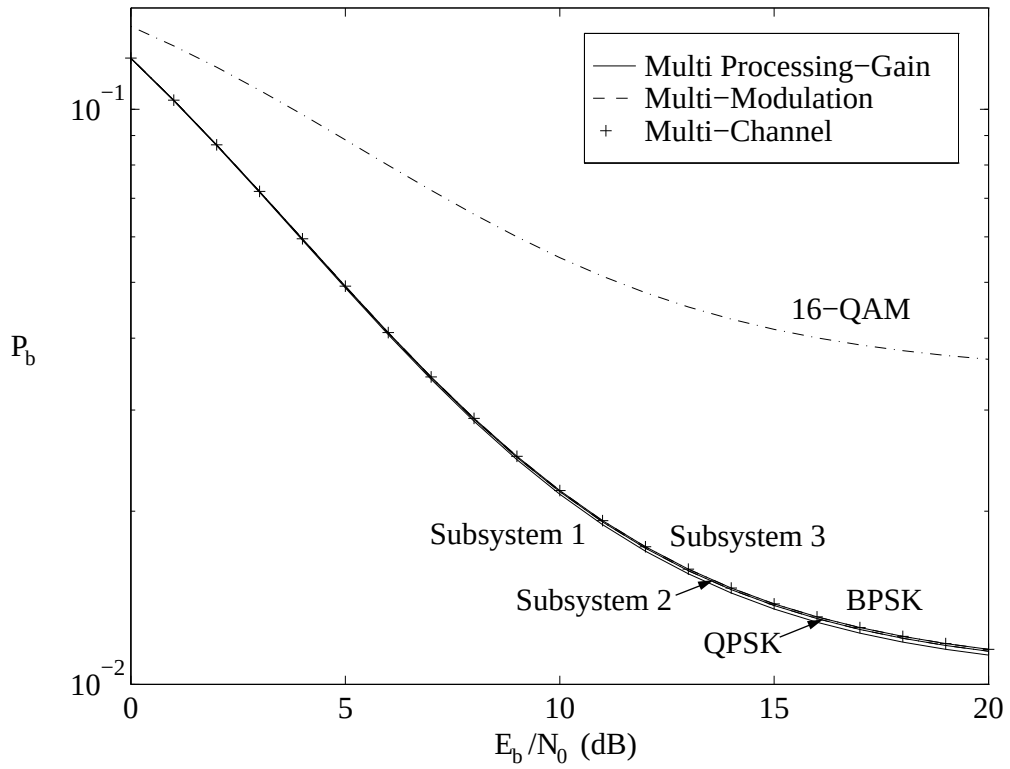

Figure 2-4. Performance of various multirate schemes for SYSTEM II in a multipath Rayleigh fading channel with $L = 3$ paths and MRC diversity. Observe that "BPSK" and "16-QAM" denotes the performance of the different rate users in the multi-modulation scheme. The "QPSK" user performance curve is almost on top of the "BPSK" curve. Further "Subsystem 1", "Subsystem 2" and "Subsystem 3" denotes multi processing-gain performance for bit rate R_1, R_2 and R_3, respectively. There exist $K_1 = 5$, $K_2 = 10$ and $K_3 = 40$ users in subsystem 1, 2, and 3, respectively.

As stated, the performance of the multi processing-gain and the multi-channel scheme is about the same. Nonetheless, in a more realistic comparison we have to know the available system bandwidth and the amount of external interference in the frequency band to make a fair comparison. In addition, there is a dependence on the amount of intersymbol interference (ISI) in the system, which of course depends on the symbol rate. In a multi-channel scheme the symbol rate is low and therefore we can neglect the ISI, but for

high bit rates in the multi processing-gain scheme, the ISI will degrade the performance.

The performance on multipath fading channels depends mainly on the system bandwidth and the type of diversity used. In Figure 2-4, the performance of the same system as in Figure 2-3, but in multipath fading with $L = 3$ paths, MRC diversity and average power control, is shown. As seen, the performance degrades significantly in fading but the relations between the different multirate schemes remain the same. To investigate the difference between narrowband and wideband CDMA channels further, we assume a Rayleigh fading channel with 2 or 3 paths, representing a narrowband and wideband CDMA channel, respectively. Furthermore, assume a RAKE receiver using maximum ratio combining or selection combining. The performance is measured in terms of the number of supported high rate users K_1 given the number of low rate users K_2 for SYSTEM I. We only consider the multi processing-gain scheme since the multi-channel scheme has about the same performance. In Figure 2-5 we show the number of sup-

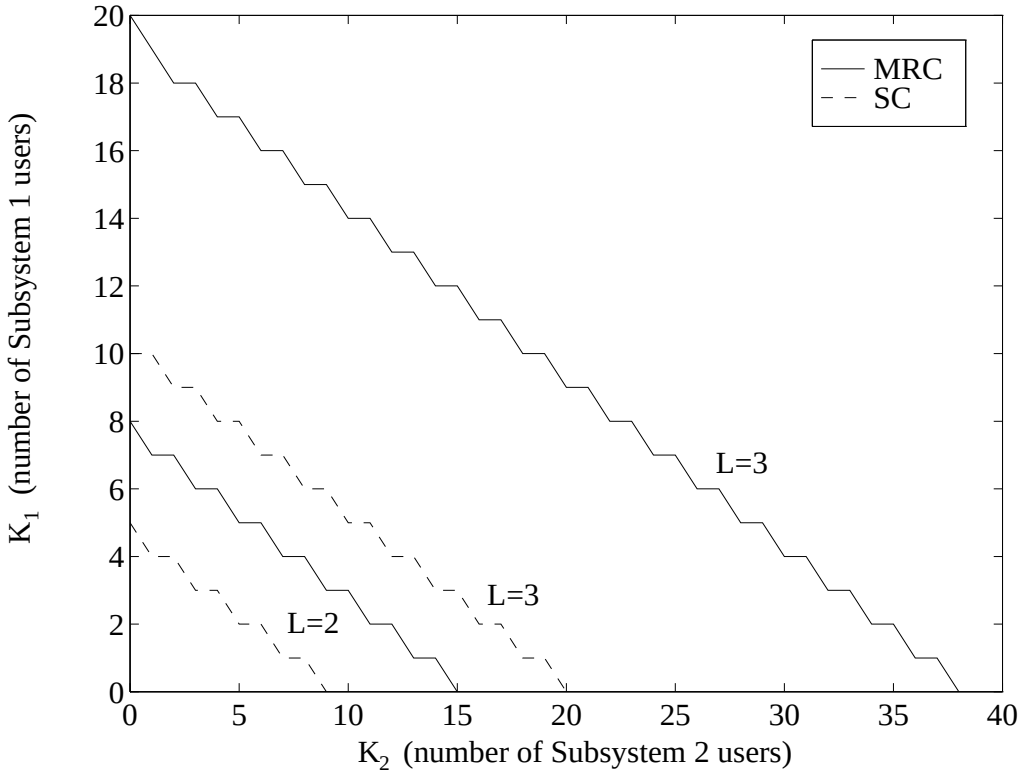

Figure 2-5. Performance of SYSTEM I for the multi processing-gain scheme. The processing gain is $N_{max} = 256$ and the channel is a multipath Rayleigh fading channel with $L = 2$ or $L = 3$ paths. RAKE receiver diversity with MRC and SC. The signal-to-noise ratio for all users is $E_b/N_0 = 10$ dB and the bit error probability upper bound is $P_b \leq 10^{-2}$.

ported users of subsystem 1 and 2, respectively, in order for the bit error probability to be at $P_b \leq 10^{-2}$ when $E_b/N_0 = 10$ dB. Notice that if a 2 path channel is assumed there is not much to gain in using an MRC receiver, but if 3 paths is assumed, the MRC receiver has about twice the capacity of the SC receiver. The conclusion is therefore that the number of paths is very critical to achieve good performance with a RAKE receiver, and that there should be at least 3 paths to use maximum ratio combining. In a narrowband system, that is, a bandwidth of about 1 MHz it is maybe possible to get a two path channel, but in a wideband channel with a bandwidth greater than 6 MHz, we expect that 3 or more paths will be present in the propagation at all times, assuming an urban environment.

2-6 CONCLUSIONS

We have investigated several multirate schemes for a DS/CDMA system and found that the use of multi processing-gain and multi-channel schemes give almost the same performance, both in AWGN and multipath fading channels. Moreover, we have seen that it is possible to use a multi-modulation scheme, which only degrades the performance for the users with high data rates, that is, users that use higher level of modulation than QPSK. If the system is to support many data rates up to about 1 Mbps, a multi processing-gain system will only has a small processing gain for the highest rates and is therefore sensitive for external interference. Further a considerable amount of intersymbol interference will be introduced. The multi-channel scheme has the same processing gain for all users, independently of their data rates. It may also be easier to design codes that have good properties and construct a multiuser receiver using only one processing gain in the system. One disadvantage of the multi-channel scheme is the need for linear amplifiers for mobiles receiving a high signal. Additionally, users with different rates have different powers, which increases the near-far problem for all schemes, except the multi-channel scheme. If we allow, or even request, for the performance to depend on the service, the users could of course vary their powers. Hence, the near-far problem would decrease for the high rate users. As for the other schemes mentioned, only the multi-chip rate modulation will be able to give the same multirate support as the multi processing-gain and multi-channel schemes.

2-7 FUTURE WORK

In this paper we have only considered the performance of a single cell system without external interference. Another interesting topic is the comparison of the capacity of the different multirate schemes in a cellular system, with or without external interference. It would also be interesting to find efficient coding methods and multiuser detection algorithms to further increase the capacity of the system.

APPENDIX 2A
THE GAUSSIAN APPROXIMATIONS

The Gaussian approximations described in this paper assume that we approximate all interference as Gaussian noise with zero mean. For convenience and ease of computation we also assume that the spreading codes are random code sequences. If we assume that the interference from the other users are independent of the Gaussian distributed noise W_j, we can calculate the variance of the interference for M-ary PAM I_{jl} (see (2-5)) separately as

$$\mathrm{Var}\,[I_{jl}] = \tag{2A-1}$$

$$\sum_{\substack{i=1 \\ i\neq j,\, k\neq l}}^{n} \sum_{k=1}^{K_i} \frac{1}{T_j^2}\frac{P_i}{P_j} E\left[\left(\int_0^{T_j} b_{ik}(t-\tau_{ik})\, c_{ik}(t-\tau_{ik})\, c_{jl}(t)\, \cos\varphi_{ik}\, dt\right)^2\right] =$$

$$\sum_{\substack{i=1 \\ i\neq j,\, k\neq l}}^{n} \sum_{k=1}^{K_i} \frac{1}{T_j^2}\frac{P_i}{P_j} E_{c,\, b_{ik},\, \tau_{ik}}[J_{ik}^2]\, \frac{1}{2\pi}\int_0^{2\pi} \cos^2\varphi_{ik}\, d\varphi_{ik} =$$

$$\sum_{\substack{i=1 \\ i\neq j,\, k\neq l}}^{n} \sum_{k=1}^{K_i} \frac{1}{2T_j^2}\frac{P_i}{P_j} E_{c,\, b_{ik},\, \tau_{ik}}[J_{ik}^2]$$

where $E_{c,\, b_{ik},\, \tau_{ik}}[\cdot]$ is the expectation with respect to the random variables $c(t)$, b_{ik} and τ_{ik}. Further the delays τ_{ik} and the phases φ_{ik} are uniformly distributed on $[0,T_i]$ and $[0,2\pi]$, respectively, and J_{ik} is given as

$$J_{ik} = \int_0^{T_j} b_{ik}(t-\tau_{ik})\, c_{ik}(t-\tau_{ik})\, c_{jl}(t)\, dt \tag{2A-2}$$

It is possible to do the same calculation for I_{jl}^{I} and I_{jl}^{Q} in the case of M-ary QAM, giving the same results. Now assume that all users have the same chip-rate $1/T_c$. Hence, we can separate the calculation of $E_{c,\, b_{ik},\, \tau_{ik}}[J_{ik}^2]$ into two cases: $T_j \geq T_i$ and $T_j < T_i$.

where

$T_j \geq T_i$:

In this case, J_{ik} will depend on several consecutive data symbols assumed independent, and we therefore get

$$\begin{aligned} E[J_{ik}^2] &= E\Bigg[b_{ik}^{(-1)} R_{ik,\, jl}(0, \tau_{ik}) + \\ &\sum_{s=0}^{L-2} b_{ik}^{(s)} R_{ik,\, jl}(\tau_{ik} + sT_i, \tau_{ik} + (s+1)\, T_i) + \\ &b_{ik}^{(L-1)} R_{ik,\, jl}(\tau_{ik} + (L-1)\, T_i, LT_i) \Bigg]^2 = \\ &E[(b_{ik}^{(-1)})^2]\, E[R_{ik,\, jl}^2(0, \tau_{ik})] + \\ &\sum_{s=0}^{L-2} E[(b_{ik}^{(s)})^2]\, E[R_{ik,\, jl}^2(\tau_{ik} + sT_i, \tau_{ik} + (s+1)\, T_i)] + \\ &E[(b_{ik}^{(L-1)})^2]\, E[R_{ik,\, jl}^2(\tau_{ik} + (L-1)\, T_i, LT_i)] \end{aligned} \tag{2A-3}$$

where $L = T_j/T_i$ and $R_{ik,\, jl}(t_1, t_2) = \int_{t_1}^{t_2} c_{ik}(t-\tau_{ik})\, c_{jl}(t)\, dt$.

$T_j < T_i$:

Here J_{ik} depend on the delays τ_{ik} and therefore we first have to calculate the expectation with respect to τ_{ik}. Hence, calculation gives

$$E_{c,\, b_{ik},\, \tau_{ik}}[J_{ik}^2] = \frac{1}{T_i}\int_0^{T_i} E_{c,\, b_{ik}}[J_{ik}^2]\, d\tau_{ik} = \tag{2A-4}$$

$$\frac{1}{T_i}\int_0^{T_j} E[(b_{ik}^{(-1)})^2]\, E[R_{ik,\, jl}^2(0, \tau_{ik})]\, d\tau_{ik} +$$

$$\frac{1}{T_i}\int_0^{T_j} E[(b_{ik}^{(0)})^2]\, E[R_{ik,\, jl}^2(\tau_{ik}, T_j)]\, d\tau_{ik} +$$

$$\frac{1}{T_i}\int_{T_j}^{T_i} E[(b_{ik}^{(-1)})^2]\, E[R_{ik,\, jl}^2(0, T_j)]\, d\tau_{ik}$$

The two cases derived above have expressions that depend on $R_{ik,\, jk}(t_1, t_2)$, where t_1 and t_2 are given by multiples of T_c plus a conditional τ_{ik} term. Therefore all these expectations can be divided into three groups: $R_{ik,\, jl}(mT_c,\ (m+n)\,T_c + \tau_{ik})$, $R_{ik,\, jl}(mT_c + \tau_{ik},\ (m+n)\,T_c)$ and $R_{ik,\, jl}(mT_c + \tau_{ik},\ (m+n)\,T_c + \tau_{ik})$.

To compute these integrals assume that the delay τ_{ik} is such that $pT_c \le \tau_{ik} \le (p+1)\,T_c$, where p is an integer. Using the illustrations in Figure 2-6 it can be seen that

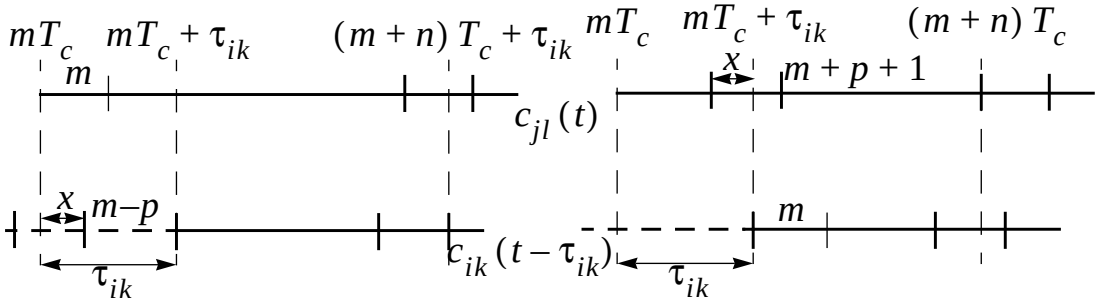

Figure 2-6. Illustration to the computation of $R_{ik,\, jk}(mT_c,\ (m+n)\,T_c + \tau_{ik})$ left figure, and $R_{ik,\, jk}(mT_c + \tau_{ik},\ (m+n)\,T_c)$ right figure.

$$R_{ik,\,jl}(mT_c,\ (m+n)\,T_c+\tau_{ik}) \ = \tag{2A-5}$$

$$\sum_{q=0}^{n+p} c_{jl}^{(m+q)}\, c_{ik}^{(m+q-p-1)} \int_{(m+q)\,T_c}^{(m+q)\,T_c+x} p_{T_c}(t)\,dt +$$

$$\sum_{q=0}^{n+p-1} c_{jl}^{(m+q)}\, c_{ik}^{(m+q-p)} \int_{(m+q)\,T_c+x}^{(m+q+1)\,T_c} p_{T_c}(t)\,dt \ =$$

$$\sum_{q=0}^{n+p-1} c_{jl}^{(m+q)}\ \{\, c_{ik}^{(m+q-p-1)}\ (\tau_{ik}-pT_c) \ + c_{ik}^{(m+q-p)}\ (\,(p+1)\,T_c-\tau_{ik})\,\} \ +$$

$$c_{jl}^{(m+n+p)}\, c_{ik}^{(m+n-1)}\ (\tau_{ik}-pT_c)$$

$$R_{ik,\,jl}(mT_c+\tau_{ik},\ (m+n)\,T_c) \ = \tag{2A-6}$$

$$\sum_{q=0}^{n-p-2} c_{ik}^{(m+q)}\ \{\, c_{jl}^{(m+p+q)}\ (\,(p+1)\,T_c-\tau_{ik}) \ + c_{jl}^{(m+p+1+q)}\ (\tau_{ik}-pT_c)\,\} \ +$$

$$c_{ik}^{(m+n-p-1)}\, c_{jl}^{(m+n-1)}\ (\,(p+1)\,T_c-\tau_{ik})$$

$$R_{ik,\,jl}(mT_c+\tau_{ik},\ (m+n)\,T_c+\tau_{ik}) \ = \tag{2A-7}$$

$$\sum_{q=0}^{n-1} c_{ik}^{(m+q)}\ \{\, c_{jl}^{(m+p+q)}\ (\,(p+1)\,T_c-\tau_{ik}) \ + c_{jl}^{(m+p+1+q)}\ (\tau_{ik}-pT_c)\,\}$$

where $x = \tau_{ik} - pT_c$ and the rectangular pulse shape $p_{T_c}(t) = 1$ for $t \in [0,T_c]$. If we assume that the codes are random, and observe that $(c_{ik}^{(j)})^{\,2} = 1$ we get

$$E_c\,[R^2_{ik,\,jl}\,(mT_c,\ (m+n)\,T_c+\tau_{ik})\,]\ =\ (n+p+1)\,x^2+\ (n+p)\ (T_c-x)^{\,2} \tag{2A-8}$$

$$E_c\,[R^2_{ik,\,jl}\,(mT_c+\tau_{ik},\ (m+n)\,T_c)\,]\ =\ (n-p-1)\,x^2+\ (n-p)\ (T_c-x)^{\,2}$$

$$E_c\,[R^2_{ik,\,jl}\,(mT_c+\tau_{ik},\ (m+n)\,T_c+\tau_{ik})\,]\ =\ nx^2+n\,(T_c-x)^{\,2}$$

By the use of these derived results it can be seen that the expectations in the two cases discussed are:

$T_j \geq T_i$:

$$E_{c,\,b_{ik},\,\tau_{ik}}\,[J^2_{ik}]\ =\ \frac{2LN_i^2}{T_i}\frac{T_c^3}{3} \tag{2A-9}$$

$T_j < T_i$:

$$E_{c,\,b_{ik},\,\tau_{ik}}\,[J^2_{ik}]\ =\ \frac{2N_iN_j}{T_i}\frac{T_c^3}{3} \tag{2A-10}$$

The multirate schemes presented in this chapter can now be analyzed with respect to the bit error performance for the users.

Multi-Modulation Systems:

As earlier defined, all users in the multi-modulation system have the same processing gain and symbol period. Hence, the variance of the interference I_{jl} is

$$\mathrm{Var}\,[I_{jl}]\ =\ \frac{2}{3N}\left(\sum_{i\,=\,1}^{n}\frac{R_i}{R_j}K_i-1\right) \tag{2A-11}$$

for the M-ary QAM users, but for the BPSK users we get

$$\mathrm{Var}\,[I_{jl}]\ =\ \frac{1}{3N}\left(\sum_{i\,=\,1}^{n}\frac{R_i}{R_j}K_i-1\right). \tag{2A-12}$$

Multi Processing-Gain Systems:

Here all T_i and N_i are different. If we observe that for equal signal-to-noise ratio per bit the power ratios between users with different rates are $P_i/P_j = R_i/R_j$, resulting in the variance of I_{jl} as

$$\mathrm{Var}\,[I_{jl}] = \frac{1}{3N_j}\left(\sum_{i=1}^{n} \frac{R_i}{R_j} K_i - 1 \right) \tag{2A-13}$$

Multi-Channel Systems:

In a multi-channel system, the processing gain, the symbol period and the modulation are constant for all users. Assuming QPSK modulation is used, the variance of I_{jl} is

$$\mathrm{Var}\,[I_{jl}] = \frac{2}{3N_j}\left(\sum_{i=1}^{n} \frac{R_i}{R_j} K_i - 1 \right) \tag{2A-14}$$

The performance, measured in bit error performance can then easily be found by the use of the variances of I_{jl} above and the equations (2-4),(2-7) and (2-8).

APPENDIX 2B
LINEARITY MEASURE FOR THE MULTI-CHANNEL SCHEME

The multi-channel scheme requires linear amplifiers also in the mobile, since the sum of several parallel channels causes a signal with large envelope variations. One linearity measure that is often used for amplifiers is the *Peak-to-Mean Envelope Power Ratio* (PMEPR) defined as

$$\mathrm{PMEPR} = \frac{\mathrm{PEP}}{\mathrm{MEP}} \tag{2B-1}$$

where PEP is the *Peak Envelope Power* and MEP is the *Mean Envelope Power*. If QPSK is used, the output from the L channels is of the form

$$y = \left(\sum_{i=0}^{L-1} b_i^I c_i^I \right) \cos \omega_c t + \left(\sum_{i=0}^{L-1} b_i^Q c_i^Q \right) \sin \omega_c t . \qquad \text{(2B-2)}$$

The maximum envelope power $\mathrm{PEP} = (y^2)_{max} = L^2$ is easily found when all channels are co-phased. The average envelope power (MEP), however, can be calculated accordingly

$$\begin{aligned}
\mathrm{MEP} &= E_{b,c,t}\left[\left(\sum_{i=0}^{L-1} b_i^I c_i^I \right)^2 \cos^2 \omega_c t + \left(\sum_{i=0}^{L-1} b_i^Q c_i^Q \right)^2 \sin^2 \omega_c t + \right. \\
&\left. 2 \left(\sum_{i=0}^{L-1} b_i^I c_i^I \right) \left(\sum_{i=0}^{L-1} b_i^Q c_i^Q \right) \cos \omega_c t \sin \omega_c t \right] = (a) \\
&E_{b,c}\left[\left(\sum_{i=0}^{L-1} b_i c_i \right)^2 \right] \overset{(b)}{=} E_a \left[\left(\sum_{i=0}^{L-1} a_i \right)^2 \right] = (c) \\
&2^{-L} \sum_{\forall (a_0, \ldots, a_{L-1})} \left(\sum_{i=0}^{L-1} a_i \right)^2 = (d) \\
&2^{-L} \sum_{\forall (a_0, \ldots, a_{L-1})} \left(\sum_{i=0}^{L-1} 1 - 2a'_i \right)^2 = \\
&2^{-L} \sum_{j=0}^{L} \binom{L}{j} (L-2j)^2 = \\
&2^{-L} \left[L^2 \sum_{j=0}^{L} \binom{L}{j} + 4L \sum_{j=0}^{L} \binom{L}{j} j + 4 \sum_{j=0}^{L} \binom{L}{j} j^2 \right] = \\
&L^2 - 2L^2 + L^2 + L = L
\end{aligned}$$

(2B-3)

where (a) are from the facts that $E_t[\cos \omega_c t \sin \omega_c t] = 0$ and $E_t[\cos^2 \omega_c t] = E_t[\sin^2 \omega_c t] = 1/2$, (b) assuming that both bits and code chips are random and independent, (c) assuming that all bits are equally likely, and (d) converting $a_i \in \{-1, 1\}$ to $a'_i \in \{0, 1\}$. The result is that, $\mathrm{PMEPR} = L$, which is the same linearity constraint as for the multi-carrier modulation scheme [5].

APPENDIX 2C
THE ACCURACY OF THE GAUSSIAN APPROXIMATION

Throughout this chapter we have used the Gaussian approximation, that is, we have approximated the interference from the other users with a Gaussian distributed variable. As earlier stated, this approximation is accurate for low signal-to-noise ratios and many users. In this appendix, we will justify this approximation for single rate systems (n=1). Therefore we calculate a more accurate performance figure using the characteristic function method [18] [19] and compare it to the Gaussian approximation.

In the *characteristic function method* the interference is estimated using characteristic functions. The characteristic function $\phi_X(\omega)$ for the random variable X is defined as

$$\phi_X(\omega) = E[\exp(j\omega X)]. \tag{2C-1}$$

Hence, the symbol error rate for M-ary amplitude modulation with the matched filter output given in (2-4) can be expressed as

$$P_{e,1l} = \frac{(M-1)}{M}\Pr(|Z_{1l} - E[Z_{1l}]| > 1) = \tag{2C-2}$$

$$2\frac{(M-1)}{M}P(I_{1l} + W_1 > 1) =$$

$$\frac{M-1}{M}\left(1 - 2\int_0^1 p(I_{1l} + W_1)\,dx\right) =$$

$$\frac{M-1}{M}\left(1 - \frac{2}{\pi}\int_0^\infty \omega^{-1}\phi(\omega)\sin(\omega)\,d\omega\right)$$

Here $p(I_{1l} + W_1)$ is the probability density function (pdf) of the total interference, that is, $I_{1l} + W_1$ and $\phi(\omega)$ is the characteristic function corresponding to this pdf. Using the assumption that the Gaussian noise is independent of the interference from all the users, we get

$$\phi(\omega) = \phi_{W_1}(\omega)\phi_{I_{1l}}(\omega) = \phi_{W_1}(\omega) - \phi_{W_1}(\omega)[1 - \phi_{I_{1l}}(\omega)] \tag{2C-3}$$

Hence, the symbol error probability can be calculated as

$$P_{e,jl} = \frac{M-1}{M}\left(Q\left(\sqrt{\frac{3}{M^2-1}\cdot\frac{2\bar{E}}{N_0}}\right) + \frac{2}{\pi}\int_0^{\infty} \omega^{-1}\phi_{W_1}(\omega)\,[1-\phi_{I_{1l}}(\omega)]\sin(\omega)\,d\omega \right) \tag{2C-4}$$

where

$$\phi_{W_1}(\omega) = \exp\left(-\frac{Var[W_1]}{2}\right) \tag{2C-5}$$

and the variance

$$Var[W_1] = \frac{(M^2-1)\,N_0}{6\bar{E}}. \tag{2C-6}$$

Following the outline in [18] for a single-rate system it can be shown that the characteristic function for M-ary PAM is given by

$$\phi_{I_{1l}}(\omega) = \frac{4}{\pi}\prod_{\substack{k=1\\k\neq l}}^{K}\sum_{p=0}^{N-1}\sum_{\forall \boldsymbol{b}_k \notin -\boldsymbol{b}_k} \int_0^{\pi/2}\cos\left(\omega\,[g_k(p+1)+g_k(p)]\,\frac{\cos\varphi_k}{2N}\right)\cdot \operatorname{sinc}\left(\omega\,[g_k(p+1)-g_k(p)]\,\frac{\cos\varphi_k}{2\pi N}\right) \tag{2C-7}$$

where $\boldsymbol{b}_k = (b_k^{(-1)}, b_k^{(0)})$, $g_k(p) = b_k^{(-1)} C_{k,l}(p-N) + b_k^{(0)} C_{k,l}(p)$, and the aperiodic cross-correlation

$$C_{k,\,l}(p) \;=\; \begin{cases} \displaystyle\sum_{j\,=\,0}^{N-1-p} c_k^{(j)}\, c_i^{(j+p)}, & 0 \le p \le N-1 \\ \displaystyle\sum_{j\,=\,0}^{N-1+p} c_k^{(j-p)}\, c_i^{(j)}, & 1-N \le p < 0 \\ 0, & |p| \ge N \end{cases} \tag{2C-8}$$

For M-ary QAM the corresponding expression is

$$\phi_{I_{1l}^{I}}(\omega) \;=\; \prod_{\substack{k\,=\,1 \\ k \neq l}}^{K} \frac{8}{\pi N M^2} \sum_{p\,=\,0}^{N-1} \sum_{\forall \boldsymbol{b}_k^I \notin -\boldsymbol{b}_k^I} \sum_{\forall \boldsymbol{b}_k^Q \notin -\boldsymbol{b}_k^Q} \int_0^{\pi/2} \tag{2C-9}$$

$$\cos\!\left(\left(g_k^{II}(\boldsymbol{b}_k^I, p+1) + g_k^{II}(\boldsymbol{b}_k^I, p)\right) \frac{\omega}{2N} \cos\varphi_k \right) \cdot$$

$$\operatorname{sinc}\!\left(\left(g_k^{QI}(\boldsymbol{b}_k^Q, p+1) - g_k^{QI}(\boldsymbol{b}_k^Q, p)\right) \sin\varphi_k + \right.$$

$$\left. \left(g_k^{II}(\boldsymbol{b}_k^I, p+1) - g_k^{II}(\boldsymbol{b}_k^I, p)\right) \cos\varphi_k \right) \frac{\omega}{2\pi N} \Bigg) d\varphi_k$$

Observe that this result is for the I-phase but is easily adjusted for the Q-phase: substitute $\sin\varphi_k$ with $\cos\varphi_k$ and $\cos\varphi_k$ with $-\sin\varphi_k$.

To exemplify the derived formulas we have done some numerical calculations using different M-ary AM formats. The codes used in these calculations are *m*-sequence codes [52] with period $N = 127$ and of the whole set of such codes we have selected the best codes according to the AO/LSE (Auto Optimal phase and Least Sidelobe Energy) criterion. These codes are tabulated in [51]. All calculations have been performed using the Characteristic function method, the Gaussian approximation (GA) with deterministic sequences and the Gaussian approximation with random sequences and we assume rectangular pulse shape for all calculations. In Figure 2-7 and Figure 2-8 we show results for the symbol error rate (SER) for BPSK and 4-PAM.

We see from the given results that both Gaussian approximations are slightly optimistic (lower SER than for the characteristic function method),

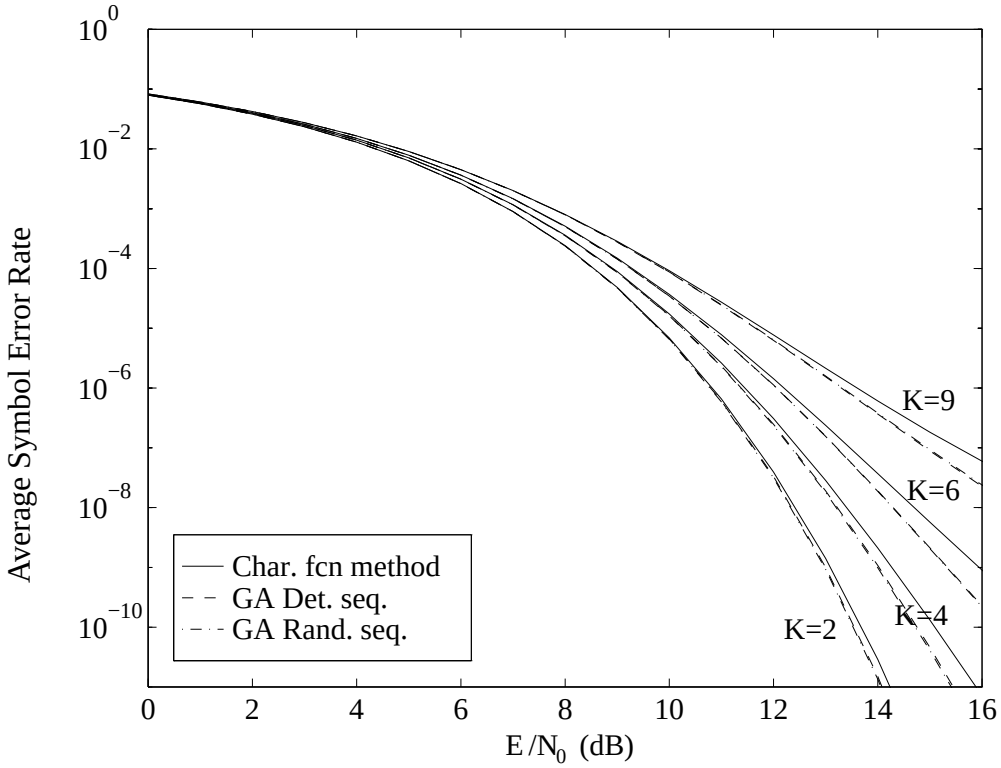

Figure 2-7. BPSK modulation with AO/LSE *m*-sequences. *N*=127.

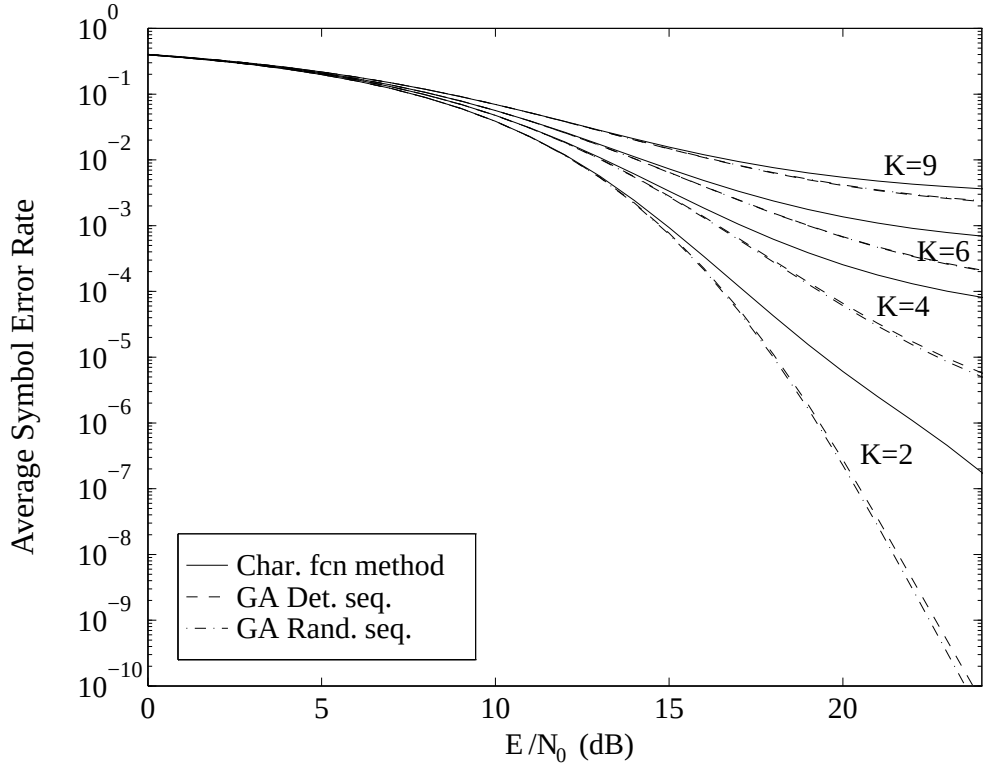

Figure 2-8. 4-PAM modulation with AO/LSE *m*-sequences. *N*=127.

but become more valid at low signal-to-noise ratios, many users and many levels of modulation. Further we do not see much difference between the two Gaussian approximations, meaning that the system with AO/LSE *m*-sequences performs approximately the same as a system using random sequences. For many users, however, there are a slight advantage for the random sequences, because of the relatively small number of good *m*-sequences.

For the QAM schemes we have used Gold-sequences, with period $N = 127$, created by the shift-register polynomial 41567, given in octal form [51]. The results are shown in Figure 2-9 and Figure 2-10 and the same conclusions as for M-ary PAM can be drawn. Observe, though, that the Gaussian approximation is slightly pessimistic for QPSK using Gold sequences (worse SER than for the characteristic function method), due to the good cross-correlation properties for the Gold sequences and that QPSK is slightly better than BPSK. The same observation was done in [19] for *m*-sequences.

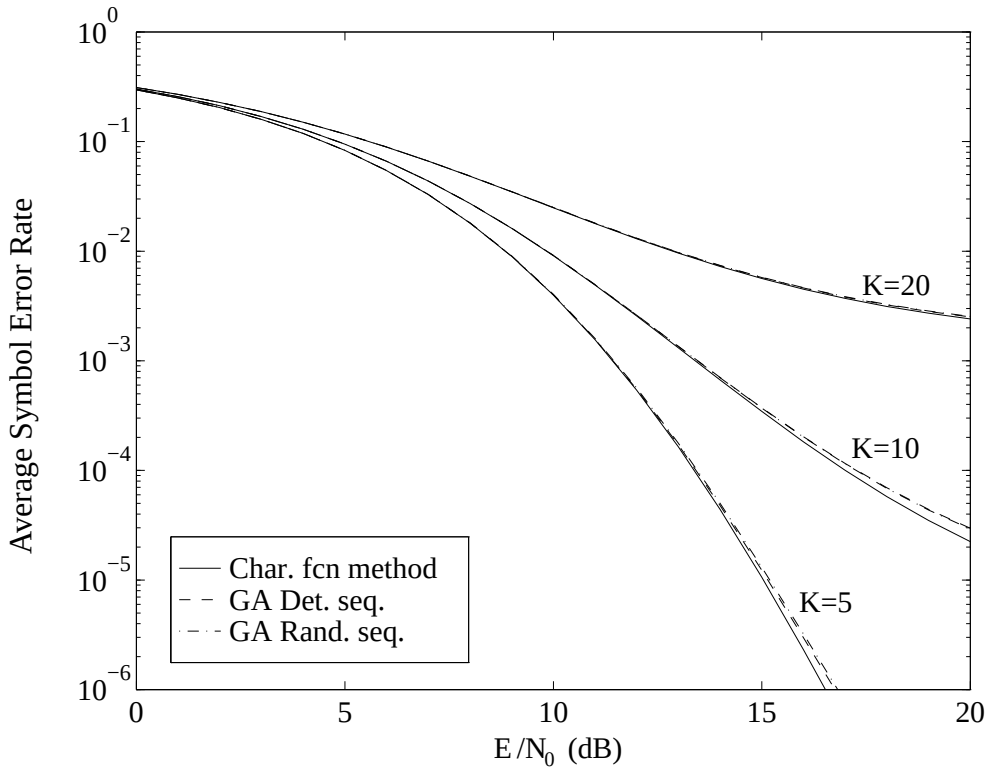

Figure 2-9. QPSK modulation with Gold-sequences. *N*=127.

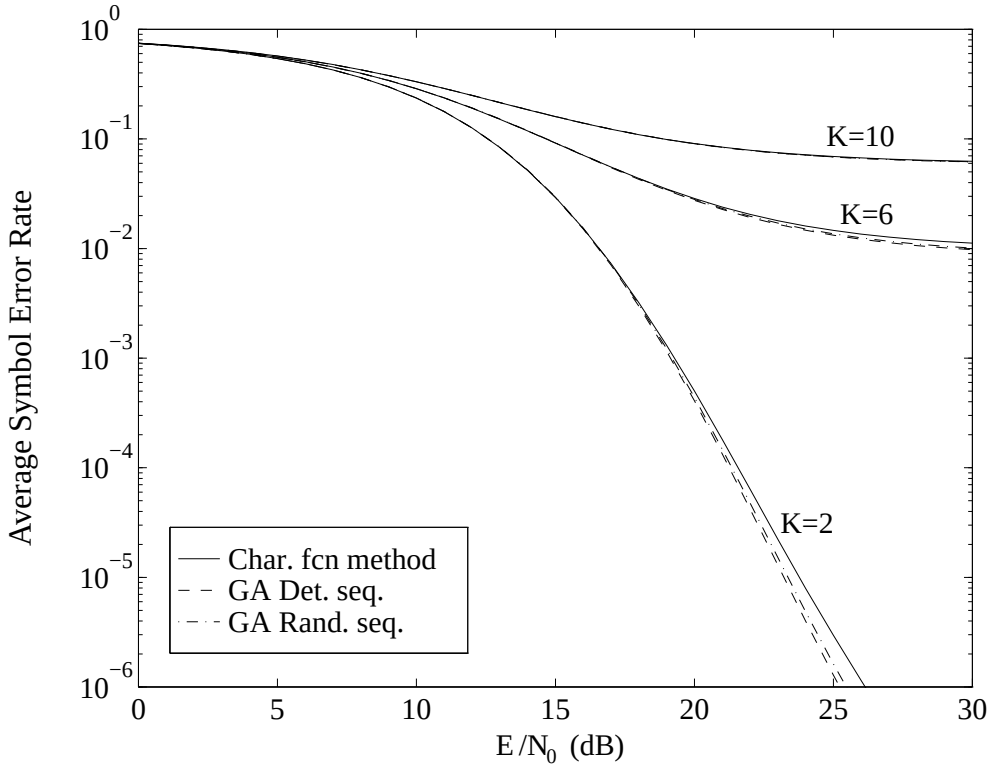

Figure 2-10. 16-QAM modulation with Gold-sequences. *N*=127.

CHAPTER
3

MULTIUSER DETECTION

3-1 INTRODUCTION

Multiuser detection concerns detection of information sent simultaneously by several transmitters sharing a multiple-access channel. There exist several types of strategies: for example Frequency Division Multiple Access (FDMA), Time Division Multiple Access (TDMA), and ALOHA. For these strategies, however, the different sub-channels are either independent or, as in the ALOHA case, each user transmits packets uncoordinated, and if a collision occurs, the packets are retransmitted (see [35] page 785, and [3]). A more challenging channel sharing strategy is the Code Division Multiple Access (CDMA) approach, where all users share the same time and frequency band. To distinguish between the different users, a unique waveform (code) is assigned to each user. Hence, the received signal from all users is a superposition of the individual transmitted signals. Therefore the task of the multiuser detector is to reliably demodulate the information from a specific user (or subset of users). In the following we will only consider multiuser detection for CDMA systems.

The conventional detector, used in single-user systems, is the matched filter receiver (correlation receiver) [49]. It is well known that this receiver is optimum in minimum probability of error sense in demodulation of a single existing user in Additive White Gaussian Noise (AWGN). In demodulation of a user in a CDMA system one can argue that the correlation receiver is close-to optimal, since the interference from the other users adds up to be

Gaussian (the central limit theorem). The central limit theorem does not apply, however, if the users have very different powers. Furthermore, the noise components from the different matched filters are not uncorrelated, due to the cross-correlation between users. Hence, this colored noise should be taken into account in the demodulation. Nevertheless, even if the interference looks white and Gaussian, its power density increases with the number of users and the performance degrades. Even worse is the case for a system with few users, where the noise cannot be accurately modeled as Gaussian.

The performance for the conventional detector can in some cases be acceptable for received user signals with similar energies and waveforms with low cross-correlations. However, if the powers of the users are very different, it is impossible to do a reliable detection of the weak users, even with very low cross-correlations. This fact, that users with high powers make detection of users with low powers impossible, is known as the *near-far effect*. Therefore a way to, in some extent, circumvent the multiuser detection problem and the near-far effect, is to use strict power control and design waveforms with low enough cross-correlations. However, a major drawback of such an approach is that the system performance is dictated by the user whose signal is received with the lowest power and therefore power control actually decreases the overall capacity [13]. As for the search of good codes with low cross-correlations, it is not possible to design codes that are orthogonal in the receiver, either due to that all users transmit uncoordinated (asynchronous system) or that the channel is a multipath channel. The conclusion is that in asynchronous CDMA systems, the conventional correlation receiver will always suffer from the near-far effect, and the performance will therefore be limited by the interference from other users. Multiuser detection is a way to deal with the problems of near-far effects and the interference limited performance.

Horwood and Gagliardi [26] and Schneider [54] [55] considered multiuser detection for synchronous systems. In [54], Schneider claimed that he had found the optimum detector. This was, however, not completely true. The derived receiver, later referred to as the decorrelator, was found to be optimal only if no information on the powers of the different users is available [39]. Schneider also briefly treated the asynchronous case, recognized that it could be modeled as a finite state machine, and suggested the use of the Viterbi algorithm to solve the detection. The major breakthrough in the area,

was triggered by Verdú in 1984, when he presented the optimum maximum likelihood sequence detector for the asynchronous case (see [72] and [73]). Complexity was, however, the main drawback for the optimum detector. Therefore, several suboptimum detectors have been presented (see Section 3-4). A survey of multiuser detection for CDMA for both optimal and suboptimal receivers can be found in [13].

In Section 3-2 the model for the synchronous CDMA channel corrupted by additive white Gaussian noise is presented. Maximum likelihood detectors are presented in Section 3-3, and several suboptimum detectors in Section 3-4. A comparison between the presented detectors is made in Section 3-5 for the Gaussian channel. The asynchronous case and the multipath fading channel are briefly discussed in Section 3-6.

3-2 SYSTEM MODEL

Assume a Direct-Sequence Code Division Multiple-Access (DS/CDMA) system as given in Figure 3-1, where the kth user is assigned a finite energy waveform, $\{c_k(t), t \in [0, T]\}$. Further assume that the data is BPSK modulated and that all users transmit synchronously over a Gaussian multiple-access channel. Hence, the received signal is

$$r(t) = \sum_{i} \sum_{k=1}^{K} w_k b_k(i)\, c_k(t - iT) + n(t) \tag{3-1}$$

where K is the number of users in the system, $\{b_k(i) \in \{-1, 1\}, \forall i\}$ is the kth user's information sequence, and w_k the amplitude. The noise $n(t)$ is additive white Gaussian with zero-mean and a power spectral density σ^2. It can be shown that the outputs of a bank of matched filters

$$y_k(i) = \int_{iT}^{(i+1)T} r(t)\, c_k(t - iT)\, dt \tag{3-2}$$

at time i are the sufficient statistics for ML-detection of the transmitted data at time i [39]. Hence, the optimal receiver is a one shot receiver. Collect the outputs from all filters in the vector[1] $\mathbf{y} = (y_1, y_2, \ldots y_K)^T$. In this way, the matched filter outputs can be expressed in matrix notation as

$$\mathbf{y} = \mathbf{RWb} + \mathbf{n} \tag{3-3}$$

where $\mathbf{R}$ is the cross-correlation matrix consisting of the elements

$$\{\mathbf{R}\}_{j,k} = \int_0^T c_j(t)\, c_k(t)\, dt. \tag{3-4}$$

The transmitted bits are contained in the vector $\mathbf{b} = (b_1, b_2, \ldots b_K)^T$, and the matrix $\mathbf{W}$ is a diagonal amplitude matrix. Due to the cross-correlation between users, the noise vector $\mathbf{n}$ is colored Gaussian distributed with zero-mean and covariance matrix $\sigma^2\mathbf{R}$.

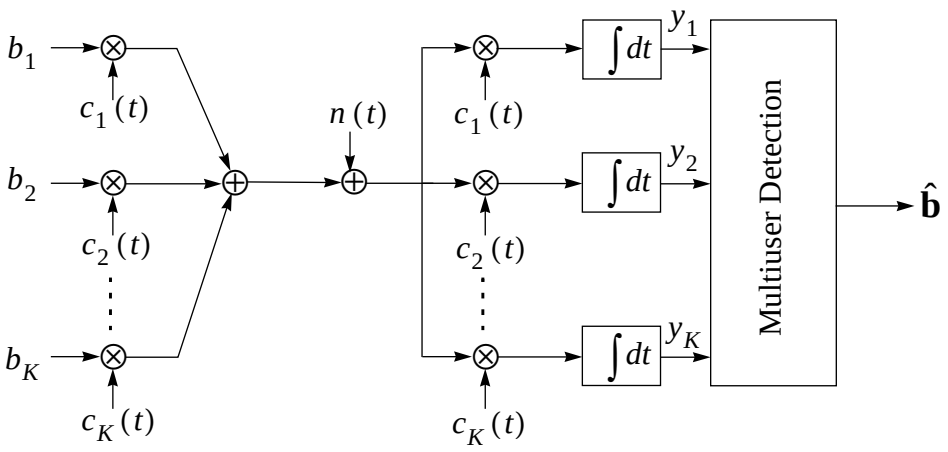

Figure 3-1. A synchronous DS/CDMA system model.

3-3 ML OPTIMUM RECEIVERS

Introduction

The optimum *maximum likelihood* receiver is not unambiguously defined. For example it is possible to maximize either $p(\mathbf{y}|b_k)$ or $p(\mathbf{y}|\mathbf{b})$, resulting in minimum bit (b_k) error or minimum symbol ($\mathbf{b}$) error, respectively. It is also possible to do these maximizations with different constraints, for example, known, unknown or partially known $\mathbf{R}$, and $\mathbf{W}$. Thus, the two criteria are different. The minimum bit error criterion is a Bayes symbol detector with the costs corresponding to the number of bit errors. On the other hand, if all symbol error costs are assigned to be equal, the minimum

1. We will frequently drop the time argument i in the following treatment.

symbol error criterion is given. Even if the criteria are different they are asymptotically equal, when the signal-to-noise ratio approaches infinity (shown in [24] for two users) and when the cross-correlations approaches zero (orthogonal codes) and therefore the difference is small for high signal-to-noise ratios and low cross-correlations between the users. This and that the minimum bit error criterion is more complex, are the main reasons why the minimum symbol error criterion is the most common, and therefore we adopt the minimum symbol error criterion in this work. Further, we will assume that the cross-correlation matrix and the amplitude matrix are known by the receiver. In practice these matrices have to be estimated.

Using the fact that $\mathbf{y}|\mathbf{b}$ is Gaussian with mean $\mathbf{RWb}$ and covariance matrix $\sigma^2\mathbf{R}$, the ML symbol decision is given by

$$\begin{aligned}\hat{\mathbf{b}}_{ML} &= \arg \min_{\mathbf{b} \in \{\pm 1\}^K} (\mathbf{y} - \mathbf{RWb})^T \mathbf{R}^{-1} (\mathbf{y} - \mathbf{RWb}) \\ &= \arg \max_{\mathbf{b} \in \{\pm 1\}^K} \{2\mathbf{y}^T\mathbf{Wb} - \mathbf{b}^T\mathbf{WRWb}\}\end{aligned} \tag{3-5}$$

The complexity of (3-5) is $O(K \cdot 2^K)$ for detection of all users (per symbol $\mathbf{b}$), because all the 2^K points $\mathbf{b} \in \{\pm 1\}^K$ have to be tested. However, if $\mathbf{b}^T\mathbf{WRWb}$ is precomputed and stored, the evaluation of $2\mathbf{y}^T\mathbf{Wb} - \mathbf{b}^T\mathbf{WRWb}$, for all possible $\mathbf{b}$ simultaneously, can be done in a tree structure (see [74] for details) using $O(2^K)$ operations and then $O(2^K)$ operations are needed to select the optimum $\mathbf{b}$.

An intuitive way to look at multiuser detectors is a to draw a decision space. There are of course several ways to do that. One could for example draw the $\mathbf{y}$-space, the $(\mathbf{RW})^{-1}\mathbf{y}$-space or the whitened $\mathbf{R}^{-1/2}\mathbf{y}$ space. Which of the three to use is a matter of opinion. However, the whitened space has the advantage to be the space in which the ML receiver is equivalent to finding the point with the minimum squared distance to the received signal point. For the ML receiver the decision boundaries in the three different spaces are given in Figure 3-2, for a system with two equally strong (in power) users and the cross-correlation 0.7. As seen in the whitened space, the decision lines divides the virtual line between any two symbols in the middle and perpendicularly. Further, the decision lines meet at common points, which is known from the theory of detection ([68], page 48).

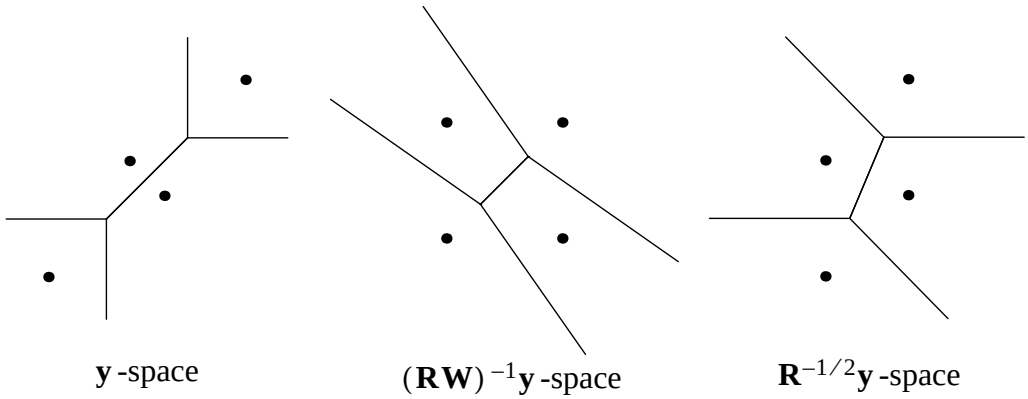

Figure 3-2. Decision spaces for the maximum likelihood receiver for a system with K=2 users and the cross-correlation between the users equal to 0.7.

A Reduced Complexity ML Receiver

As seen from the previous section, the complexity of the ML receiver is inhibiting. Thus, there is a need for reducing this complexity. Usually this is done with a suboptimal receiver. However, in this section we derive a ML optimal receiver with reduced complexity (first presented in [1]).

We start from the model given in (3-3). Further, if the noise is whitened (assuming $\mathbf{R}$ to be positive definite), the model can be written as

$$\mathbf{u} = \mathbf{R}^{-1/2}\mathbf{y} = \mathbf{T}\mathbf{b} + \mathbf{z}, \tag{3-6}$$

where $\mathbf{T} = \mathbf{R}^{1/2}\mathbf{W}$ is the whitening transform, and the covariance matrix of the Gaussian noise $\mathbf{z}$ is $\sigma^2\mathbf{I}$. If vectors are regarded as points in K-dimensional space, then the 2^K vectors $\mathbf{b}$ constitute the vertices of a hypercube. Similarly, the constellation $\mathcal{X} = \{\mathbf{T}\mathbf{b}\}_{\mathbf{b} \in \{\pm 1\}^K}$ spans a K-dimensional parallelotope; that is, a linear transformation of a hypercube, where $\mathbf{T}$ is the transformation matrix. Given an observation vector $\mathbf{u}$, the most likely point in $\mathcal{X}$ is given by the minimum Euclidean distance to $\mathbf{u}$, that is

$$\hat{\mathbf{b}}_{ML} = \arg \min_{\mathbf{b} \in \{\pm 1\}^K} \|\mathbf{u} - \mathbf{T}\mathbf{b}\| \tag{3-7}$$

This detection rule, which is equivalent to (3-5), partitions the space into 2^K convex polytopes, called *Voronoi regions*, given by

$$\mathcal{V}(\mathbf{x}) = \{\mathbf{u} \in \Re^K : \|\mathbf{u} - \mathbf{x}\| \le \|\mathbf{u} - \mathbf{x}'\|; \forall \mathbf{x}' \in \mathcal{X}\} \tag{3-8}$$

with one region for each $\mathbf{x} \in \mathcal{X}$. The ML decision on $\mathbf{b}$ given $\mathbf{u}$ is thus to find $\hat{\mathbf{b}}_{ML}$ such that $\mathbf{u} \in \mathcal{V}(\mathbf{T}\hat{\mathbf{b}}_{ML})$.

Some of the $2^K - 1$ nontrivial inequalities in (3-8) may be redundant, so that the same regions can be described as

$$\mathcal{V}(\mathbf{x}) = \{\mathbf{u} \in \Re^K: \|\mathbf{u} - \mathbf{x}\| \leq \|\mathbf{u} - \mathbf{x}'\|; \forall \mathbf{x}' \in \mathcal{N}(\mathbf{x})\} \tag{3-9}$$

The minimal set $\mathcal{N}(\mathbf{x})$ for which this is true is called the set of "neighbors" of $\mathbf{x}$. Geometrically, each element of $\mathcal{N}(\mathbf{x})$ corresponds to one facet ((*K*-1)-dimensional face) of the polytope $\mathcal{V}(\mathbf{x})$. Thus, to check if a given vector $\mathbf{u}$ belongs to the Voronoi region $\mathcal{V}(\mathbf{x})$, it is sufficient to compute[1] $|\mathcal{N}(\mathbf{x})|$ distances, a number that is often considerably smaller than $2^K - 1$. Hence, the iterative approach in Table 3-1, called the *neighbor descent (ND) algorithm* [2], can be used.

Table 3-1. The Neighbor Descent (ND) algorithm.

1. Start with a guess $\mathbf{x} = \mathbf{T}\hat{\mathbf{b}}^{(0)}$.
2. **repeat for** $\forall \mathbf{x}' \in \mathcal{N}(\mathbf{x})$:
   if $\|\mathbf{u} - \mathbf{x}'\| < \|\mathbf{u} - \mathbf{x}\|$ **then**
   replace $\mathbf{x}$ with $\mathbf{x}'$; **Go to** 2.
   end repeat
3. $\hat{\mathbf{b}}_{ML} = \mathbf{T}^{-1}\mathbf{x}$.

The guess $\hat{\mathbf{b}}^{(0)}$ can, for example, be the conventional or the decorrelating receiver. It can be proven that this algorithm is equivalent to the ML receiver [2]. Further the algorithm assumes that the neighbors $\mathcal{N}(\mathbf{x})$ for all $\mathbf{x} \in \mathcal{X}$ have been precomputed and stored in memory. The following theorem can be used to find the neighbors (can be proved using the theory of "indecomposable vectors" [73]):

Theorem: If every pair of points in $\mathcal{X}$ are joined by a line, the neighbors are given by the lines that are only intersected by longer lines.

1. $|\mathcal{N}(\mathbf{x})|$ is the size of the set $\mathcal{N}(\mathbf{x})$.

To calculate the complexity: Think of the lines between points in $\mathcal{X}$ as diagonals in a parallelotope. These lines can only intersect each other at the points

$$\mathcal{Y} = \{\mathbf{Tb}\}_{\mathbf{b} \in \{-1, 0, 1\}^K} \setminus \mathcal{X} \tag{3-10}$$

and nowhere else. Since at most one pair of neighbors can meet at each intersection point, the total number of neighbor pairs in the point set is upperbounded by $|\mathcal{Y}| = 3^K - 2^K$. In other words, an average point in $\mathcal{X}$ has $< 2\,(3^K - 2^K)\,/\,2^K < 2\,(3/2)^K$ neighbors, and since most of the time for the ND-algorithm is used for verification [2] (part of step 2 in the algorithm) the asymptotic complexity is $O\,(1.5^K)$.

3-4 SUBOPTIMUM RECEIVERS

The Conventional Receiver

The conventional receiver (matched filter receiver) uses no information of the transmitted signals of the other users and therefore regards them as noise. Hence, the receiver is simply a signum decision

$$\hat{\mathbf{b}}_{conv} = \text{sgn}\,(\mathbf{y})\ . \tag{3-11}$$

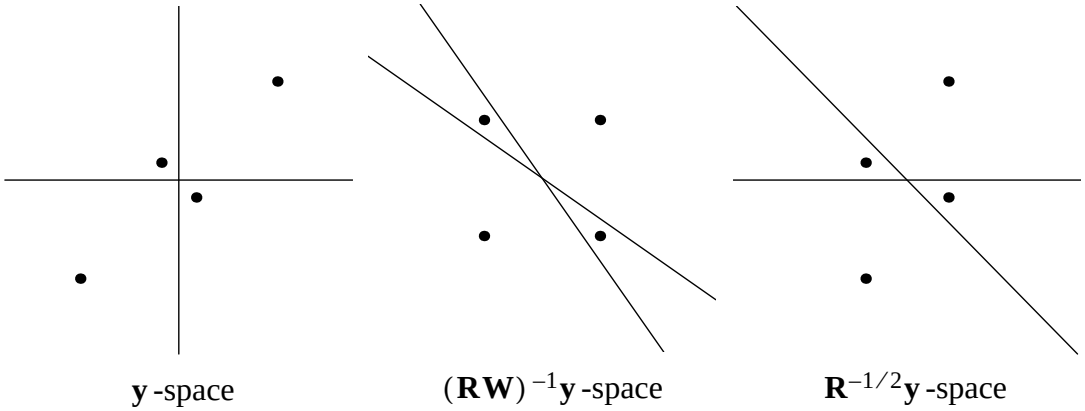

Figure 3-3. Decision spaces for the conventional receiver for a system with *K*=2 users and the cross-correlation between the users equal to 0.7.

The performance of this receiver is interference limited as stated in the introduction, and this is also seen in Figure 3-2, where the distance between

symbols and the decision lines are very different for the different symbols, $\mathbf{b}$, resulting in a high symbol error rate. We also see the signum decision lines in the $\mathbf{y}$-space, that defines the receiver. If one user increases its power, more than one symbol will eventually be placed in some regions, and no symbols in other regions (see Figure 3-4, where $w_1 = 2, w_2 = 1$ and the cross-correlation between users is equal to 0.7). Hence, the conventional receiver suffers from the near-far effect. That is, a user with a high received power makes it impossible to detect a user with a low received power level.

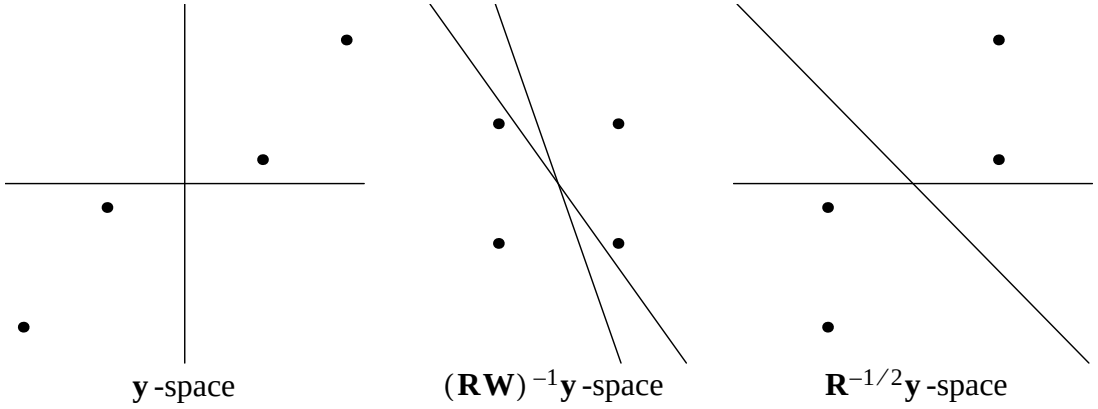

Figure 3-4. Decision spaces for the conventional receiver for a system with K=2 users in a near-far situation. The amplitudes are $w_1 = 2$ and $w_2 = 1$ and the cross-correlation between the users is equal to 0.7.

The Decorrelator Receiver

The conventional receiver suffers from the near-far effect, as stated above. On the other hand, the ML receiver is resistant to this effect, but the complexity is high. A simple, low complexity detector that is resistant to the power of the other users is the decorrelator, which is the ML optimum receiver if the amplitude matrix $\mathbf{W}$ is unknown.

The receiver is simply a linear transformation $\mathbf{R}^{-1}$, that projects the matched filter outputs $\mathbf{y}$ (see (3-3)) onto a space where all users are independent, that is $\mathbf{R}^{-1}\mathbf{y} = \mathbf{Wb} + \mathbf{R}^{-1}\mathbf{n}$. The decisions are then obtained by simple signum decisions on the transformed signal as

$$\hat{\mathbf{b}}_{decorr} = \text{sgn}\,(\mathbf{R}^{-1}\mathbf{y})\ . \tag{3-12}$$

The drawback, though, is the noise enhancement. Drawing the decision spaces for this receiver is especially illustrative. In Figure 3-2, we see that the decorrelator is a signum decision detector in the $(\mathbf{RW})^{-1}\mathbf{y}$-space. Furthermore, it is easy to see that the decision lines do not depend on the power of the users, that is the scaling of points in one or both dimensions. Hence, the receiver is also near-far resistant.

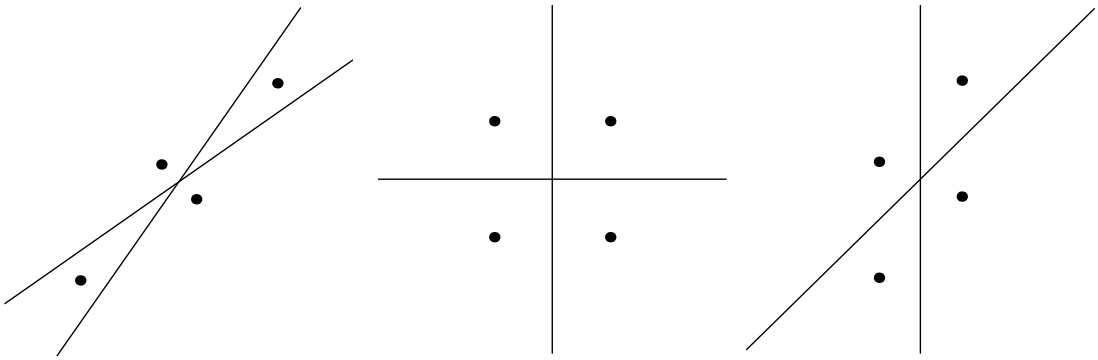

Figure 3-5. Decision spaces for the decorrelator receiver for a system with K=2 users and the cross-correlation between the users equal to 0.7.

Since the outputs from the different users now spans an orthogonal signal space (the $\mathbf{b}$-space) it is easy to see that the average bit error probability for transmission over an AWGN channel is

$$P_{b,k} = Q\left(\sqrt{\frac{w_k^2}{\sigma^2 \{\mathbf{R}^{-1}\}_{k,k}}}\right) \tag{3-13}$$

where

$$Q(x) = 1/(\sqrt{2\pi}) \cdot \int_x^\infty \exp(-z^2/2)\, dz, \tag{3-14}$$

and $\{\mathbf{R}\}_{k,k}$ is the kth element on the diagonal of $\mathbf{R}$.

The Multistage Receiver

There exist several ways to iteratively maximize the ML criterion (equation (3-5)) to a local maximum. One such receiver is the multistage algorithm [70] shown in Table 3-2.

Table 3-2. The multistage algorithm.

1. Start with a first stage guess $\hat{\mathbf{b}}(0)$.

2. **repeat for** m=1,...,$\alpha - 1$

   repeat for k=1,...,K

   $$\mathbf{b} = \left[\hat{b}_1(m-1), \ldots, b_k, \ldots, \hat{b}_K(m-1)\right]^T$$

   $$\hat{b}_k(m) = \underset{b_k \in \{-1, 1\}}{\arg\max} \{2\mathbf{y}^T\mathbf{W}\mathbf{b} - \mathbf{b}^T\mathbf{W}\mathbf{R}\mathbf{W}\mathbf{b}\}$$

   end repeat

end repeat

As a guess to the first stage, the conventional matched filter receiver or the decorrelator can be used. The number of stages, α, is usually chosen to $\alpha = 2$. However, if the number of stages is increased, it is not guaranteed that the receiver becomes better with each iteration [70]. Furthermore, it can be shown that [70]

$$\hat{b}_k(m) = \text{sgn}\{y_k - \sum_{k' \neq k} \hat{b}_{k'}(m-1)\, w_{k'}\{\mathbf{R}\}_{k',k}\} \tag{3-15}$$

where $\{\mathbf{R}\}_{k',k}$ is the (k', k)-component of $\mathbf{R}$. Hence, the multistage algorithm is a canceller that uses the previous stage decisions to cancel the interference of all other users from the matched filter output, and then use a conventional signum detector. This scheme is sometimes referred to as a parallel cancellation scheme, since all users are canceled at the same time (in parallel). Observe, that it is easier (less complex) to implement (3-15) than using the expression for $\hat{b}_k(m)$ in Table 3-2.

The type of iteration that is used, with the ML criterion as a measure, gives peculiarly looking decision spaces. As seen in Figure 3-2, the decision lines are the same as for the ML receiver (compare Figure 3-2) but for the two closed regions in the middle, labelled C and D. Observe also that these occur because some decision errors in the first stage are fed into the iteration, forcing the detector to the wrong region. Since, the decision lines

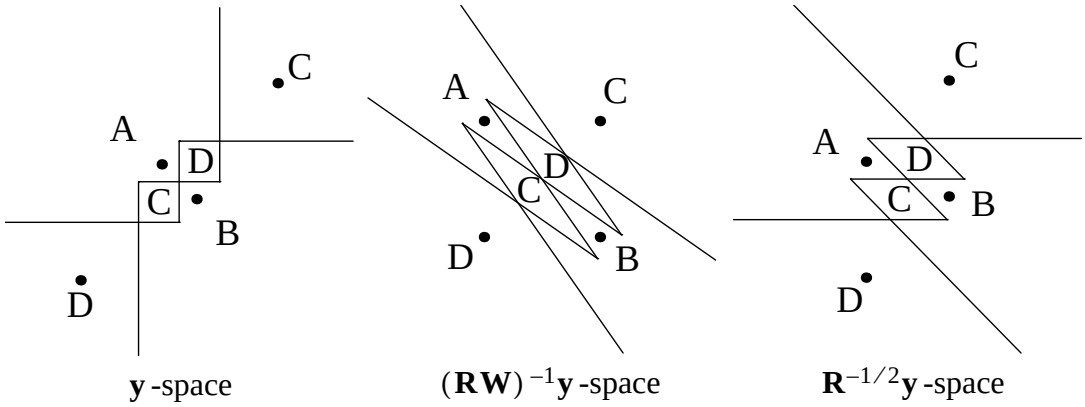

Figure 3-6. Decision spaces for the multistage receiver ($\alpha = 2$) with the conventional receiver as the first stage. The system has K=2 users and the cross-correlation between the users is equal to 0.7.

essentially are the same as for the ML receiver, the multistage receiver is near-far resistant.

The Successive Interference Cancellation Receiver

In the previous section a multistage or parallel cancellation receiver was presented. It is also possible to design a successive cancellation scheme. The *successive Interference Cancellation* (IC) scheme [47] finds the user with the strongest influence on the received signal, detects it and cancels it from the received signal. Now the strongest remaining user is detected and canceled. This algorithm iterates until all users are detected. Mathematically this can be expressed as in Table 3-3.

Here $\{\mathbf{R}\}_k$ is the kth column of $\mathbf{R}$. Observe that the algorithm use estimates, $\widehat{b_k w_k}$, of the product, $b_k w_k$. A simple estimate is to use the matched filter outputs [47], that is, $\widehat{b_k w_k} = y_k^{(s)}$. However, due to this suboptimal estimator, the performance is in some cases worse than the conventional receiver, see Figure 3-9. Another possible estimate is to use the decisions, $\widehat{b_k w_k} = \hat{b}_k w_k$, that is, we assume perfect estimates of the amplitudes of the users. If all users have the same power and if the cross-correlations between all users are equal and positive, the IC algorithm using this type of estimates, is equivalent to the ML optimal receiver [32].

Also, in this case of interference cancellation it is useful to draw the decision space, see Figure 3-2. Since the ordering of decisions are made dynamically (first test in step 2 of the algorithm), it is easy to show that the IC in

this case (two users) is equivalent to the decorrelator. This is, however, only true for two users. The IC with signum decisions, on the other hand, is identical to the ML receiver, as stated earlier.

Table 3-3. The Successive Interference Cancellation algorithm.

1. $\mathbf{y}^{(1)} = \mathbf{y}$, $\Omega = \{1, 2, \ldots, K\}$.

2. **repeat for** s=1,...,K

$$k = \arg\max_{\forall k' \in \Omega} \left| y_{k'}^{(s)} \right|$$

$$\hat{b}_k = \operatorname{sgn}(y_k^{(s)})$$

$$\Omega = \Omega \backslash \{k\}$$

$$\mathbf{y}^{(s+1)} = \mathbf{y}^{(s)} - \hat{b_k} w_k \cdot \{\mathbf{R}\}_k$$

end repeat

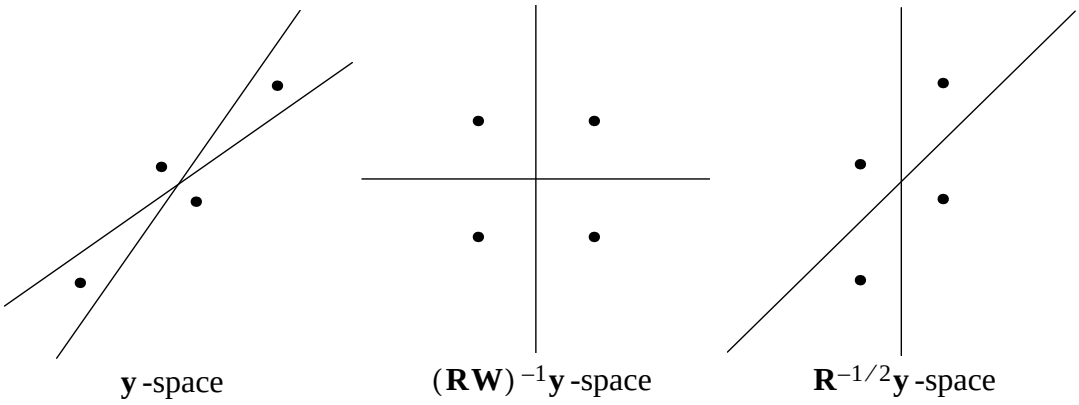

Figure 3-7. Decision spaces for the successive interference cancellation receiver in a system with K=2 users and the cross-correlation between the users equal to 0.7.

3-5 PERFORMANCE IN AWGN CHANNELS

To exemplify the described receivers and their relative performance on an AWGN channel, we have simulated a system with $K = 4$ users and the cross-correlation matrix

$$\mathbf{R} = \frac{1}{7}\begin{bmatrix} 7 & -1 & 3 & 3 \\ -1 & 7 & 3 & -1 \\ 3 & 3 & 7 & -1 \\ 3 & -1 & -1 & 7 \end{bmatrix}. \tag{3-16}$$

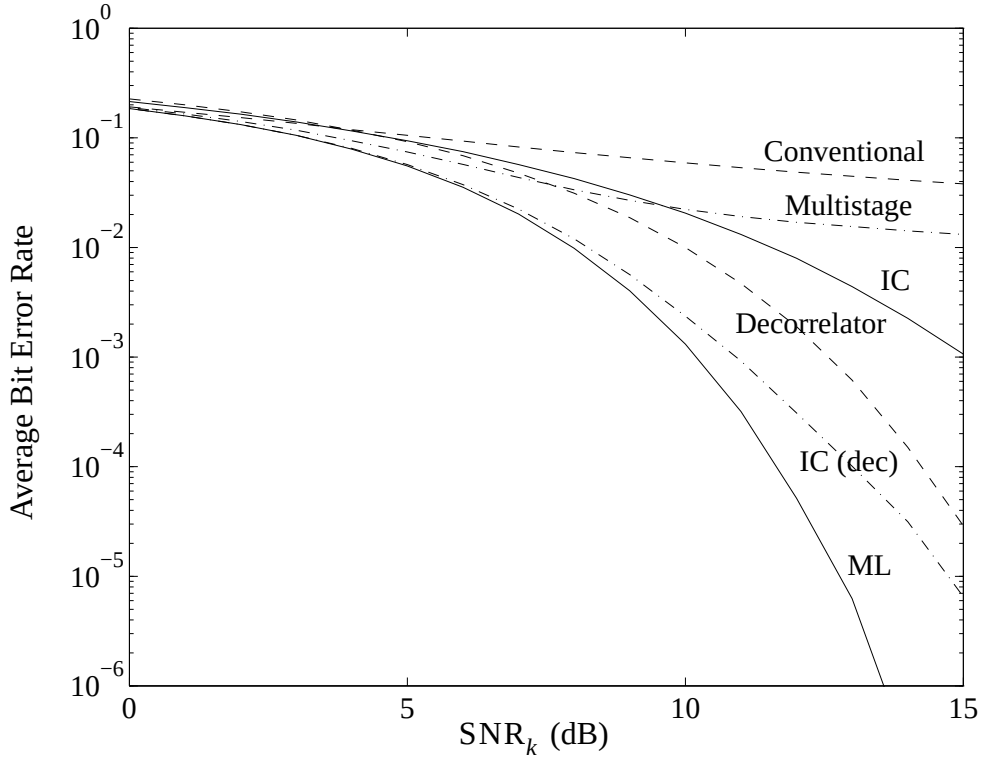

Figure 3-8. Average bit error rate for different multiuser receivers with $K = 4$.

The IC algorithm uses either the matched filter outputs as estimates (labeled "IC") or the decision estimates (labeled "IC (dec)"), and the multistage receiver begins with a conventional receiver, followed by one iteration. In Figure 3-8, we show the average bit error rate versus the signal-to-noise ratio, $SNR_k = w_k^2/\sigma^2$, for equally strong users. Observe, that the ML optimum receiver treated in this chapter optimizes the symbol error, and therefore not optimal regarding the bit error rate. As seen in Figure 3-8, the ML optimal receiver outperforms the other receivers. The decorrelator is better than the multistage and successive interference cancellation receivers (with matched filter outputs as estimates, labeled "IC") for high signal-to-noise ratios. However, if the cross-correlations between the users are low, for example, if selected Gold sequences are used, the multistage and successive interference cancellation receivers will outperform the decorrelator [1].

Observe, that the interference cancellation scheme using decisions in the cancellation (labeled “IC(dec)”) performs much better than the other IC scheme. This is due to the perfect knowledge of the amplitudes of the users. The conventional receiver has worst performance, except for very low signal-to-noise ratios, where the noise enhancement of the decorrelator makes it worse.

As for the near-far resistance of the different detectors, we have simulated a system with four users and the same cross-correlation matrix as above. The signal-to-noise ratio for user one is fixed to $\mathrm{SNR}_1 = 10$ dB. However, the other users have all same power but this power level is varied such that different near-far ratios are obtained. That is, $\mathrm{SNR}_k - \mathrm{SNR}_1$ is altered, and the bit error rate of user one is monitored. The result is shown in Figure 3-9. As expected, we see that the decorrelator is insensitive to near-far effects and has a constant bit error performance. Also, the multistage detector and of course the ML detector are near-far resistant as well. However, neither the conventional nor the interference cancellation detectors are near-far resistant, and the IC detector is even worse than the conventional for high near-far ratios. It can also be observed that the IC detector is worse than the conventional detector at very low near-far ratios, and this is due to the simple estimation procedure, when selecting the strongest user. If user 1 was chosen at all times, the IC and the conventional receiver would be the same for this user, since the first step in the IC is a conventional receiver for the strongest user. Furthermore, if the IC algorithm with decisions and perfect knowledge of the amplitudes of the users is used (labeled “IC (dec)”), the performance is much better. The knowledge of the amplitudes of the users must in practise be replaced by estimates. However, also the ML-MUD and the Multistage detectors assume perfect knowledge of $\mathbf{W}$ and $\mathbf{R}$. The decorrelator and the IC, on the other hand, only assume that $\mathbf{R}$ is known and the conventional receiver only assumes that the code of the user to detect is known.

3-6 ASYNCHRONOUS CDMA AND MULTIPATH FADING

The model used in this chapter is valid only for the synchronous AWGN channel, but it is possible to extend the model to asynchronous channels and channels with multipath, and it is possible to derive multiuser detectors for

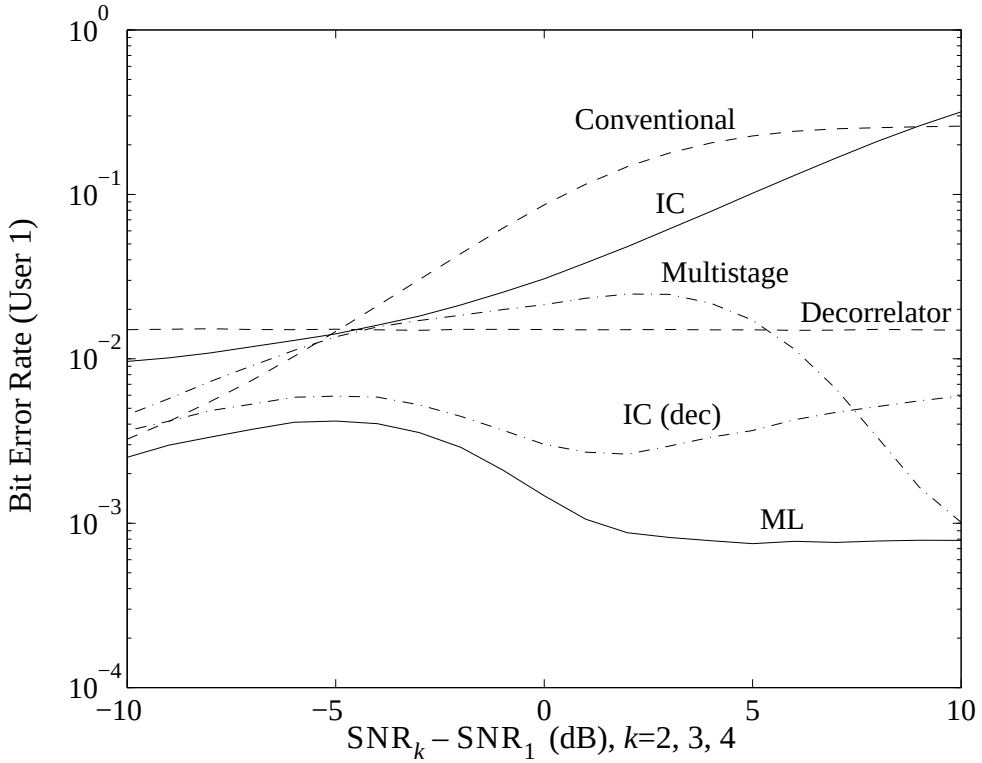

Figure 3-9. Near-far resistance for different multiuser detectors. Plotted is the bit error probability for user 1, which has a fixed signal-to-noise ratio SNR_1=10 dB. The other users vary their power according to the abscissa.

these cases. For further reading on this subject see for example [13], [39], [40], [47], [71], [73] and [77] and references therein.

CHAPTER
4

SOFT MULTIUSER DECODING FOR VECTOR QUANTIZATION

4-1 INTRODUCTION

A communication system is usually designed for data transmission, and thus the assumptions of independent and equally likely transmitted bits are most often valid. However, many of these systems are then used for speech and image communications, in which such assumptions are generally not valid. The solution is to take the source statistics into account in designing the receiver.

Furthermore, most system components, such as source encoder/decoder, channel encoder/decoder and modulator/demodulator, are generally optimized separately. For example, the modulation format is decided and a detector derived. Then a channel coding scheme is applied to the system, assuming now that the modulator/detector is a part of the channel and therefore fixed. Finally the source encoder/decoder pair is designed, typically for a binary symmetric channel. According to information theory [56], this tandem strategy (system components in cascade), see Figure 4-1, is optimal for most channels if the code lengths of both the source and channel codes are infinitely long. This would however require infinite delay, making two-way communications impossible. Hence, it may be possible to get a better overall performance if joint optimization is used. It has, for example, been shown that combined source-channel coding, see Figure 4-2, for vector quantization (VQ) can give a considerable performance gain over the tan-

dem approach at a specific transmission rate, finite decoding delay and moderate complexity (for example, [15], [25] and [37]).

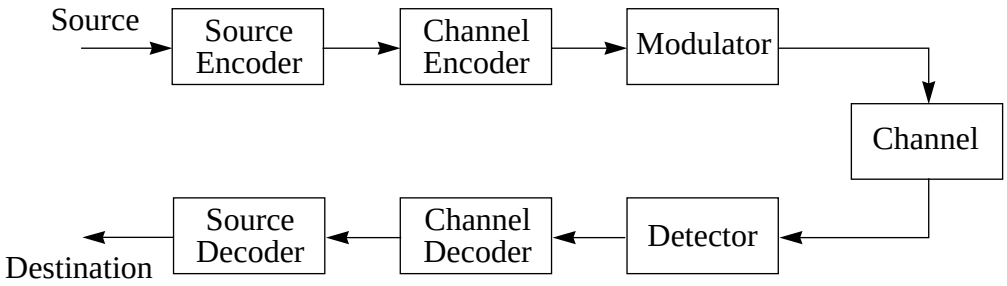

Figure 4-1. Communication model. Tandem approach.

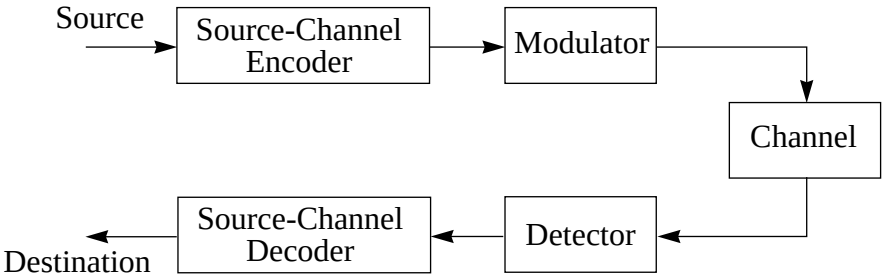

Figure 4-2. Communication model. Approach for combined source-channel coding.

However, such optimization is still suboptimal, because the modulator and detector are optimized separately, if optimized at all. To get around this, either side information from the detector can be used in the decoding of the source-channel codes or a joint optimization of the detector and the source-channel decoder can be carried out, see Figure 4-3. This has successfully been done for single-user AWGN and Rayleigh fading channels in [37] [38] [57] [58] and [69], as well as for channels with intersymbol interference in [29] and [63].

A multiuser communication system, see Figure 4-4 is essentially several independent or dependent parallel channels, one for each user. For FDMA and TDMA these channels are independent (if frequency or time guard intervals, respectively are used). Hence, it is no use to optimize the system with respect to all users. In CDMA however, the multiple access channel introduces cross-correlations between the users, and thus it may be possible

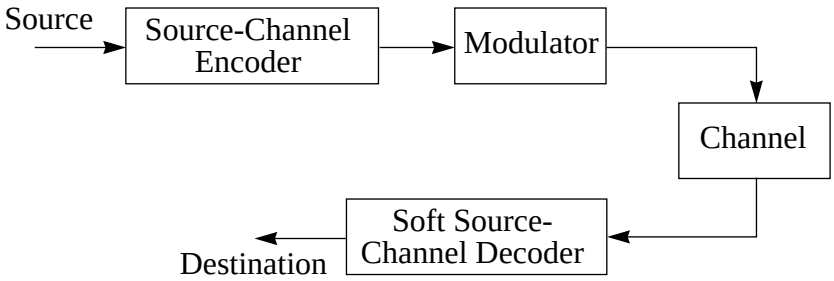

Figure 4-3. Communication model. Approach for jointly optimized detection and source-channel decoding.

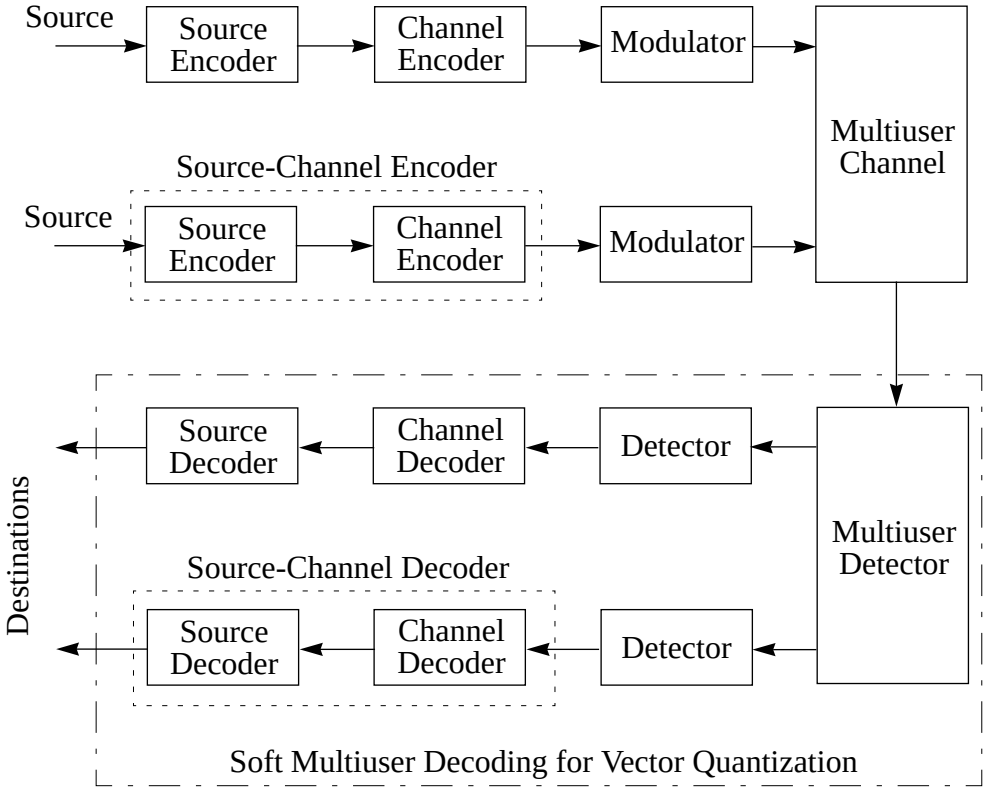

Figure 4-4. Multiuser communication model.

to improve the performance through joint optimization of the multiuser detector and the source-channel decoders. To the best of our knowledge the first work considering this kind of optimization in multiuser systems is [61] and [62] by Skoglund and Ottosson, where the optimum and several suboptimal receivers were derived for the synchronous CDMA channel corrupted

by additive white Gaussian noise. We will, for example, show that it is possible to solve the optimization, and get a considerable performance gain compared to the optimal tandem approach.

We will assume that the reader is familiar with basic source coding theory, and especially vector quantization. For a good introduction to this subject, we recommend [20] and [22]. Also, as description of the vector quantizers, we will use the Hadamard transform representation due to Hedelin et. al., which is thoroughly treated in [25] (a short description is also available in the Appendix 4A). For a treatment of multiuser detection for synchronous CDMA channels, see chapter 3, of this thesis.

4-2 MODELS AND ASSUMPTIONS

The model of a synchronous CDMA multiuser communication system, with K users, is shown in Figure 4-5. User k produces a d-dimensional sample vector, $\mathbf{x}_k$, which is encoded into an index $I_k \in \{0, 1, \ldots, N-1\}$ by the *encoder* of user k, using the condition

$$\left\| \mathbf{x}_k - \mathbf{c}_{I_k}^{(k)} \right\| \leq \left\| \mathbf{x}_k - \mathbf{c}_{i'}^{(k)} \right\|, \forall i' , \tag{4-1}$$

where $\mathbf{c}_i^{(k)}$ is the ith encoder centroid of user k, defined as

$$\mathbf{c}_i^{(k)} = E\left[\mathbf{x}_k \middle| I_k = i\right] . \tag{4-2}$$

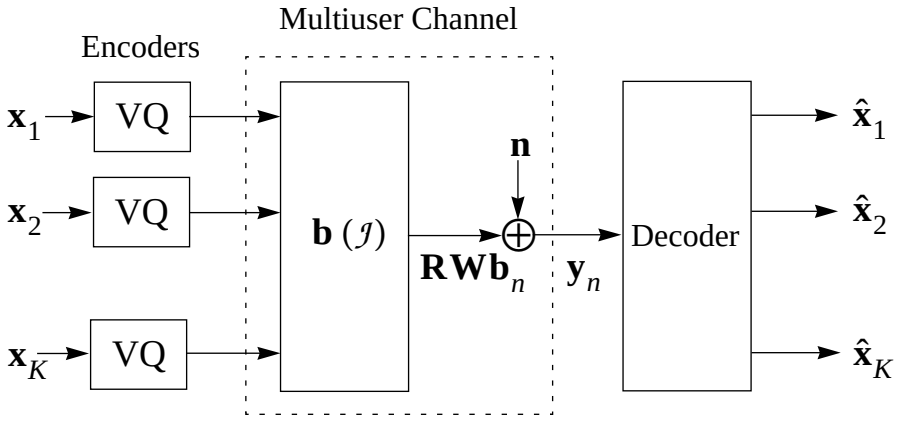

Figure 4-5. Multiuser communication system.

Note that $\mathbf{c}_i^{(k)}$ is the MMSE estimate ([68], page 56) of $\mathbf{x}_k$ given $I_k = i$. Thus, for a vector quantizer with a mean squared error distortion measure, the centroids, $\mathbf{c}_i^{(k)}$, are the optimal reconstruction vectors for the noiseless channel [20]. If the Hadamard representation of the vector quantizer is used (see Appendix 4A and [25]), the centroids can be written as

$$\mathbf{c}_i^{(k)} = \mathbf{T}_k \mathbf{h}_i^{(N)} \tag{4-3}$$

where $\mathbf{T}_k$ is a real-valued transform matrix, and $\mathbf{h}_i^{(N)}$ denotes the ith column vector of a size N by N Hadamard matrix[1]. In the following we will assume that the vector quantizers are known, that is, the centroids and the index probabilities $P_i^{(k)} = \Pr(I_k = i)$ are known. We also assume that the sources of the different users are independent, which is reasonable for most applications. The *encoder entropy* of user k is defined as

$$H_k = -\sum_{l=0}^{N-1} P_l^{(k)} \log_2 P_l^{(k)} . \tag{4-4}$$

The maximum entropy [11] of encoder k is $H_k = \log_2 N$, which we refer to as *full* encoder entropy.

The index I_k is converted into a block $(b_L(I_k), \ldots, b_1(I_k))$ of $L = \log_2 N$ bits in BPSK format, that is $b_n(I_k) \in \{\pm 1\}$. For simplicity we assume that all users have the same block length L. For notational reasons we construct an augmented index $\mathcal{I}$, where user K define the L most significant bits of $\mathcal{I}$ and the bits of user 1 the L least significant bits of $\mathcal{I}$, that is

$$\mathcal{I} \leftrightarrow (b_L(I_K), \ldots, b_1(I_K), \ldots, b_L(I_1), \ldots, b_1(I_1)) . \tag{4-5}$$

The corresponding index probabilities are now given as $P_j = \Pr(\mathcal{I} = j)$. In the same way we define an augmented sample vector $\mathbf{x}$ as

1. The Hadamard vector $\mathbf{h}_i^{(N)}$ is, by definition, obtained from the bit representation of i as $\mathbf{h}_i^{(N)} = (1, b_L(i))^T \otimes \ldots \otimes (1, b_1(i))^T$, where $\otimes$ is the Kronecker product (see Appendix 4B for the definition and properties). Furthermore, the transform matrix, $\mathbf{T}_k$, is given by $\mathbf{T}_k = (1/N)\mathbf{C}^{(k)}\mathbf{H}_N$, where $\mathbf{C}^{(k)} = [\mathbf{c}_0^{(k)}, \ldots, \mathbf{c}_{N-1}^{(k)}]$ and $\mathbf{H}_N = [\mathbf{h}_0^{(N)}, \ldots, \mathbf{h}_{N-1}^{(N)}]$ (see Appendix 4A).

$$\mathbf{x} = (\mathbf{x}_1^T, \mathbf{x}_2^T, \ldots, \mathbf{x}_K^T)^T \tag{4-6}$$

and the corresponding augmented centroid vectors $\mathbf{c}_j$ as[1]

$$\mathbf{c}_j = ((\mathbf{c}_{i_1}^{(1)})^T, (\mathbf{c}_{i_2}^{(2)})^T, \ldots, (\mathbf{c}_{i_K}^{(K)})^T) . \tag{4-7}$$

At the transmitter the bits of the user indices are transmitted one by one over a symbol synchronous DS/CDMA channel. Thus, the matched filter outputs of the received signal $\mathbf{y}_n = (y_n(1), y_n(2), \ldots y_n(K))^T$, at time n, can be expressed as (see Chapter 3, equation (3-3))

$$\mathbf{y}_n = \mathbf{RWb}_n(\jmath) + \mathbf{n}, \tag{4-8}$$

where $\mathbf{R}$ is the cross-correlation matrix and $\mathbf{W}$ is a diagonal matrix of user amplitudes w_k. The bits of the users at time n are contained in the vector $\mathbf{b}_n(\jmath) = (b_n(I_1), \ldots, b_n(I_K))^T$. The channel noise term, $\mathbf{n}$, is Gaussian with zero mean and covariance matrix $\sigma^2\mathbf{R}$.

4-3 THE OPTIMAL MULTIUSER DECODER

The optimum decoder measures $\mathbf{Y} = [\mathbf{y}_1, \mathbf{y}_2, \ldots, \mathbf{y}_L]$ for a transmitted index $\jmath$. Using the minimum mean squared error as distortion measure, the optimum receiver minimizes

$$D_k = E\|\mathbf{x}_k - \hat{\mathbf{x}}_k(\mathbf{Y})\|^2 \tag{4-9}$$

for each user k. Since this distortion measure is additive, minimizing

$$\sum_{k=1}^{K} D_k = \sum_{k=1}^{K} E\|\mathbf{x}_k - \hat{\mathbf{x}}_k(\mathbf{Y})\|^2 \tag{4-10}$$

---

1. Now the centroids can be represented by $\mathbf{c}_j = \mathbf{T}\mathbf{h}_j^{(M)}$, where $M = 2^{KL}$, and the Hadamard vector is given by $\mathbf{h}_j^{(M)} = (1, b_{KL}(j))^T \otimes \ldots \otimes (1, b_1(j))^T$, that is $\mathbf{h}_j^{(M)} = \mathbf{h}_{i_K}^{(N)} \otimes \ldots \otimes \mathbf{h}_{i_1}^{(N)}$. The transform matrix $\mathbf{T}$ is given in the same way as before.

is equivalent to minimizing the individual D_k separately. Hence, we have from estimation theory ([68], page 56) that the estimate of the augmented sample vector $\mathbf{x}$ is

$$\hat{\mathbf{x}}(\mathbf{Y}) = E[\mathbf{x}|\mathbf{Y}], \tag{4-11}$$

which can be rewritten, using the Hadamard representation as

$$\hat{\mathbf{x}}(\mathbf{Y}) = E[\mathbf{c}_j|\mathbf{Y}] = \mathbf{T} \cdot E\left[\mathbf{h}_j^{(M)}\middle|\mathbf{Y}\right] = \mathbf{T}\hat{\mathbf{h}}(\mathbf{Y}), \tag{4-12}$$

where $\mathbf{c}_j$ is a centroid in the augmented vector quantizer of all users. Using the definition of expectation we get

$$\hat{\mathbf{h}}(\mathbf{Y}) = \frac{\sum_j \mathbf{h}_j^{(M)} p(\mathbf{Y}|j) P_j}{\sum_j p(\mathbf{Y}|j) P_j}, \tag{4-13}$$

where $p(\mathbf{Y}|j)$ is the probability density function of the random variable $\mathbf{Y}$ given the index j. Inserting the pdf

$$p(\mathbf{Y}|j) = \lambda \exp\left(-\frac{1}{2\sigma^2}\sum_{n=1}^{L}(\mathbf{RWb}_n - \mathbf{y}_n)^T\mathbf{R}^{-1}(\mathbf{RWb}_n - \mathbf{y}_n)\right) \tag{4-14}$$

where $\lambda = (2\pi\sigma^2|\mathbf{R}|)^{-KL/2}$ into (4-13), cancelling common factors in the nominator and denominator and introducing the function

$$g(j) = \exp\left(-\frac{1}{2\sigma^2}\sum_{n=1}^{L}\mathbf{b}_n^T(j)\,\mathbf{WRWb}_n(j)\right) \tag{4-15}$$

the estimate $\hat{\mathbf{h}}(\mathbf{Y})$ from (4-13) can be written as

$$\hat{\mathbf{h}}(\mathbf{Y}) = \frac{\sum_j \mathbf{h}_j^{(M)} P_j g(j) \exp\left(\sigma^{-2}\sum_n \mathbf{y}_n^T\mathbf{Wb}_n(j)\right)}{\sum_j P_j g(j) \exp\left(\sigma^{-2}\sum_n \mathbf{y}_n^T\mathbf{Wb}_n(j)\right)}. \tag{4-16}$$

Observing that

$$\sum_n \mathbf{y}_n^T \mathbf{W} \mathbf{b}_n(j) = \sum_{n,k} w_k b_n(i_k) y_n(k) \tag{4-17}$$

and using the equality $e^{ax} = \cosh(x)\,(1 + a \cdot \tanh(x))$ for $a \in \{-1, 1\}$ (Appendix 4C and [46]) we have

$$\begin{aligned}
&\exp\left(\sigma^{-2} \sum_{n,k} w_k b_n(i_k) y_n(k) \right) = \\
&\prod_{n,k} \exp\left(\sigma^{-2} w_k b_n(i_k) y_n(k)\right) = \\
&\prod_{n,k} \cosh\left(\sigma^{-2} w_k y_n(k)\right)\left(1 + b_n(i_k) \tanh\left(\sigma^{-2} w_k y_n(k)\right)\right) = \\
&C \cdot \prod_{n,k} \left(1 + b_n(i_k) \tanh\left(\sigma^{-2} w_k y_n(k)\right)\right) = C \cdot \mathbf{h}_j^T \cdot \hat{\mathbf{p}}(\mathbf{Y})
\end{aligned} \tag{4-18}$$

where C is a constant with respect to the transmitted data. The vector $\hat{\mathbf{p}}(\mathbf{Y})$ is defined by

$$\begin{cases} \hat{\mathbf{p}}(\mathbf{Y}) = \hat{\mathbf{p}}_K \otimes \ldots \otimes \hat{\mathbf{p}}_1 \\ \hat{\mathbf{p}}_k = \begin{bmatrix} 1 \\ \hat{b}_L(k) \end{bmatrix} \otimes \ldots \otimes \begin{bmatrix} 1 \\ \hat{b}_1(k) \end{bmatrix} \end{cases} \tag{4-19}$$

where

$$\hat{b}_n(k) = \tanh\left(\sigma^{-2} w_k y_n(k)\right). \tag{4-20}$$

Observe that $\hat{b}_n(k)$ is an estimate of the transmitted bit $b_n(I_k)$, which takes on values in the interval $(-1, 1)$.

Finally, inserting (4-18) and (4-16) into (4-12), the estimator $\hat{\mathbf{x}}(\mathbf{Y})$ is given by

$$\hat{\mathbf{x}}(\mathbf{Y}) = \mathbf{T} \cdot \frac{\mathbf{R_{hh}}}{\mathbf{m}_\mathbf{h}^T \cdot \hat{\mathbf{p}}(\mathbf{Y})} \cdot \hat{\mathbf{p}}(\mathbf{Y}) \tag{4-21}$$

where

$$\begin{cases} \mathbf{R_{hh}} = \sum_j P_j g(j)\, \mathbf{h}_j \mathbf{h}_j^T \\ \mathbf{m_h} = \sum_j P_j g(j)\, \mathbf{h}_j \end{cases} \tag{4-22}$$

Note that $\mathbf{R_{hh}} = E[g(\mathcal{J})\,\mathbf{h}_{\mathcal{J}}\mathbf{h}_{\mathcal{J}}^T]$ and $\mathbf{m_h} = E[g(\mathcal{J})\,\mathbf{h}_{\mathcal{J}}]$, where the expectations are taken over the statistics of the transmitted VQ-indices. Furthermore, $\hat{\mathbf{p}}(\mathbf{Y})$ is independent of the set $\{P_j\}$, and thus, the a-priori index information is confined to $\mathbf{R_{hh}}$ and $\mathbf{m_h}$. Note also that the MMSE decoding is based on the bit-estimates of (4-20), and that the estimates $\hat{b}_n(k)$ are only dependent on $y_n(k)$. Hence, in the calculation of $\hat{\mathbf{p}}$ the channel can be regarded as K independent channels, where the vector $\hat{\mathbf{p}}$ can be viewed as an estimate of the "transmitted" value of $\mathbf{h}_j^{(M)}$. This under the assumptions of full encoder entropies and independent channels (i.e. orthogonal code sequences). To modify the vector $\hat{\mathbf{p}}$ to account for the source statistics and the correlation between users, $\hat{\mathbf{p}}$ is mapped and scaled by the matrix $[\mathbf{m}_\mathbf{h}^T \cdot \hat{\mathbf{p}}(y)]^{-1}\mathbf{R_{hh}}$. We name the decoder (4-21) the *Hadamard-based Soft Multiuser Decoder* (HSMUD). Since the HSMUD is MSE-optimal it shows how to utilize the a-priori and channel information in an optimal fashion to counteract channel noise and multiuser interference.

On the basis of the recursive nature of the Hadamard matrix, an algorithm for computing $\hat{\mathbf{h}}(\mathbf{Y})$ was derived in [58]. The algorithm requires an asymptotic order of $KL \cdot 2^{KL}$ operations to compute $\hat{\mathbf{h}}(\mathbf{Y})$ from $\mathbf{Y}$. Finally, for decoding, a matrix multiplication is needed to obtain $\hat{\mathbf{x}}(\mathbf{Y})$. The transform matrix $\mathbf{T}$ is sparse in a way that allows this additional operation to be performed in an order of $K \cdot d \cdot N$ operations.

4-4 SUBOPTIMUM DECODERS

The Single-User Decoder

In this section we consider the decoding of one user, user *k*, under the assumption that the source statistics of the *other* users are unknown. In this case, we assume that the encoder outputs of the other users have uniform probability masses. That is, these users have full encoder entropies. The result is a decoder giving a lower computational complexity than that of (4-

21) and therefore well suited for the decoding of a single user in a mobile station.

As in the derivation of the HSMUD, we express the encoder centroid of user k as $\mathbf{c}_i^{(k)} = \mathbf{T}_k \mathbf{h}_i^{(N)}$ where $\mathbf{T}_k$ is the transform matrix for user k. Now, consider the decoding of user k, under the assumption that $P_i^{(k')} = 2^{-L}$ for $k' \neq k$. Since

$$\mathbf{h}_j^{(M)} = \mathbf{h}_{i_K}^{(N)} \otimes \mathbf{h}_{i_{K-1}}^{(N)} \otimes \ldots \otimes \mathbf{h}_{i_1}^{(N)}, \tag{4-23}$$

the vector $\hat{\mathbf{h}}_k(\mathbf{Y})$ consists of N elements counted from the $(K-k)N+1$ element from the top of the vector $\mathbf{h}_j^{(M)}$. Starting from the optimal decoder (4-13), and using the orthogonality of the Hadamard columns ($\mathbf{h}_m^T \mathbf{h}_n = N \cdot \delta_{mn}$) we get [46]:

$$\hat{\mathbf{h}}(\mathbf{Y}) = \frac{\sum_j \mathbf{h}_j^{(M)} p(\mathbf{Y}|j) P_j}{\sum_j p(\mathbf{Y}|j) P_j} = \frac{\sum_j P_j \mathbf{h}_j^{(M)} (\mathbf{h}_j^{(M)})^T \sum_\ell \mathbf{h}_\ell^{(M)} p(\mathbf{Y}|\ell)}{\sum_j P_j (\mathbf{h}_j^{(M)})^T \sum_\ell \mathbf{h}_\ell^{(M)} p(\mathbf{Y}|\ell)} \tag{4-24}$$

Now using properties of the Hadamard transform and the Kronecker product it is possible to proceed according to

$$\begin{aligned}
&\sum_j P_j \mathbf{h}_j^{(M)} (\mathbf{h}_j^{(M)})^T = (a) \\
&\sum_j P_j (\mathbf{h}_{i_K}^{(N)} \otimes \ldots \otimes \mathbf{h}_{i_1}^{(N)}) ((\mathbf{h}_{i_K}^{(N)})^T \otimes \ldots \otimes (\mathbf{h}_{i_1}^{(N)})^T) = (b) \\
&\sum_j (P_{i_K} \mathbf{h}_{i_K}^{(N)} (\mathbf{h}_{i_K}^{(N)})^T) \otimes \ldots \otimes (P_{i_1} \mathbf{h}_{i_1}^{(N)} (\mathbf{h}_{i_1}^{(N)})^T) = (c) \\
&\left(\sum_{i_K} P_{i_K} \mathbf{h}_{i_K}^{(N)} (\mathbf{h}_{i_K}^{(N)})^T \right) \otimes \ldots \otimes \left(\sum_{i_1} P_{i_1} \mathbf{h}_{i_1}^{(N)} (\mathbf{h}_{i_1}^{(N)})^T \right) = \\
&\mathbf{R}_{\mathbf{hh}}(K) \otimes \ldots \otimes \mathbf{R}_{\mathbf{hh}}(1)
\end{aligned} \tag{4-25}$$

where (a) is from the definition of $\mathbf{h}_j^{(M)}$ and (b) using basic algebra for Kronecker products (the theorems 4 and 6 in Appendix 4B) and that the different indices i_k are independent, and (c) from the theorem 2 in Appendix 4B (algebra for Kronecker products).

Also observe that, since for $k' \neq k$, we have that $P_{i_{k'}} = N^{-1}$ and therefore

$$\mathbf{R}_{\mathbf{hh}}(k') = \frac{1}{N} \cdot \sum_{i_{k'}} \mathbf{h}_{i_{k'}}^{(N)} (\mathbf{h}_{i_{k'}}^{(N)})^T = \frac{1}{N} \cdot N \cdot \mathbf{I}_N = \mathbf{I}_N \tag{4-26}$$

where $\mathbf{I}_N$ is the identity matrix of size N. In the same way we get for the expression

$$\begin{aligned} &\sum_j P_j (\mathbf{h}_j^{(M)})^T = \\ &\quad \left(\sum_{i_K} P_{i_K} (\mathbf{h}_{i_K}^{(N)})^T \right) \otimes \ldots \otimes \left(\sum_{i_1} P_{i_1} (\mathbf{h}_{i_1}^{(N)})^T \right) = \\ &\quad \mathbf{m}_{\mathbf{h}}^T(K) \otimes \ldots \otimes \mathbf{m}_{\mathbf{h}}^T(1) \end{aligned} \tag{4-27}$$

where we, due to the balance property of the Hadamard matrix, observe that

$$\mathbf{m}_{\mathbf{h}}(k') = \frac{1}{N} \cdot \sum_{i_{k'}} \mathbf{h}_{i_{k'}}^{(N)} = \mathbf{0}. \tag{4-28}$$

Hence, the estimated Hadamard column, $\hat{\mathbf{h}}(\mathbf{Y})$, can be expressed as

$$\hat{\mathbf{h}}(\mathbf{Y}) = \tag{4-29}$$

$$\frac{(\mathbf{I}_N \otimes \ldots \otimes \mathbf{R}_{\mathbf{hh}}(k) \otimes \ldots \otimes \mathbf{I}_N) \sum_{\ell} (\mathbf{h}_{i_K}^{(N)} \otimes \ldots \otimes \mathbf{h}_{i_1}^{(N)}) p(\mathbf{Y}|\ell)}{(\mathbf{0}^T \otimes \ldots \otimes \mathbf{m}_{\mathbf{h}}^T(k) \otimes \ldots \otimes \mathbf{0}^T) \sum_{\ell} (\mathbf{h}_{i_K}^{(N)} \otimes \ldots \otimes \mathbf{h}_{i_1}^{(N)}) p(\mathbf{Y}|\ell)}$$

and hence, the estimated Hadamard vector, $\hat{\mathbf{h}}_k(\mathbf{Y})$, is

$$\hat{\mathbf{h}}_k(\mathbf{Y}) = \frac{\mathbf{R}_{\mathbf{hh}}(k) \cdot \sum_{\ell} \mathbf{h}_{i_k}^{(N)} p(\mathbf{Y}|\ell)}{\mathbf{m}_{\mathbf{h}}^T(k) \cdot \sum_{\ell} \mathbf{h}_{i_k}^{(N)} p(\mathbf{Y}|\ell)} \tag{4-30}$$

However, it is convenient to rewrite the summation in the last equation using expectations

$$\begin{aligned}
&\sum_{\ell} \mathbf{h}_{i_k}^{(N)} p(\mathbf{Y}|\ell) = \\
&\sum_{\ell} \mathbf{h}_{i_k}^{(N)} \lambda \exp\left(-\frac{1}{2\sigma^2} \sum_{n=1}^{L} (\mathbf{RWb}_n(\ell) - \mathbf{y}_n)^T \mathbf{R}^{-1} (\mathbf{RWb}_n(\ell) - \mathbf{y}_n) \right) \underline{(a)} \\
&\left[\lambda \sum_{\mathbf{b}_L} \begin{bmatrix} 1 \\ b_L(i_k) \end{bmatrix} \exp\left(-\frac{1}{2\sigma^2} (\mathbf{RWb}_L - \mathbf{y}_L)^T \mathbf{R}^{-1} (\mathbf{RWb}_L - \mathbf{y}_L) \right) \right] \otimes \dots \\
&\otimes \left[\lambda \sum_{\mathbf{b}_1} \begin{bmatrix} 1 \\ b_1(i_k) \end{bmatrix} \exp\left(-\frac{1}{2\sigma^2} (\mathbf{RWb}_1 - \mathbf{y}_1)^T \mathbf{R}^{-1} (\mathbf{RWb}_1 - \mathbf{y}_1) \right) \right]
\end{aligned} \tag{4-31}$$

where (a) follows from the definition of $\mathbf{h}_{i_k}^{(N)}$. Introducing the estimates $\hat{b}_n(k)$, defined as

$$\begin{aligned}
\hat{\mathbf{b}}_n(\mathbf{y}_n) &= (\hat{b}_n(1), \dots, \hat{b}_n(K))^T = \\
&E\left[\mathbf{b}_n \middle| \mathbf{y}_n, \Pr(\mathbf{b}_l) = 2^{-K}, \forall l\right]
\end{aligned} \tag{4-32}$$

and inserting (4-32) and (4-31) in (4-30), the MMSE decoder for user *k*, assuming that the indices of the other users are equally probable, is [46]

$$\hat{\mathbf{x}}_k(\mathbf{Y}) = \mathbf{T}_k \cdot \frac{\mathbf{R}_{\mathbf{hh}}(k)}{\mathbf{m}_{\mathbf{h}}^T(k) \cdot \hat{\mathbf{q}}_k(\mathbf{Y})} \cdot \hat{\mathbf{q}}_k(\mathbf{Y}), \tag{4-33}$$

where

$$\begin{cases} \mathbf{R}_{\mathbf{hh}}(k) = E\left[\mathbf{h}_{I_k}^{(N)} (\mathbf{h}_{I_k}^{(N)})^T\right] \\ \mathbf{m}_{\mathbf{h}}(k) = E\left[\mathbf{h}_{I_k}^{(N)}\right] \end{cases}. \tag{4-34}$$

The expectations are taken over the statistics of the index I_k. Furthermore, the vector $\hat{\mathbf{q}}_k(\mathbf{Y})$ is defined by

$$\hat{\mathbf{q}}_k(\mathbf{Y}) = \begin{bmatrix} 1 \\ \hat{b}_L(k) \end{bmatrix} \otimes \ldots \otimes \begin{bmatrix} 1 \\ \hat{b}_1(k) \end{bmatrix}. \tag{4-35}$$

Note that the a-priori information of user k is confined to $\mathbf{R}_{\mathbf{hh}}(k)$ and $\mathbf{m}_{\mathbf{h}}(k)$, and that the expectation of (4-32) is taken under the condition $Pr(\mathbf{b}_l) = 2^{-K}$ for all l, that is, full encoder entropies for *all* users. We will refer to (4-33) as the *single-user version* of the HSMUD.

Since the evaluation of the expectation in (4-32) has a complexity that is $O(K \cdot 2^K)$, the total complexity for decoding of all user vectors, given the value of $\mathbf{Y}$, is $O(KL \cdot 2^K)$. Also, an additional $O(KL \cdot 2^L)$ operations for the calculation of all $\mathbf{h}$, and an order of $K \cdot d \cdot N$ operations for the matrix multiplications, $\mathbf{T}_k\hat{\mathbf{h}}_i$ are needed.

The Approximated Single-User Decoder

In spite of the reduction in complexity for the single-user version, with respect to the HSMUD, it is still exponential in the number of users. When using the expectation of (4-32) in (4-33), the expression

$$\sum_{\mathbf{b} \in \{\pm 1\}^K} \mathbf{b} \cdot \exp\left(-\frac{1}{2\sigma^2} (\mathbf{RWb} - \mathbf{y}_n)^T \mathbf{R}^{-1} (\mathbf{RWb} - \mathbf{y}_n) \right) \tag{4-36}$$

has to be evaluated. The sum in (4-36) is taken over all vertices of the hypercube $\{-1, 1\}^K$. However, many of the terms of the sum will not contribute significantly to the result. Thus, we have examined the limitation of the summation to a sub-set of $\{-1, 1\}^K$. There are a number of ways to choose this sub-set. The approach taken here is to use a decision, $\hat{\mathbf{b}}$, on the value of $\mathbf{b}$ and then evaluate the sum over a limited number of "neighbors" to $\hat{\mathbf{b}}$ (for example, can the Voronoi neighbors be used, Section 3-3). To take the first decision with a reasonable low complexity we use a decorrelating detector (see Section 3-4). This detector has a complexity of $O(K^2)$. Then the summation sub-set is taken to be the α (a positive number less than 2^K) vectors $\mathbf{b}$ with the lowest distance to $\hat{\mathbf{b}}$. As a distance measure between $\mathbf{b}$ and $\hat{\mathbf{b}}$ the value of

$$\left\| \mathbf{R}^{1/2}\mathbf{W}\left(\mathbf{b} - \hat{\mathbf{b}}\right) \right\|^2 \tag{4-37}$$

was used, that is the distance in the whitened signal space. Thus, the vertices to include, given $\hat{\mathbf{b}}$, can be computed in advance and stored (see Section 3-3). Using this approach the complexity for evaluating (4-36) for all L is $O\left(KL \cdot (1+\alpha)\right)$, plus an additional $O\left(KL \cdot 2^L\right)$ operations for the calculation of all $\mathbf{h}$, and the final matrix multiplication is of the order of $K \cdot d \cdot N$ operations. Note that the choice of α depends on the number of users K, for a specific performance. The maximum value of α is $2^K - 1$. For this case we evaluate all points, and therefore the receiver is equivalent to the single-user decoder. The complexity can be further reduced if a conventional detector (matched filter) is used as a first decision.

Maximum Likelihood Multiuser Detection with Table Look-Up VQ Decoding

The conventional maximum likelihood multiuser detector (ML-MUD), see Section 3-3, gives hard decisions on the transmitted bits for all users, $\hat{\mathbf{b}}_L, \ldots, \hat{\mathbf{b}}_1$. For each user k, the bits $\hat{b}_L \ldots, \hat{b}_1$ are converted to the corresponding index $\hat{i}_k$. The decoder then find and output the centroid $\mathbf{c}_{\hat{i}_k}$ [20]. Hence, the complexity of this decoder is $O\left(KL \cdot 2^K\right)$.

4-5 RESULTS

In this section we present results and compare the presented decoders to the standard multiuser detection and VQ decoding. We measure the quality of the noisy channel in terms of the *Channel Signal-to-Noise Ratio* (CSNR), w_k^2/σ^2, where all amplitudes are the same ($w_k = w$). In the simulations we assume perfect knowledge of the CSNR, since the soft decoders are updated with a varying channel quality. In practice, the perfect knowledge has to be replaced by estimates. The reproduction fidelity of the system is given in terms of the output *Signal-to-Noise Ratio* (SNR), $E\|\mathbf{x}\|^2 / E\|\mathbf{x} - \hat{\mathbf{x}}\|^2$. As decoders we used the HSMUD, the single-user decoder and the ML-MUD plus table look-up VQ decoding. In the ML-MUD simulations the decoder is not updated according to the channel quality. This represents the usual approach where the a-priori index information and the channel quality information are not utilized in the decoding. Also included in the simulations is

an upper bound on the performance that was obtained from simulating the HSMUD with orthogonal codes.

First, we trained VQs for a noiseless channel. In these cases the VQ encoders have almost full entropies. The *encoders* of these VQs were then used in comparing the different decoders. The sources were modeled as first order Gauss-Markov processes with correlation 0.9 between samples. The correlation matrices used are

$$\mathbf{R}_2 = \begin{bmatrix} 1 & 0.7 \\ 0.7 & 1 \end{bmatrix} \text{ and } \mathbf{R}_4 = \frac{1}{7}\begin{bmatrix} 7 & -1 & 3 & 3 \\ -1 & 7 & 3 & -1 \\ 3 & 3 & 7 & -1 \\ 3 & -1 & -1 & 7 \end{bmatrix} \tag{4-38}$$

for two and four users.

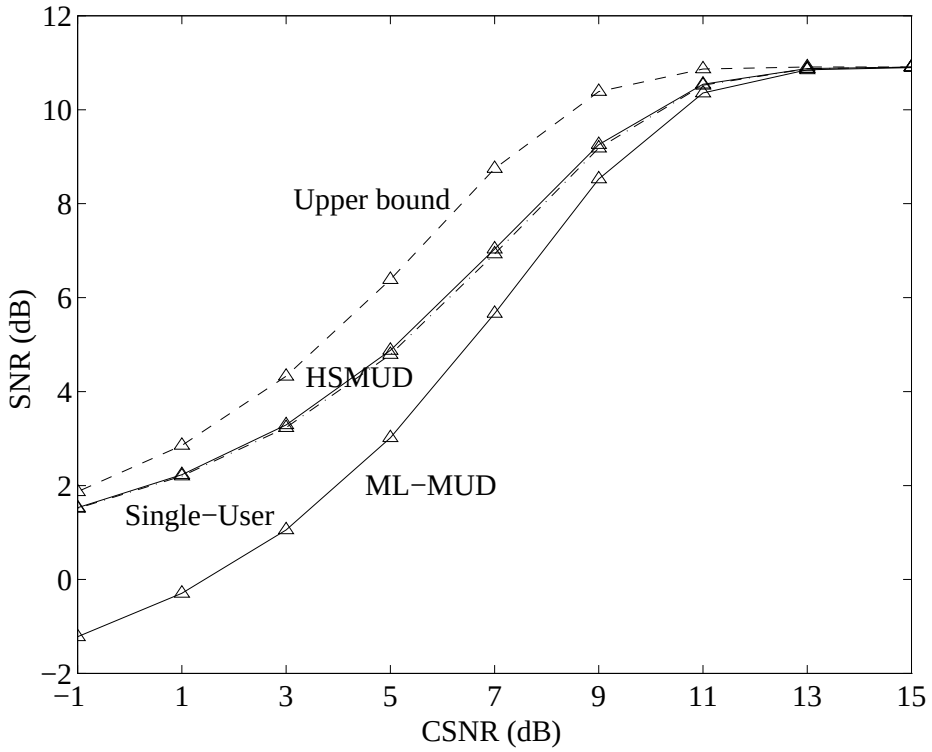

Figure 4-6. Signal-to-noise ratio for a system with two users (average SNR), $d = 6$ and $L = 6$, $H_k = 5.87$ bits. The single-user decoder (dashdot line) is almost on top of the HSMUD (solid line).

The results are shown in Figure 4-6 and Figure 4-7, for two and four users, respectively. As can be seen, there is a considerable difference between the

performance of the optimal soft decoder and the ML-MUD plus table look-up VQ decoding, both for two and four users. Part of the performance gain of the soft decoders is inherent from the knowledge of the user source statistics and the multiuser interference. Therefore, the performance gain over ML-MUD increases with the interference from the other users as well as with lower VQ output entropy. Also, as has been found for single-user channels ([37] and [57]), the soft decoding alone has a large gain over VQ-decoding based on hard decisions. This is due to the knowledge of the noise variance and that hard ML-decisions destroy information that can be utilized by a soft VQ-decoder.

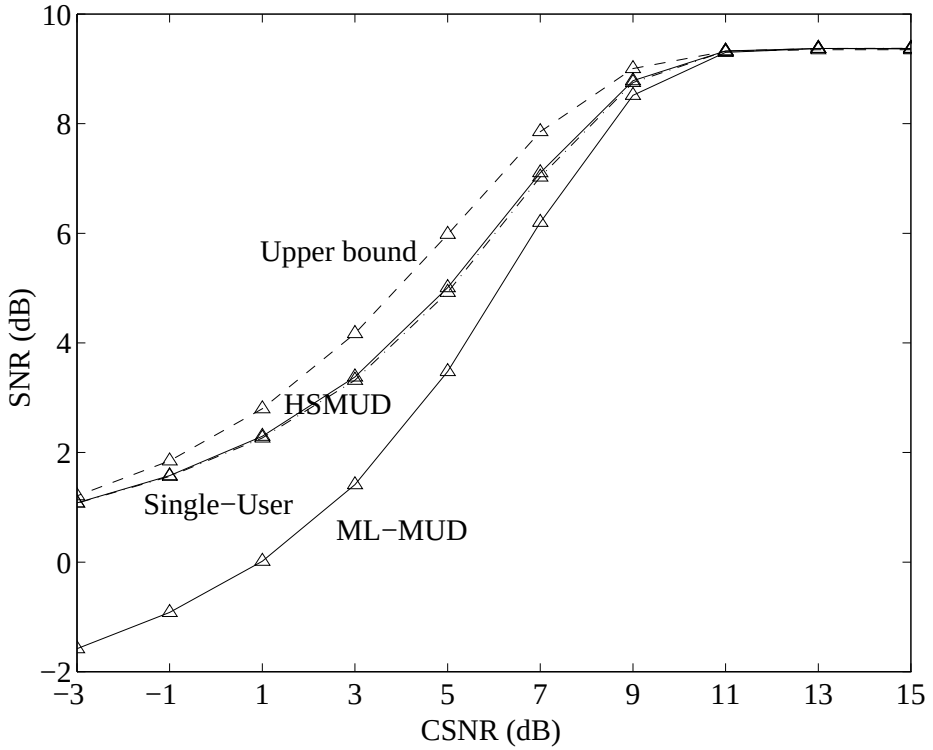

Figure 4-7. Signal-to-noise ratio for system with four users (user 1 is illustrated), $d = 3$ and $L = 3$, $H_k = 2.88$ bits. The curve of the single-user decoder (dashdot line) is almost on top of the HSMUD curve (solid line).

In training a VQ for a noisy channel, referred to as Channel Optimized VQ (COVQ), redundancy is incorporated, resulting in a lower encoder entropy [16]. The redundancy of the transmitted indices counteracts channel imperfections. To exemplify this, we have trained a COVQ with dimension $d = 6$ and block length $L = 6$ for a single-user binary symmetric channel with a bit error probability of 5%, resulting in an encoder output entropy of 4.77 bits (compared to 5.87 bits for a noiseless channel). A bit error rate of

5% corresponds to the two-user CDMA channel and a channel SNR of about 5 dB. Then the *encoder* (the encoder regions) of this COVQ was employed in the simulation giving Figure 4-8. As we can see the gain of the HSMUD is even larger in this case, due to the increased redundancy in the transmitted indices that can be utilized efficiently by the HSMUD. Also in this case the soft algorithms have a large gain in that they are adaptive regarding the channel quality. It can also be observed that even if the COVQs are trained for a certain CSNR, the adaptability of the decoder makes the HSMUD robust against changes in CSNR.

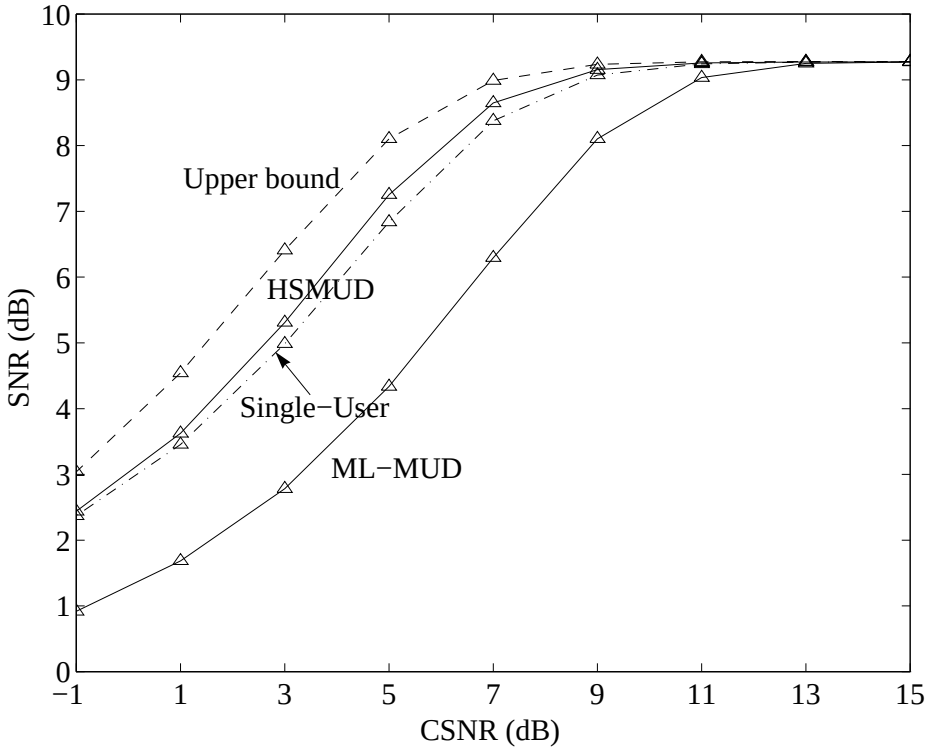

Figure 4-8. Signal-to-noise ratio for a system with two users (average SNR), $d = 6$ and $L = 6$, $H_k = 4.77$ bits.

As can be seen, the difference between the HSMUD and the single-user decoder is almost negligible in the simulations of Figure 4-6 and Figure 4-7. This is due to the facts that the VQ encoders have almost full entropy in these figures. On the other hand, in Figure 4-8 the difference is small but not negligible, due to the lower encoder entropies.

To investigate the difference between the HSMUD and its single-user version further, we have simulated a case with two users where the users have different encoders. In Figure 4-9, user one employs the COVQ encoder used

in Figure 4-8, and user two utilizes the encoder of Figure 4-6. Here we can see that the difference between the HSMUD and the single-user version is notable for user two, and almost negligible for user one. We interpret this observation as follows: In the decoding of user two the single-user version is unaware of the source statistics of user one, while the HSMUD uses the knowledge of both user sources. Thus, the HSMUD can utilize the redundancy of user *one* (which is higher) when decoding user two. However, in the decoding of user one the redundancy of user two is almost negligible.

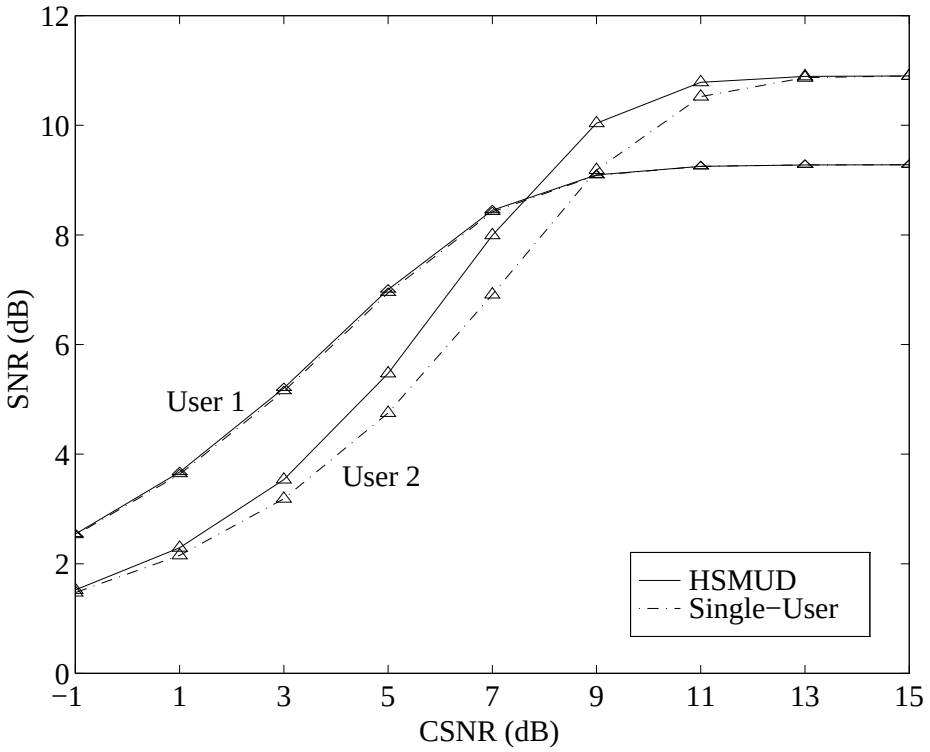

Figure 4-9. Signal-to-noise ratio for a system with two users, $d = 6$ and $L = 6$. User one use a low entropy encoder, $H_1 = 4.77$ bits, and user two a high entropy encoder, $H_2 = 5.87$ bits.

To exemplify the performance of the low complexity version of the single-user HSMUD, a system with Gold-sequences [52] of length 31 has been simulated. The number of users is eight and the same VQs as in Figure 4-6 have been used. The performance for $\alpha = 255$ (full complexity) and $\alpha = 7$ neighbors are presented in Figure 4-10. As can be seen $\alpha = 7$ suffices to give almost full performance. When $\alpha = 31$ and $\alpha = 127$ the performance is indistinguishable from the full complexity case of $\alpha = 255$. Note also that the case of $\alpha = 255$ almost gives the performance of a system with orthogonal codes.

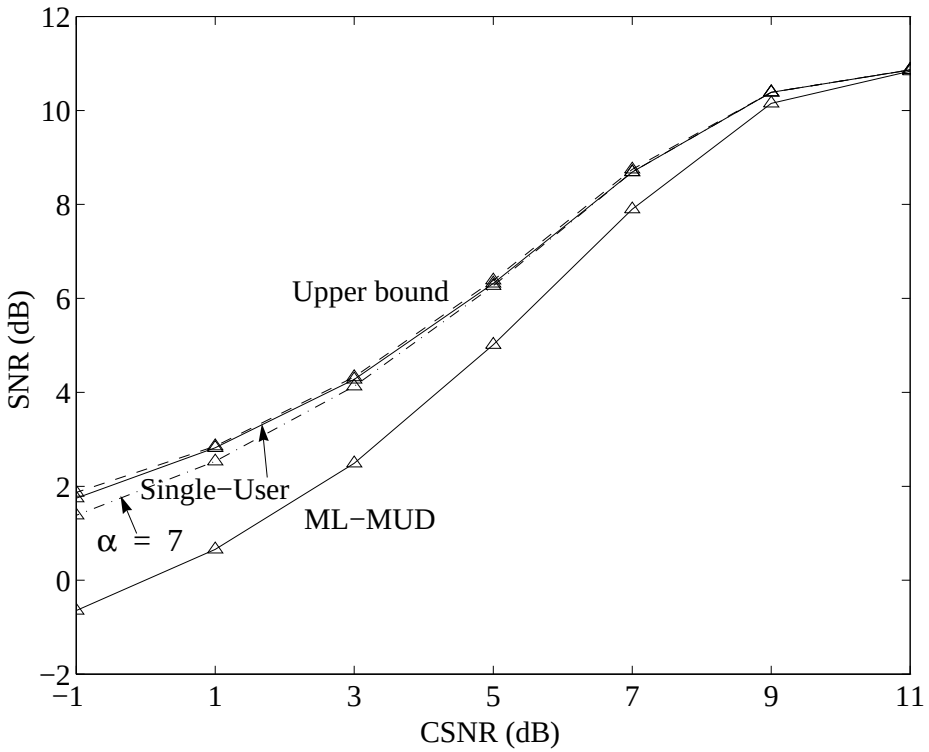

Figure 4-10. Signal-to-noise ratio for a system with eight users (user 1 is illustrated). Gold sequences of length 31 are used. d=6 and L=6. $H_k = 5.87$ bits.

4-6 CONCLUSIONS

We have presented a combined source and channel coding scheme for vector quantization over a CDMA channel. The optimal soft joint multiuser and VQ decoder is presented. This decoder is referred to as the *Hadamard-based soft multiuser decoder* (HSMUD). Simulations demonstrate that the HSMUD outperforms the conventional tandem scheme using an ML multiuser detector followed by a table look-up VQ decoder. However, the complexity of the optimal soft decoder is limiting. Therefore, a single-user version, of lower complexity, is presented. In our simulations the performance of the single-user version is comparable to that of the HSMUD for VQs with high output entropies. Also, an approximation to the single-user version with further reduced complexity has been derived. This algorithm has especially good performance for low cross-correlations.

Note that in the presented simulations all users have the same amplitudes, $w_k = w$. However, we have also investigated the near-far resistance of the

HSMUD and simulations indicate that the soft decoders are near-far resistant.

4-7 FUTURE WORK

In this work we have considered a synchronous CDMA channel. One interesting generalization to investigate in the future is the asynchronous CDMA channel and the corresponding HSMUD. Furthermore, we have used VQ encoders designed for a noiseless channel or a noisy binary channel. To increase the performance of the system further, the encoder can be trained for the CDMA channel according to the COVQ philosophy of [16]. However, in practice, it is hard to update the encoder as the channel is varying, because the receiver and transmitter must agree on which encoder is used. Thus, the encoder has to be trained for the "worst case" channel, and then instead it is possible to modify the decoder with regard to the varying channel.

APPENDIX 4A
VECTOR QUANTIZATION AND THE HADAMARD TRANSFORM REPRESENTATION

Vector Quantization

A vector quantizer (VQ), see Figure 4-11, takes a real-valued d-dimensional vector, $\mathbf{x} \in \Re^d$, as input and tries to approximate this vector using a finite set of codevectors. The vector $\mathbf{x}$ is fed to the encoder of the VQ, and the output of the encoder is an index, I, corresponding to one of N regions in $\Re^d$, resulting in the encoder rate $R = \log(N)/d$. The encoder uses a "nearest neighbor" strategy to find the correct region, given by the condition

$$I = i: \ \|\mathbf{x} - \mathbf{y}_i\| \leq \|\mathbf{x} - \mathbf{y}_j\|, \forall j \in \{0, 1, \ldots, N-1\}, \tag{4A-1}$$

where

$$\{\mathbf{y}_0, \mathbf{y}_1, \ldots, \mathbf{y}_{N-1}\} \tag{4A-2}$$

is the set of reconstruction vectors (one vector for each region). These regions, defined by (4A-1), are called *Voronoi regions*. An example of Voronoi regions for a 4-bit vector quantizer with dimension $d = 2$, trained for an uncorrelated Gaussian source is shown in Figure 4-12.

Figure 4-11. A vector quantization system.

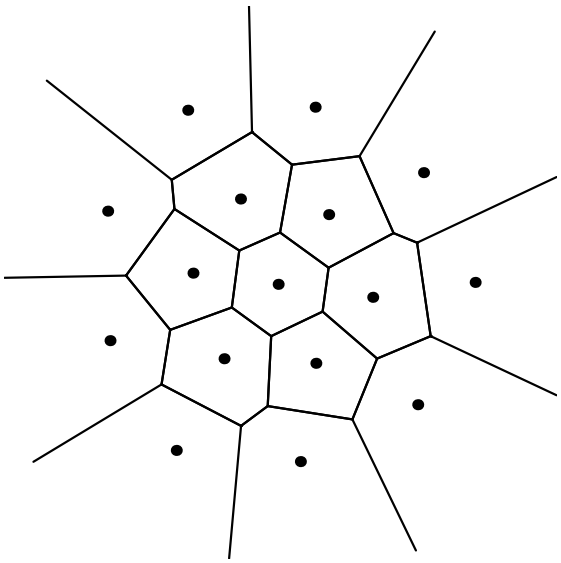

Figure 4-12. Voronoi regions for a 4-bit vector quantizer of dimension *d*=2. (from Knagenhjelm [34]).

In designing a vector quantizer, that is, designing the encoder-decoder functions, a distortion measure has to be chosen. The most common is the squared error distortion measure. In this case, the distortion of the vector quantizer is $D = E\|\mathbf{x} - \hat{\mathbf{x}}\|^2$. Using elementary estimation theory, it can be shown [20] that the optimal reconstruction vectors, given that the channel is noiseless, should be chosen as $E[\mathbf{x}|I]$. These vectors are often called the centroids $\{\mathbf{c}_i\}$ of the encoder regions, defined as $\mathbf{c}_i = E[\mathbf{x}|I = i]$

The decoder, on the other hand, takes an index J as input, which may be different from the "transmitted" index I, and outputs the vector, $\hat{\mathbf{x}} = \mathbf{c}_J$, as an estimate of the transmitted vector, $\mathbf{x}$.

The Hadamard Representation

A convenient way to analyze vector quantizers, and especially the robustness against channel errors is the Hadamard transform representation by Hedelin, Knagenhjelm and Hagen (see for example [23], [25] and [33]). The Hadamard transform of an N-size column vector $\mathbf{u}$ is defined as (see for example [21] and [28])

$$\mathbf{v} = \frac{1}{N}\mathbf{H}_N \cdot \mathbf{u} \tag{4A-3}$$

and the inverse transform is

$$\mathbf{u} = \mathbf{H}_N \cdot \mathbf{v}, \tag{4A-4}$$

where $\mathbf{H}_N$ is the N size square Hadamard matrix defined as

$$\begin{cases} \mathbf{H}_N = \mathbf{H}_{N-1} \otimes \mathbf{H}_1 \\ \mathbf{H}_1 = \begin{bmatrix} 1 & 1 \\ 1 & -1 \end{bmatrix} \end{cases} \tag{4A-5}$$

For $N = 2^L$, the Hadamard matrix has some useful properties [28]:

1. $\mathbf{H}_N^T = \mathbf{H}_N$.
2. $\mathbf{H}_N\mathbf{H}_N = N\mathbf{I}_N$, where $\mathbf{I}_N$ is the identity matrix of size N.
3. $\mathbf{H}_N^{-1} = N^{-1}\mathbf{H}_N$.

Furthermore, if the integer i is represented by the natural binary representation $(b_L, b_{L-1}, \ldots, b_1)$, using +1 for a “zero” and -1 for a “one”, we have [59]

$$\mathbf{h}_i^{(N)} = \begin{bmatrix} 1 \\ b_L \end{bmatrix} \otimes \begin{bmatrix} 1 \\ b_{L-1} \end{bmatrix} \otimes \ldots \otimes \begin{bmatrix} 1 \\ b_1 \end{bmatrix}. \tag{4A-6}$$

Here, $\mathbf{h}_i^{(N)}$ denotes the ith column of $\mathbf{H}_N$.

A vector quantizer is represented by its centroids. Hence, collect all centroids in the matrix $\mathbf{C} = [\mathbf{c}_0, \mathbf{c}_1, \ldots, \mathbf{c}_{N-1}]$, and take the Hadamard transform of each row in $\mathbf{C}$. That is, the transform $\mathbf{t}_i$ of row i of $\mathbf{C}$ is

$$\mathbf{t}_i = \frac{1}{N}\mathbf{H}_N \cdot \{\mathbf{C}^T\}_i \tag{4A-7}$$

and therefore using the inverse transform, we have

$$\mathbf{C} = \mathbf{T} \cdot \mathbf{H}_N, \tag{4A-8}$$

where the real-valued transform matrix is given by

$$\mathbf{T} = [\mathbf{t}_0, \mathbf{t}_1, \ldots, \mathbf{t}_{N-1}]^T = \mathbf{C} \cdot \mathbf{H}_N^{-1} = \frac{1}{N}\mathbf{C}\mathbf{H}_N. \tag{4A-9}$$

APPENDIX 4B
THE KRONECKER PRODUCT

Assume that $\mathbf{A}$ is a $(p \times q)$-size matrix and $\mathbf{B}$ a $(m \times n)$-size matrix. Hence, the Kronecker product is the $(pm \times qn)$-size matrix

$$\mathbf{A} \otimes \mathbf{B} = \begin{bmatrix} a_{11}\mathbf{B} & a_{12}\mathbf{B} & \ldots & a_{1q}\mathbf{B} \\ a_{21}\mathbf{B} & & & \\ & & & \\ a_{p1}\mathbf{B} & \ldots & & a_{pq}\mathbf{B} \end{bmatrix}. \tag{4B-1}$$

The basic algebra for Kronecker products can be found in [6], but some of the more useful theorems are repeated here for convenience.

1. $(\mathbf{A} \otimes \mathbf{B}) \otimes \mathbf{C} = \mathbf{A} \otimes (\mathbf{B} \otimes \mathbf{C})$
2. $(\mathbf{A} + \mathbf{B}) \otimes \mathbf{C} = \mathbf{A} \otimes \mathbf{C} + \mathbf{B} \otimes \mathbf{C}$
3. $(\mathbf{A} \otimes \mathbf{B})^T = (\mathbf{A}^T \otimes \mathbf{B}^T)$
4. $(\mathbf{A} \otimes \mathbf{B})(\mathbf{C} \otimes \mathbf{D}) = \mathbf{AC} \otimes \mathbf{BD}$
5. $(\mathbf{A} \otimes \mathbf{B})^{-1} = (\mathbf{A}^{-1} \otimes \mathbf{B}^{-1})$
6. $\alpha(\mathbf{A} \otimes \mathbf{B}) = (\alpha\mathbf{A}) \otimes \mathbf{B} = \mathbf{A} \otimes (\alpha\mathbf{B})$, where α is scalar.

APPENDIX 4C
PROOF OF LEMMA

In the derivation of the optimum decoder the following lemma [46] is needed (see (4-18)).

Lemma: For $a \in \{-1, 1\}$ and $x \in \Re$ is

$$e^{ax} = \cosh(x)\,(1 + a \cdot \tanh(x)) . \tag{4C-1}$$

Proof: Using the definitions of $\cosh(x)$ and $\tanh(x)$ we get

$$\cosh(x)\,(1 + a \cdot \tanh(x)) = \tag{4C-2}$$

$$\frac{e^x + e^{-x}}{2} \cdot \left(1 + a \cdot \frac{e^x - e^{-x}}{e^x + e^{-x}}\right) =$$

$$\frac{(1+a)}{2} \cdot e^x + \frac{(1-a)}{2} \cdot e^{-x} = \begin{cases} e^x, & a = 1 \\ e^{-x}, & a = -1 \end{cases}$$

and the lemma follows easily.

BIBLIOGRAPHY

[1] E. Agrell and T. Ottosson, "ML optimal CDMA multiuser receiver," *Electronics Letters*, Vol. 31, No. 18, pp. 1554-1555, August 1995.

[2] E. Agrell, "Spectral coding by fast vector quantization," *Proc. IEEE Workshop on Speech Coding for Telecommunications*, Sainte-Adèle, Québec, Canada, 1993, pp. 61-62.

[3] N. Abramson, *The ALOHA system*. Prentice-Hall, 1973.

[4] A. Baier, U.C. Fiebig, W. Granzow, P. Teder, and J. Thielecke, "Design study for a CDMA-based third-generation mobile radio system," *IEEE J. Select. Areas Commun.*, Vol. 12, No. 4, pp. 733-743, May 1994.

[5] D. W. Bennet, R. J. Wilkinson, and P. B. Kenington, "Determining the power rating of a multichannel linear amplifier," *IEE Proc.-Commun.*, Vol. 142, No. 4, pp. 274-280, August 1995.

[6] J. W. Brewer, "Kronecker products and matrix calculus in system theory," *IEEE Trans. Circuits and Systems*, Vol. CAS-25, No. 9, pp. 772-781, September 1978.

[7] M. H. Callendar, "Future public land mobile telecommunication systems," *IEEE Personal Commun.*, Vol. 1, No. 4, pp. 18-22, Fourth Quarter 1994.

[8] I. Chih-Lin and K. K. Sabnani, "Variable spreading gain CDMA with adaptive control for true packet switching wireless network," in *Proc. ICC'95*, Seattle, USA, 1995, pp. 725-730.

[9] I. Chih-Lin and R. D. Gitlin, "Multi-code CDMA wireless personal communications networks," in *Proc. ICC'95*, Seattle, USA, 1995, pp. 1060-1064.

[10] N. Doi, T. Yano, and N. Kobayashi, "DS/CDMA prototype system transmitting low bit-rate voice and high bit-rate ISDN signals," in *Proc. IEEE VTC'94*, Stockholm, Sweden, 1994, pp. 51-55.

[11] T. M. Cover and J. A. Thomas, *Elements of Information Theory.* John Wiley & Sons, Inc., 1991.

[12] D. C. Cox, "Wireless Personal Communications: What is it?," *IEEE Personal Commun.*, Vol. 2, No. 2, pp. 20-35, April 1995.

[13] A. Duel-Hallen, J. Holtzman, and Z. Zvonar, "Multiuser detection for CDMA systems," *IEEE Personal Commun.*, Vol. 2, No. 2, pp. 46-58, April 1995.

[14] T. Eng and L. B. Milstein, "Comparison of hybrid FDMA/CDMA systems in frequency selective Rayleigh fading," *IEEE J. Select. Areas Commun.*, Vol. 12, No. 5, pp. 938-951, June 1994.

[15] N. Farvardin, "A study of vector quantization for noisy channels," *IEEE Trans. Inform. Theory*, Vol. 36, No. 4, pp. 799-809, July 1990.

[16] N. Farvardin and V. Vaishampayan, "On the performance and complexity of channel-optimized vector quantizers," *IEEE Trans. Inform. Theory*, Vol. 37, No. 1, pp. 155-159, January 1991.

[17] M-.H. Fong, V. K. Bhargava, and Q. Wang, "Concatenated orthogonal/PN spreading scheme for cellular DS-CDMA systems with integrated traffic," in *Proc. ICC'95*, Seattle, USA, 1995, pp. 905-909.

[18] E. Geraniotis and M. B. Pursley, "Error probability for direct-sequence spread-spectrum multiple-access communications - Part II: Approximations," *IEEE Trans. Commun.*, Vol. COM-30, No. 5, pp. 985-995, May 1982.

[19] E. Geraniotis and B. Ghaffari, "Performance of binary and quaternary direct-sequence spread-spectrum multiple-access systems with random signature sequences," *IEEE Trans. Commun.*, Vol. 39, No. 5, pp. 713-724, May 1991.

[20] A. Gersho and R. M. Gray, *Vector quantization and signal compression*. Kluwer Academic Publishers, 1992.

[21] R. C. Gonzalez and P. Wintz, *Digital image processing*. Addison-Wesley, 1987.

[22] R. M. Gray, "Vector quantization," *IEEE ASSP Magazine*, pp. 4-29, April 1984.

[23] R. Hagen and P. Hedelin, "Robust vector quantization in spectral coding," in *Proc. ICASSP'93*, Minneapolis, USA, 1993, pp. II:13-16.

[24] B. Hagerman, “Single-user receivers for partly known co-channel interference,” *Technical Report TRITA-IT R 94:11*, Royal Institute of Technology, Stockholm, Sweden, ISSN 1103-534X, 1994.

[25] P. Hedelin, P. Knagenhjelm, and M. Skoglund, “Theory for transmission of vector quantization data,” in *Speech coding and synthesis*, W. B. Kleijn and K. K. Paliwal, eds. Elsevier Science, 1995.

[26] D. Horwood and R. Gagliardi, “Signal design for digital multiple access communications,” *IEEE Trans. Commun.*, Vol. COM-23, No. 3, pp. 378-383, March 1975.

[27] A. Jalali and P. Mermelstein, “Effects of diversity, power control, and bandwidth on the capacity of microcellular CDMA systems,” *IEEE J. Select. Areas Commun.*, Vol. 12, No. 5, pp. 952-961, June 1994.

[28] A. K. Jain, *Fundamentals of digital image processing*. Prentice-Hall, 1989.

[29] V. Kafedziski and D. Morrell, “Vector quantization over Gaussian channels with memory,” in *Proc. ICC’95*, Seattle, USA, 1995, pp. 1433-1437.

[30] R. H. Katz, “Adaption and mobility in wireless information systems,” *IEEE Personal Commun.*, Vol. 1, No. 1, pp. 6-17, First Quarter 1994.

[31] M. Kavehrad and P. J. McLane, “Performance of low-complexity channel coding and diversity for spread spectrum in indoor, wireless communication,” *Bell Syst. Tech. J.*, Vol. 64, No. 8, pp. 1927-1965, October 1985.

[32] P. Kempf, “A non-orthogonal synchronous DS-CDMA case, where successive cancellation and maximum-likelihood multiuser detectors are equivalent,” in *Proc. ISIT’95*, Whistler, Canada, 1995, p. 321.

[33] P. Knagenhjelm, “How good is your index assignment?,” in *Proc. ICASSP’93*, Minneapolis, USA, 1993, pp. II:423-426.

[34] P. Knagenhjelm, “Competitive learning in robust communication,” *Ph.D Thesis*, Dept. of Information Theory, Chalmers University of Technology, Göteborg, Sweden, 1993.

[35] E. A. Lee and D. G. Messerschmitt, *Digital Communication, 2nd ed.*, Kluwer Academic Publishers, 1994.

[36] V. O. K. Li and X. Qiu, “Personal communication systems (PCS),” in *Proc. IEEE*, Vol. 83, No. 9, pp. 1210-1243, September 1995.

[37] F.-H. Liu, P. Ho, and V. Cuperman, “Joint source and channel coding using a non-linear receiver,” in *Proc. ICC '93*, Geneva, Switzerland, 1993, pp. 1502-1507.

[38] F.-H. Liu, P. Ho, and V. Cuperman, "Sequential reconstruction of vector quantized signals transmitted over Rayleigh fading channels," in *Proc. ICC '94*, New Orleans, USA, 1994, pp. 23-27.

[39] R. Lupas and S. Verdú, "Linear multiuser detectors for synchronous code-division multiple-access channels," *IEEE Trans. Inform. Theory*, Vol. 35, No. 1, pp. 123-136, January 1989.

[40] R. Lupas and S. Verdú, "Near-far resistance of multiuser detectors in asynchronous channels," *IEEE Trans. Commun.*, Vol. 38, No. 4, pp. 496-508, April 1990.

[41] D. T. Magill, F. D. Natali, and G. P. Edwards, "Spread-spectrum technology for commercial applications," in *Proc. IEEE*, Vol. 82, No. 4, pp. 572-584, April 1994.

[42] I. Okazaki and T. Hasegawa, "Spread spectrum pulse position modulation - A simple approach for Shannon's limit," *IEICE Trans. Commun.*, Vol. E76-B, No. 8, pp. 929-940, August 1993.

[43] T. Ottosson and A. Svensson, "Performance of different multi-rate schemes in DS/CDMA systems," in *Proc. NRS seminar on Radio communication networks*, Linköping, Sweden, 1994, pp. 15-18.

[44] T. Ottosson and A. Svensson, "Multi-rate schemes in DS/CDMA systems," in *Proc. VTC'95*, Chicago, USA, 1995, pp. 1006-1010.

[45] T. Ottosson and A. Svensson, "Multi-rate performance in DS/CDMA systems," *Tech. Report No. 14*, Dept. Information Theory, Chalmers University of Technology, Göteborg, Sweden, ISSN 0283-1260, March 1995.

[46] T. Ottosson and M. Skoglund, "Hadamard-based soft multiuser decoding for vector quantization over a synchronous CDMA channel," *in preparation*.

[47] P. Patel and J. Holtzman, "Analysis of a simple successive interference cancellation scheme in a DS/CDMA system," *IEEE J. Select. Areas Commun.*, Vol. 12, No. 5, pp. 796-807, June 1994.

[48] R. L. Pickholtz, D. L. Schilling, and L. B. Milstein, "Theory of spread-spectrum communications - A tutorial," *IEEE Trans. Commun.*, Vol. COM-30, No. 5, pp. 855-884, May 1982.

[49] J. G. Proakis, *Digital communications, 2nd Ed.*, McGraw-Hill, 1989.

[50] M. B. Pursley, "Performance evaluation for phase-coded spread-spectrum multiple-access communication - Part I: System analysis," *IEEE Trans. Commun.*, Vol. COM-25, No. 8, pp. 795-799, August 1977.

[51] M. B. Pursley and H. F. A. Roefs, “Numerical evaluation of correlation parameters for optimal phases of binary shift-register sequences,” *IEEE Trans. Commun.*, Vol. COM-27, No. 10, pp. 1597-1604, October 1979.

[52] D. V. Sarwate and M. B. Pursley, “Crosscorrelation properties of pseudorandom and related sequences,” in *Proc. IEEE*, Vol. 68, No. 5, pp. 593-618, May 1980.

[53] Shigenobu Sasaki, Jinkang Zhu, and Gen Marubayashi, “Performance of the parallel combinatory spread spectrum multiple access communication system with error control technique,” in *Proc. IEEE Int. Symposium on Spread Spectrum Techniques and Applications (ISSSTA’92)*, Yokohama, Japan, 1992, pp. 159-162.

[54] K. Schneider, “Optimum detection of Code Division Multiplexed Signals,” *IEEE Trans. Aerospace and Electronic Systems*, Vol. AES-15, No. 1, pp. 181-185, January 1979.

[55] K. Schneider, “Crosstalk resistant receiver for M-ary multiplexed communications,” *IEEE Trans. Aerospace and Electronic Systems*, Vol. AES-16, No. 4, pp. 426-433, July 1980.

[56] C. E. Shannon, “A mathematical theory of communication,” *Bell Sys. Tech. Journal*, Vol. 27, pp. 379-423, 623-656, 1948.

[57] M. Skoglund and P. Hedelin, “Vector quantization over a noisy channel using soft decision decoding,” in *Proc. ICASSP '94*, Adelaide, Australia, 1994, pp. V605-V608.

[58] M. Skoglund, “A soft decoder vector quantizer for a Rayleigh fading channel - Application to image transmission,” in *Proc. ICASSP '95*, Detroit, USA, 1995, pp. 2507-2510.

[59] M. Skoglund, “Soft decoding vector quantization for noisy channels,” *Tech. report, No. 190L*, Dept. Information Theory, School of Electrical and Computer Engineering, Chalmers University of Technology, Göteborg, Sweden, ISBN 91-7197-079-7, January 1995.

[60] M. Skoglund and P. Hedelin, “Hadamard-based soft decoding for vector quantization over noisy channels,” *to be submitted*.

[61] M. Skoglund and T. Ottosson, “Optimal soft multi-user decoding for vector quantization in a synchronous CDMA system,” in *Proc. ISIT’95*, Whistler, Canada, 1995, p. 315.

[62] M. Skoglund and T. Ottosson, "Vector quantization over a CDMA channel using soft multiuser decoding," in *Proc. 4th Commun. Theory Mini-Conf. in conjunction with Globecom'9*5, Singapore, 1995.

[63] M. Skoglund and T. Ottosson, "Joint equalization and soft decoding for vector quantization over channels with intersymbol interference," *subm. to ICC'96*.

[64] S. Tachikawa, "Modulation in spread spectrum communication systems," *IEICE Trans. Commun.*, Vol. E75-B, No. 6, pp. 445-452, June 1992.

[65] S. Tachikawa, "Recent spreading codes for spread spectrum communication systems," *Electronics and Communications in Japan*, Part I, Vol. 75, No. 6, pp. 41-49, 1992.

[66] TIA/EIA/IS-95, "Mobile station-base station standard for dual-mode wideband spread spectrum cellular system," *Telecommunication Industry Association*, July 1993.

[67] G. L. Turin, "Introduction to spread-spectrum antimultipath techniques and their application to urban digital radio," in *Proc. IEEE*, Vol. 68, No. 3, pp. 328-353, March 1980.

[68] H. L. van Trees, *Detection, Estimation, and Modualtion Theory, Part I*. New York: Wiley, 1968.

[69] V. A. Vaishampayan and N. Farvardin, "Joint design of block source codes and modulation signal sets," *IEEE Trans. Inform. Theory*, Vol. 36, No. 4, pp. 1230-1248, 1992.

[70] M. K. Varanasi and B. Aazhang, "Near-optimum detection in synchronous code-division multiple-access systems," *IEEE Trans. Commun.*, Vol. 39, No. 5, pp. 725-736, May 1991.

[71] M. K. Varanasi and B. Aazhang, "Multistage detection in asynchronous code-division multiple-access communications," *IEEE Trans. Commun.*, Vol. 38, No. 4, pp. 509-519, April 1990.

[72] S. Verdú, "Optimal multi-user signal detection," Ph.D Thesis, University of Illinois at Urbana-Champaign, Coordinated Science Laboratory, Urbana, USA, September 1984.

[73] S. Verdú, "Minimum probability of error for asynchronous gaussian multiple-access channels," *IEEE Trans. Inform. Theory*, Vol. IT-32, No. 1, pp. 85-96, January 1986.

[74] S. Verdú, "Computional complexity of optimum multiuser detection," *Algorithmica*, Vol. 4, pp. 303-312, 1989.

[75] T. H. Wu and E. Geraniotis, "CDMA with multiple chip rates for multimedia communications," in *Proc. Information Science and Systems*, Princeton University, 1994, pp. 992-997.

[76] Jinkang Zhu and Gen Marubayashi, "Properties and application of parallel combinatory SS communication system," in *Proc. IEEE Int. Symposium on Spread Spectrum Techniques and Applications (ISSSTA'92)*, Yokohama, Japan, 1992, pp. 227-230.

[77] Z. Zvonar and D. Brady, "Suboptimal multiuser detector for frequency-selective Rayleigh fading synchronous CDMA channels," *IEEE Trans. Commun.*, Vol. 43, No. 2/3/4, pp. 154-157, February/March/April 1995.

[78] Special issue on the European path towards UMTS, IEEE Personal Commun., Vol. 2, No. 1, February 1995.